



UNIVERSITÀ DEGLI STUDI DI CAMERINO

School of Advanced Studies

Doctoral Course in

Chemical and Pharmaceutical Sciences and Biotechnology – Pharmaceutical Sciences

Cycle XXXI

SYNTHESIS AND BIOLOGICAL EVALUATION
OF NEW LIGANDS FOR THE
ADENOSINE RECEPTORS

Medicinal Chemistry: CHIM/08

PhD Candidate

Michael Alliance Ngouadjeu Ngnintedem

Supervisors

Prof.ssa Rosaria Volpini

Prof.ssa Catia Lambertucci

Coordinator

Prof. Sauro Vittori

2015-2018

V: Dedication

I dedicate this thesis to the Lord Jesus Christ, my Lord and my personal savior. My faithful friend and my everlasting Father.

VI: Acknowledgements

I would like to thank the Lord Jesus Christ for his strength, his love, his mercy, his health and his patience. I thank God for my family and for my life.

The institutions

I would like to thank the University of Camerino and in particular the School of Pharmacy and Health Products for its welcoming environment and facilities for international students.

I would like to thank the School of Advanced Studies (SAS) of the University of Camerino for its support, guidance and training during these three years.

I would like to thank the Volpini et al laboratory for the training and the knowledge acquired during these years.

I would like to thank the Italian government for financing my tuition and my cost of living through the ERSU grant for my entire PhD program.

I would like to thank the URCA-DSCHANG project which allowed me to move from my country to Italy thanks to a mobility grant between the University of Dschang (Cameroon) and the University of Camerino (Italy).

I would like to thank the University of Dschang where I started my university studies and the partnership they established with the University of Camerino and which allowed me to move from Cameroon to Italy.

Mentors

I would like to thank my supervisors: Professors Volpini Rosaria, Gabriella Marucci and Lambertucci Catia for their invaluable support in my studies, research training, research career and life outside the laboratory. I would also like to thank them for their patience and understanding during these three years.

I would like to thank Professor Vittori Sauro for his support and for the opportunity he has given me since he led the URCA-DSCHANG project.

I would like to thank Dr. Ajiroghene Thomas for his full support during the first year of my PhD program

I would like to thank Dr. Kenfack Bruno, who has been in charge of the university career since the beginning, even today.

Contributions

I would like to thank Professors Volpini Rosaria and Lambertucci Catia for being my supervisors during my PhD training.

I would like to thank my colleague, Dr. Andrea Spinaci, for his assistance and guidance which allowed me to grow in the field of nucleoside chemistry.

I would like to thank Professor Marucci's laboratory, especially Professor Buccioni Michella and Dr. Aleix, for providing the biological data of the synthesized compounds.

I would like to thank Professor Diego dal Ben for the docking studies of synthesized compounds.

Family

I would like to thank all my family in Cameroon for their advice, availability, encouragement and psychological support.

I would like to thank my fiancée, Dr. Marielle Azangue, for her love, kindness and understanding.

I would like to thank my cousin Dr. Yonkoua Esther and her husband for being my family in Italy and for their kindness, support and availability whenever I needed help.

I would especially like to thank my elder brother, Joel Ngouadjeu, who lives Germany for his financial support and encouragement.

Friends

I would like to thank all my friends for their daily support and encouragement. Special thanks to Manuella Lesly, Larissa, Godsglory, Dr. Roger Michel, Dr. Julienne Deholie, Dr. Misfalline Badawe, Dr. Khawla, Dr. Brice Fokom, Dr. Franks Zekoue, Dr. Nkuimie Joice, Dr. Yannick Fotio, Dr. Alain Tenoh, Dr. Azebaze Mureille, Dr. Temgue Gael, Dr. Ngahang Stephane.

Finally, I would like to thank everyone who contributed to this work.

VII: Dédicace

Je dédie cette thèse au Seigneur Jésus-Christ, mon Seigneur et Sauveur personnel. Mon fidèle ami et mon père éternel.

VIII : Remerciements

Je remercie le Seigneur Jésus-Christ pour sa force, son amour, sa miséricorde, sa santé et sa patience. Je remercie Dieu pour ma famille et pour ma vie.

Les institutions

Je voudrais remercier l'Université de Camerino et en particulier l'école de pharmacie et de produits de santé pour son environnement accueillant et ses installations pour les étudiants internationaux.

Je voudrais remercier l'école d'études avancées (SAS) de l'université de Camerino pour son soutien, son accompagnement et sa formation au cours de ces trois années.

Je voudrais remercier le laboratoire Volpini et al pour la formation et les connaissances acquises au cours de ces années.

Je voudrais remercier le gouvernement italien qui a financé mes frais de scolarité et mon coût de la vie à travers la bourse ERSU pour l'ensemble de mon programme de doctorat.

Je voudrais remercier le projet URCA-DSCHANG qui m'a permis de passer de mon pays en Italie grâce à une bourse de mobilité entre l'Université de Dschang (Cameroun) et l'université de Camerino (Italie).

Je voudrais remercier l'Université de Dschang où j'ai commencé mes études universitaires ainsi que le partenariat qu'ils ont établi avec l'Université de Camerino et qui m'a permis de quitter le Cameroun pour l'Italie.

Mentors

Je tiens à remercier mes supérieurs hiérarchiques: le Professeur Volpini Rosaria, le Professeur Gabriella Marucci et le Professeur Lambertucci Catia pour leur grand soutien, dans le cadre de mes études, de ma formation à la recherche, de la construction de ma carrière de chercheur, de ma vie en dehors du laboratoire. Je tiens également à les remercier pour leur patience et leur compréhension au cours de ces trois années.

Je voudrais remercier le Professeur Vittori Sauro pour le soutien, l'accompagnement et l'opportunité qu'il m'a donnée en sa qualité de responsable du projet URCA-DSCHANG.

Je voudrais remercier le Dr Ajiroghene Thomas pour son soutien total au cours de ma première année de thèse.

Je tiens à remercier le Dr Kenfack Bruno, qui s'occupe de ma carrière universitaire depuis le début jusqu'à aujourd'hui.

Contributions

Je voudrais remercier les professeurs Volpini Rosaria et Lambertucci Catia d'avoir été mes superviseurs lors de ma formation de doctorat.

J'aimerais remercier mon collègue, le Dr Andrea Spinaci, pour son aide et ses conseils qui m'ont permis de progresser dans le domaine de la chimie des nucléosides.

Je voudrais remercier le laboratoire du professeur Marucci, en particulier le Professeur Buccioni Michella et Dr.Aleix, pour avoir fourni les données biologiques des composés synthétisés.

Le Professeur Diego dal Ben pour les études de docking des composés synthétisés.

Famille

Je voudrais remercier toute ma famille au Cameroun pour leurs conseils, leur disponibilité, leurs encouragements et leur soutien psychologique.

J'aimerais remercier ma fiancée, le Docteur Marielle Azangue, pour son amour, sa gentillesse et sa compréhension.

Je voudrais remercier ma cousine Dr.Yonkoua Esther et son mari d'être ma famille en Italie et de leur gentillesse, leur soutien et leur disponibilité chaque fois que j'étais dans le besoin.

Je voudrais remercier tout particulièrement mon frère aîné, Joel Ngouadjeu, qui réside en Allemagne pour son soutien financier et pour ses encouragements.

Amis

Je voudrais remercier tous mes amis pour leur soutien et leurs encouragements quotidiens. Un merci particulier à Manuella Lesly, Larissa, Godsglory, Dr. Roger Michel, Dr. Julienne Dejolie, Dr. Misfalline Badawe, Dr. Khawla, Dr. Brice Fokom, Dr. Franks Zekoue, Dr. Nkuimie Joice, Dr. Yannick Fotio, Dr. Alain Tenoh, Dr. Azebaze Mureille, Dr. Temgue Gael, Dr. Ngahang Stephane.

Enfin, je voudrais remercier toute autre personne qui a contribué à la réalisation de ce travail.

Summary

Adenosine (Ado) is an endogenous nucleoside ubiquitous in mammals promoting protection and cells repair during metabolic stress conditions. Through interaction with the four Ado receptor subtypes (ARs), AR ligands have shown potential therapeutic interest for many disorders. In this work both new A_{2A} AR agonists and A_3 AR antagonists were designed, synthesized and tested *in vitro*.

Although Ado 5'-N-ethylcarboxamide derivatives like VT 7 and GCS21680 display a good affinity and selectivity for A_{2A} AR, the development of new agonists for this receptor subtype is still a big challenge in nucleoside chemistry. In this current decade, some papers have reported that a tetrazolyl residue in 4'-position of Ado derivatives led to compounds endowed with good A_{2A} AR affinity. Hence, in this work, compounds bearing the N-ethyltetrazolyl moiety in 4'- position of the Ado ribose portion together with different arylalkylthio and arylalkylamino chains in C2-position were designed and synthesized.

The new compounds were prepared using a convergent approach. To this purpose, 2,6-dichloropurine was coupled with the suitable modified sugar to afford a nucleoside which was further modified by introducing an amino group at the C6- and the suitable side chain at the C2- position. The modified sugar used in the coupling reaction was synthesized starting from the commercially available D-ribose in seven steps. The binding assay and functional study performed with the new compounds at all AR subtypes transfected on Chinese hamster ovary (CHO) cells revealed that the 2-phenylethylthio derivative was the compound endowed with the better affinity for the A_{2A} AR/ A_3 AR subtypes (**17**: K_i hA_{2A} AR = 5.8 nM; K_i hA_3 AR = 1.2 nM). It is worthwhile to note that the presence of the ethyltetrazolyl substituent in the sugar moiety favors the interaction with the receptor respect to the ethylcarboxamido group. As expected, the new derivatives show a dual behavior at ARs, resulting A_{2A} AR agonists and A_3 AR antagonists (**17**: IC_{50} at hA_3 AR of 8.4 nM). Furthermore, the wound healing potential of the news nucleosides was evaluated respect to VT 7, CGS21680 and epidermal growth factor (EGF, used as positive control). The compounds, **17**, **19**, **20**, **21** and **22** showed all better wound healing potential respect to VT 7, CGS21680 and EGF. Therefore such compounds are good candidates for further investigation in *in vivo* model of wound healing.

New A_3 AR antagonists were also prepared based on the observations that, the substitution of the 8-bromine atom of 8-bromo-9-ethyladenine (K_i hA_{2A} AR = 52 nM, K_i hA_3 AR = 2,800 nM) with phenylacetylene shifts the preference of the resulting compound (K_i hA_{3A} AR = 86

nM, $hA_{2A}AR = 600$ nM) from $A_{2A}AR$ to A_3AR . Hence, from these facts, three series of compounds were prepared. The first one was 8-phenylethynyladenine derivatives substituted at N-9 position with different alkyl/arylalkyl chains. The second one combines substitution on the phenyl ring of 8-phenylethynyladenine with either N-9 cyclopentyl or N-9 phenethyl since they resulted being the best N-9 substituents of the first series. The third series combines a fixed para-methoxy-phenylacetylene in C-8 with either N-9 cyclopentyl or N-9 phenethyl, 2-chloro, and with different N^6 substituents. The 8-arylethynyladenine derivatives substituted at 9 position with different alkyl/arylalkyl chains, and the corresponding compounds further substituted at the 2 and N^6 position, were synthesized starting from commercially available adenine or 2,6-dichloropurine in three/five steps, respectively. The results of the *in vitro* test reported that: N-9 cyclopentyl improved affinity while N-9 phenethyl improved selectivity, the chlorine atom is well tolerated especially when combined with C-8 para-methoxy-phenylacetylene, the N^6 substitution gave compounds with maintained selectivity in the same range of the non-substituted derivatives but with a slight decrease of the affinity. Most of the new compounds are endowed with high affinity and different degree of selectivity for the A_3AR subtype. In particular, the tetra-substituted adenine derivative **38** ($K_i A_3R = 8.4$ nM; $K_i A_1R$ and $K_i A_{2A}R > 30,000$ nM) resulting the most active and selective ligand and it represents a very good ligand to study the A_3AR subtype and its function.

TABLE OF CONTENTS

I: List of figures	10
II: List of tables.....	11
III: List of schemes	12
IV: Abbreviations	13
CHAPTER 1: INTRODUCTION	15
1. Overview	16
1.1 Purinergic receptors.....	16
1.2 Purinergic receptors family	17
1.3 Different P2 receptors sub-family	18
2. Production, transport, metabolism and physiological role of ATP	20
2.1 Production	20
2.2 Transport and Metabolism	21
2.3 Physiological role of ATP	21
3. From ATP to Adenosine	24
3.1 P1 Receptors.....	24
3.2 Synthesis, transport and metabolism of Ado.....	25
3.3 Adenosine receptors	27
3.4 Structure of the adenosine receptors	28
3.4 Signal transduction	31
3.5 Adenosine receptor subtypes.....	33
4.0 Adenosine.....	39
4.1 Overview	39
Introduction	39
4.2 Production, metabolism and physiological role of adenosine.....	39
5. Adenosine receptors	42

6. Adenosine derivatives: agonists, antagonists and allosteric modulators.....	43
6.3 Allosteric modulators for adenosine receptors.....	46
7. Therapeutic potential of Ado and adenosine receptor agonists.....	50
7.1 Uses of Ado receptor agonists in diagnosis and in therapy.....	50
7.2 Uses of Ado receptor antagonists in diagnostic and in therapy.....	51
CHAPTER 2: OBJECTIVES.....	55
CHAPTER 3: Synthesis of new 4'-tetrazolyl adenosine derivatives as potential agents for wound healing.....	57
3.1 Aim of the research.....	58
3.2 Chemistry.....	62
3.2.1 Synthesis of the modified sugar.....	62
3.2.2 Glycosylation reaction.....	63
3.2.3 Final compounds.....	65
3.3 Results and discussion.....	67
3.4 Wound healing assay.....	73
3.5 Conclusion.....	79
3.6 Experimental section.....	81
3.6.1 Materials and methods.....	81
3.6.2 Chemistry.....	82
3.7 Biological assay.....	89
3.7.1 Cell culture.....	89
3.7.2 Preparation of membranes.....	90
3.7.3 Binding assays.....	90
3.7.4 GloSensor cAMP Assay.....	91
3.7.5 Wound healing-migration assay.....	91
CHAPTER 4: SYNTHESIS OF NEW ADENINE DERIVATIVES AS POTENT ANTAGONIST OF THE HUMAN A₃AR.....	93

4.1 Aim of the work	94
4.2 Chemistry	96
4.2.1 First series of compounds.....	96
4.2.2 Second series of compounds	97
4.2.3 Third series of compounds	99
4.3 Results and discussion.....	101
4.4: Experimental section.....	107
4.4.1: Materials and methods	107
4.4.2: Chemistry.....	107
4.5: Biological assay.....	114

I: List of figures

Figure 1.1 : Diagram of three stages of cellular metabolism that leads to ATP production from food.....	16
Figure 1.2 : ATP hydrolysis coupled with ATP synthesis.....	17
Figure 1.3 : Chemical structure of Adenosine.....	24
Figure 1.4 : Ado synthesis, metabolism, and transport.....	26
Figure 1.5 : Classification of purinergic receptors.....	27
Figure 1.6 Structure of GPCRs.....	29
Figure 1.7 : Structure of the antagonist ZM241385-bound $A_{2A}AR$	30
Figure 1.8 : Interactions between the human $A_{2A}AR$ and a) ZM 241385 and b) Ado.....	31
Figure 1.9 : Schematic representation of the signal transduction pathways associated with ARs.....	32
Figure 1.10 : Activation mechanism of G protein	33
Figure 1.11 : Interactions between $A_{2A}AR$ and D_2 receptors.....	36
Figure 1.12 : Structure of Adenosine	40
Figure 1.13 : Production and Metabolism of Adenosine.....	41
Figure 1.14 : example of Ado receptors agonists.....	44
Figure 1.15 : example of Adenosine receptors antagonists.....	45
Figure 1.16 : structure of allosteric modulators for A_1AR , $A_{2A}AR$ and A_3AR	49

Figure 1.17: structure of ARs agonists having a very good therapeutic potential.....	51
Figure 1.18: structure of AR antagonists having a very good therapeutic potential.....	53
Figure 3.1: Some promising A _{2A} agonist	59
Figure 3.2: Lead compounds used for the design of the AR ligands in this project.....	60
Figure 3.3: Plan of the designed research project	61
Figure 3.4: NECA and 4'-N-ethyltetrazolyl Ado derivative in the A _{2A} AR binding pocket..	72
Figure 3.5: Example of the scratched wound assay.....	74
Figure 3.6: Effect of CGS21680 on wound healing assay.....	75
Figure 3.7: Effect of VT 7 on wound healing assay.....	76
Figure 4.1: previously synthesized compounds and their AR binding.....	94
Figure 4.2: structure of designed compounds	95

II: List of tables

Table 1.1: reports some key information about distribution and physiological role of P2X receptors sub-family.....	19
Table 1.2: reports some key information about distribution and physiological of P2Y receptors Sub-family.....	20
Table 1.3, 1.4 and 1.5: information's about the implication of ATP in various pathological and physiological states	22-23
Table 1.6.1: ARs receptor subtypes.	42
Table 1.7: Description of AR antagonists with very good therapeutic potential.....	52
Table 3.1: Binding studies at human A ₁ , A _{2A} , and A ₃ ARs cloned and transfected in CHO cells and functional activity at A _{2B} AR cloned and transfected in CHO cells.	68
Table 3.2: Functional studies on chosen candidates at human A ₁ , A _{2A} , A _{2B} , and A ₃ ARs cloned and transfected in CHO cells.	71
Table 3.3: Activity of tested compounds 12, 16-22 in the wound-healing assay; CGS and VT 7 were used as reference compounds.....	77
Table 4.1: Biological profile of 8-phenylethyladenine derivatives 8-10	102
Table 4.2: Biological profile of synthesized compounds 12-20	103
Table 4.3: Biological profile of synthesized compounds 24-38	104
Table 4.4: Functional data, as IC ₅₀ value (nM), at human A ₃ ARs in comparison with binding affinity data (K _i , nM) of compounds 16, 18, and 38	105

III: List of schemes

Scheme 3.1 : Synthesis of the modified sugar	63
Scheme 3.2 : N^2 Glycosylation reaction.....	64
Scheme 3.3 : N^1 Glycosylation reaction.....	65
Scheme 3.4 : Final compounds.....	66
Scheme 4.1 : First series of compounds	97
Scheme 4.2 : Second series of compounds.....	98
Scheme 4.3 : Third series of compounds.....	100

IV: Abbreviations

AC: Adenylyl cyclase

Ado: Adenosine

ADA: Ado deaminase

ADP: Adenosine diphosphate

AK: Ado kinase

AMP: Adenosine monophosphate

AR: Adenosine receptor

ARs: Adenosine receptor subtypes

ATP: Adenosine triphosphate

cAMP: cyclic AMP

CB: Cannabinoid receptor

cDNA : complementary DNA

CHO Cell: Chinese Hamster ovary cell

CNS: Central nervous system

CNTs: concentrative nucleoside transporters

CREB: cAMP responsive element binding protein

CoA: Coenzyme A

COPD: Chronic Obstructive Pulmonary Disease

CO₂: carbon dioxide

CTP: Cytosine triphosphate

DAG: diacylglycerol

DARPP-32: dopamine- and cAMP-regulated neuronal phosphoprotein

EGF: Epidermal growth factor

EL: Extracellular loops

ENTs: equilibrative nucleoside transporters

GFR: glomerular filtration rate

GDP: Guanosine diphosphate

GMP: Guanosine monophosphate

GPCR: G proteins coupled receptors

His: Histidine

IL1 : intracellular loops

cN-1: intracellular 5'- nucleotidase

IP3: Inositol triphosphate
KDa: Kilo daltons
 μ M: micromolar
nM: nanomolar
NECA: 5'- *N*-ethylcarboxamidoAdo
NOS: nitric oxide synthase
5'-NT: ecto-5'-nucleotidase
NTPDase1: ectonucleoside triphosphate diphosphohydrolase 1
O₂: molecular oxygen
PCR: polymerase chain reaction
PD: Parkinson's disease
Pi: Inorganic phosphate
PKA: protein kinase A
PLC: Phospholipase C
PLA₂: Phospholipase A₂
PLD: Phospholipase D
P: Purinergic
PX24R: Purinergic receptor subtype P2X4
PX27R: Purinergic receptor subtype P2X7
P2Y12: Purinergic receptor subtype P2Y12
RNA: Ribonucleic acid
SAH: S-adenosylhomocysteine hydrolase
Ser: Serine
TM: Transmembrane
TNF: Tumor necrotic factor
Trp: Tryptophane
UTP: Uridine triphosphate
Val: Valine

CHAPTER 1: INTRODUCTION

1. Overview

1.1 Purinergic receptors

Adenosine triphosphate (ATP) is the main energy source of the cell. ATP is produced through a complex pathway involving both physiological and biochemical processes which convert the food we eat to the useful energy source for the cell. Figure 1.1 summarizes the ATP production, which starts with food digestion followed by glycolysis and the citric acid cycle.

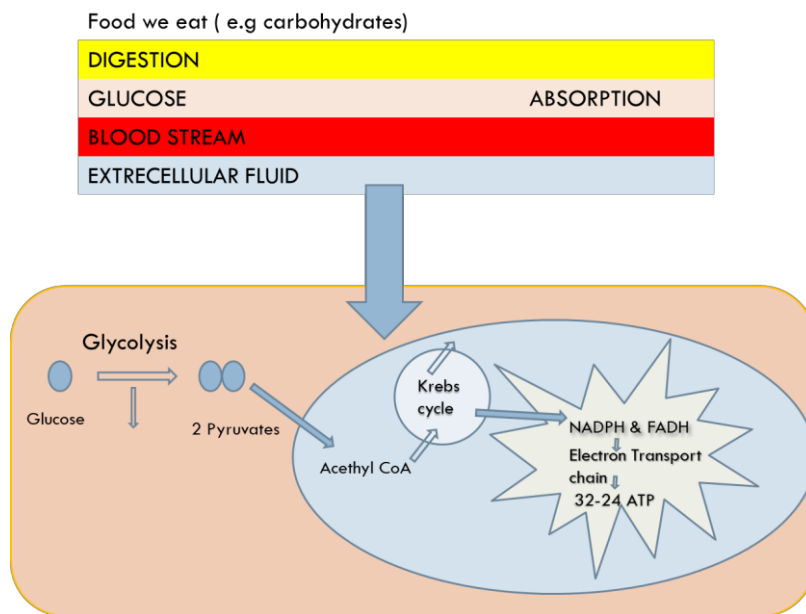


Figure 1.1: Diagram of three stages of cellular metabolism that leads to **ATP** production from food. **Stage 1:** occurs outside of the cell. **Stage 2:** occurs mainly in the cytosol, except for the final step of conversion of pyruvate to acetyl groups on acetyl CoA, which occurs in mitochondria. **Stage 3:** occurs in mitochondria¹.

ATP produced is used as a fuel for energy-needed processes in living cells. Such processes include movement of substances across the cell membranes, muscle contraction and synthesis of many macromolecules essential for the cell existence. The energy stored in ATP is released by hydrolysis, which is a breaking down of ATP in ADP and Pi. ADP and Pi production is coupled with ATP synthesis, which guarantees ATP regeneration. Figure 1.2 reports the ATP hydrolysis and ATP synthesis.

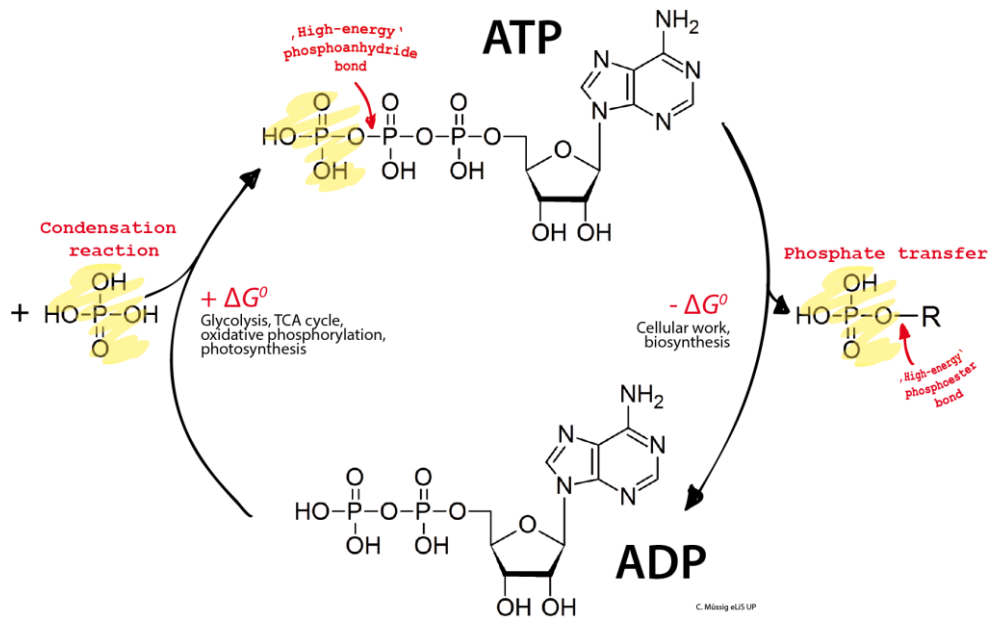


Figure 1.2: ATP hydrolysis coupled with ATP synthesis.

Concerning the storage, ATP usually reaches high concentrations within cells. However, ATP content is quickly depleted due to ATP-dependent processes together with its low stability in water. Hence, storage and compensative processes are needed to maintain the high ATP concentration within the cell. ATP itself cannot be stored easily within cells, hence ATP is stored as carbon sources (such as triglycerides or glycogen), ADP and AMP, which are converted to ATP through glycolysis and with the help of ATP synthase².

Surprisingly, Dowdall and co-workers found a noticeable amount of ATP together with acetylcholine in cholinergic vesicles from the electric organ of *Torpedo marmorata*³. Considerable similar findings (co-storage with noradrenaline, serotonin, dopamine, etc.) were observed in subsequent years in other mammalian and non-mammalian species. Hence, the evidence of co-storage of ATP with neurotransmitters has strongly supported the idea that ATP is a fundamental mediator of purinergic neurotransmission in sympathetic and parasympathetic nerves, where it can induce several purinergic responses (i.e., control of autonomic functions, neural glial interactions, pain and vessel tone control). The purinergic signaling and purinergic receptors sub-family will be discussed in the following section.

1.2 Purinergic receptors family

For years, interest in purines (ATP, ADP, AMP, GTP, GDP, GMP and IMP) and pyrimidines (CTP and UTP) nucleotides was focused on the involvement of ATP in cell metabolism and its role as an energy source⁴. Nonetheless, in 1972, Burnstock raised the possibility that ATP was a

neurotransmitter⁵ and in 1978, he proposed that specific extracellular receptors, known as P1 (will be discussed later) and P2, mediate the physiological effects of adenosine (Ado) and ATP, respectively. Subsequently, ATP was known as a co-transmitter⁵. Hence ATP is now considered either as an exclusive transmitter or as a co-transmitter in both peripheral and central nervous system (CNS)⁶. The evidence of ATP as neurotransmitter has driven a great interest in purinergic signaling and nowadays a lot has been discovered and published around P2 receptor purinergic transmission, especially, the different P2 receptors sub-family which have been well documented and are discussed in the following section.

1.3 Different P2 receptors sub-family

The work of Burnstock *et al* in 1985 allowed the classification of P2 purinoreceptors in two major sub-families known as P2X and P2Y⁷. Subsequent research always carried out by Burnstock allowed to clone and functionally characterized seven subtypes of the human P2X sub-family and eight subtypes of the human P2Y sub-family⁸.

1.3.1 P2X receptor sub-family

Members of this sub-family are seven ionotropic receptors subtypes most of which are assembled as trimers. The monomers show the following common characteristic: an intracellular N- and C-termini; two trans-membrane spanning regions (TM1 and TM2), a large extracellular loop, with 10 conserved cysteine residues forming a series of disulfide bridges and an ATP-binding site⁹. Additional details are given in Table 1.1.

Table 1.1: some key information about distribution and physiological role of P2X receptor sub-family¹⁰.

P2X Purinergic receptors Sub-Family		
P2X receptor sub-type	Body distribution	Physiological role
P2X1	Smooth muscle, platelets, cerebellum, dorsal horn, spinal neurones	Smooth muscle contraction; platelet activation
P2X2	Smooth muscle, CNS, retina, chromaffin cells, autonomic and sensory ganglia	Sensory transmission & modulation of synaptic function
P2X3	Sensory neurones, Nucleus Tractus Solarius, some sympathetic neurones	Mediates sensory transmission; facilitates glutamate release in CNS
P2X4	CNS, testis, colon	Modulates chronic inflammatory & neuropathic pain
P2X5	Proliferating cells in skin, gut, bladder, thymus, spinal cord	Inhibits proliferation & increases differentiation
P2X6	CNS, motor neurones in spinal cord	Functions as a heteromeric channel in combination with P2X2 & P2X4 subunits
P2X7	Apoptotic cells in immune cells, pancreas, skin,	Mediates apoptosis, cell proliferation & proinflammatory cytokine release

1.3.2 P2Y Receptors sub-family

P2Y receptor sub-family comprises eight metabotropic receptor-subtypes characterized by: an extracellular N-terminus, an intracellular C-terminus, and seven trans-membrane spanning regions. Each P2Y receptor subtype binds to a single heterotrimeric G protein (typically Gq/11). However, P2Y₁₂ couples to Gi while P2Y₁₁ can couple to both Gq/11 and Gs. Both purine and pyrimidine nucleotides activate P2Y₂, P2Y₄ and P2Y₆ receptors, whereas P2Y₁ and P2Y₁₁₋₁₃ are activated by purine nucleotides alone. The P2Y₁₄ is dually activated by UDP-sugars, such as UDP-glucose, and also by UDP. Activation of recombinant P2Y receptor subtype leads either to intracellular calcium release following phospholipase C activation or to cyclic AMP (cAMP) levels alteration due to interaction with adenylyl cyclase (AC)⁹. Additional details are given in Table 1.2.

Table 1.2: some key information about distribution and physiological role of P2Y receptor sub-family¹¹.

P2Y Purinergic receptors Sub-Family			
P2Y sub-type	receptor	Body distribution	Physiological role
P2Y1		Epithelial and endothelial cells , platelets, immune cells, osteoclasts , brain	Smooth muscle relaxation & mitogenic actions; platelet shape change & aggregation
P2Y2		Immune cells, epithelial and endothelial cells, kidney tubules, osteoclasts	Vasodilatation & vasoconstriction; mitogenic actions
P2Y4		Endothelial cells, placenta, T cells, spleen, thymus.	Regulates epithelial Cl ⁻ transport; vasodilatation, mitogenic actions
P2Y6		Airway and intestinal epithelial cells , placenta , T cells, thymus, microglia(activated)	NaCl secretion in colonic epithelium; role in epithelial proliferation
P2Y11		Spleen, intestine, granalocytes	Role in maturation & migration of dendritic cells; granulocytic differentiation
P2Y12		Platelets, glia cells	Platelet aggregation; role in dense granule secretion
P2Y13		Spleen, brain, lymph nodes, bone marrow , erythrocytes	Function largely unknown, but present in both the immune system and brain
P2Y14		Placenta, adipose tissue, stomach,intestine, discrete brain region,mast cells	Chemoattractant receptor in bone marrow hematopoietic stem cells; dendritic cell activation

2. Production, transport, metabolism and physiological role of ATP

2.1 Production

ATP is mainly produced from food we eat, from stored macromolecules as glycogen or triglycerides, from ADP and AMP (discussed already in more detail in the section above).

Briefly, glucose released either from digestion of sugars or from breaking down of glycogen is transported into the intracellular compartment where it is subsequently converted in pyruvate through glycolysis. At this stage, small amount of ATP and NADH is produced. Then the pyruvate obtained from glycolysis is converted to acetyl coenzyme A (Acetyl-CoA). Finally, Acetyl-CoA moves from cytosol to mitochondria where it enters in Krebs cycle to produce a considerable amount of ATP. In fact, acetyl group is oxidized to carbon dioxide (CO₂), generating a considerable amount of the electron carrier NADH. Then the NADH enter in the electron-transport chain within the mitochondrial inner membrane; during that process of transfer there is a release of energy which is used to drive a process that produces ATP and consumes molecular oxygen (O₂)¹.

2.2 Transport and Metabolism

The synthesized ATP is transported from mitochondria to cytosol by the help of the mitochondrial ADP/ATP carrier. Once in cytosol, ATP is used as energy source for vital cell processes such as cell membrane transport and synthesis of macromolecules¹². The mitochondrial ADP/ATP carrier is one of the most abundant carrier proteins of the mitochondrial inner membrane¹³. The essential activity of the carrier is to import ADP back from cytosol into the mitochondrion for ATP synthesis and to export the synthesized ATP out of the mitochondrion for use in the cytosol. The activity of mitochondrial ADP/ATP carrier allows ATP to reach high intracellular concentration. Even though ATP concentration reaches millimolar range within the cell, it is not stored. In fact, storage is mainly impeded by the high demand of energy needed processes but also partly by the low water stability of ATP. So, to maintain the high concentration of ATP necessary for the cell survival, the depletion of ATP is coupled with a compensative process which converts back ADP generated during ATP hydrolysis to ATP. The compensative process resides on the mitochondrial ADP/ATP carrier, which transports back ADP from cytosol to mitochondria allowing ADP to be reconverted in ATP. Summarizing, ATP synthesized in the mitochondria is transported in cytosol where it is used as energy source for cellular metabolism. ATP is not stored and its high concentration of ATP within the cell is maintained by the reconversion of ADP to ATP.

However, Dowdall and co-workers has brought additional knowledge about the storage of ATP showing that, even if ATP used as energy source is not stored alone, considerable amount of ATP is stored together with neurotransmitters³. An example is the case of co-storage of ATP with acetylcholine in the cholinergic vesicles. This co-storage has brought evidence that ATP, beside its energetic role, is also released in the extracellular space where it behaves like any neurotransmitter. Specifically, neurotransmitter properties of ATP have been proved in purinergic signalling where ATP is the signal molecule mediating the purinergic neurotransmission both in sympathetic and parasympathetic nerves². More details about ATP as a fundamental mediator of purinergic signalling are given in the next section.

2.3 Physiological role of ATP

Although evidences of ATP as signal molecule were already reported before, the concept of ATP as a signal molecule was accepted in 1998 after P2X and P2Y receptors sub-family were cloned and characterized as receptors for purines and pyrimidines (ATP, ADP and UTP)¹⁴. From these preliminary findings, subsequent studies (physiological, pharmacological and biochemical)

allowed to expand knowledge about the concept of ATP as signal molecule. Hence, it is now known that, beside the energetic role, ATP mediates neurotransmission in both peripheral and CNS. In addition, ATP is also known as a powerful extracellular messenger modulating the physiology of non-neuronal cells including secretory, exocrine and endocrine, endothelial, immune, musculo-skeletal and inflammatory cells^{6, 15}.

The demonstration of ATP as a neurotransmitter, but also as an extracellular signal molecule in non-neuronal cells, has driven a great interest about the implication of ATP in both physiological and pathological conditions. In the following section it will be discussed briefly some disorders focusing our interest in the implication of ATP either as the cause of the disorder or as potential repair pathway. All informations are gathered in Tables 1.3, 1.4 and 1.5.

The Tables **1.3**, **1.4** and **1.5**: content information is about the implication of ATP in various pathological and physiological states.

Table 1.3

Disorders		Example of disorders	
Central nervous system disorder	Neurodegenerative diseases	Alzheimer's Diseases (AD)	Parkinson's Disease (PD)
Implication of ATP in the disorder	P2X7R antagonists are potential therapeutic candidates ¹⁶	Both P2X7R and P2Y4R antagonists are potential therapeutic ^{17,18}	A P2X7R antagonists, brilliant blue G, was recently shown to be protective in an animal model of PD ¹⁹
Brain injury, Neuroprotection, Neuroregeneration	Brain injury	Neuroprotection	Neuroregeneration
Implication of ATP in the disorder	P2X7R antagonists are target to prevent secondary neurological injury after traumatic brain injury e and after spinal cord injury ²⁰	P2X4R are required for neuroprotection via ischemic preconditioning. Neuroprotection mediated by microglia is associated with P2X7R activation and release of tumor necrosis factor- α ²¹	Activation of P2Y2R evokes regeneration of glial cells and nerves. Neural stem cell activation leads to neuroregeneration, probably via P2X4R and P2X7R ¹⁷

Table 1.4

Disorders		Example of disorders	
Cardiovascular diseases	Heart Failure	Hypertension	Thrombosis, Inflammation, and Stroke
Implication of ATP in the disorder	Application of ATP, prior to or just after cardiac ischaemia is cardioprotective ²²	ATP released as a cotransmitter from sympathetic nerves together with noradrenaline (NA) potentializes, via P2X1R vasoconstriction in hypertension ²³	Nucleotides are mediators of vascular inflammation and thrombosis. Also P2Y12 antagonists, inhibits platelets aggregation and are widely prescribed for thrombosis and stroke ^{24,25}
Diseases of the airways	Asthma	Chronic Obstructive Pulmonary Disease (COPD)	Airway Infections
Implication of ATP in the disorder	In human lung mast cells, ATP is an important modulator of histamine release ²⁵	COPD is characterized by up-regulation of ATP in bronchoalveolar lavage fluid, which promotes inflammation and tissue degradation. ATP-induced pulmonary vasodilation occurs in patients with COPD ²⁶	Antibiotics, including erythromycin, are used widely for the treatment of lower and upper respiratory tract infections. Erythromycin blocks the P2XR-mediated Ca ²⁺ influx and could represent one mechanism by which it exerts its effects stroke ^{27, 23}

Table 1.5

Example of disorders			
	Neuropathic pain	Brain tumor	Lung injury
Implication of ATP in the disorder	Antagonists to P2X7R and P2Y12R on microglia reduce neuropathic pain ^{27,28}	Neuroblastoma, expresses P2X7R which may be target for treatment since it regulates metabolic activity, angiogenesis and mediates proliferation ^{29,30}	The initial inflammatory cells recruited during lung injury are pulmonary neutrophils and P2X7R antagonists reduced neutrophil infiltration and proinflammatory cytokine level ³¹

3. From ATP to Adenosine

The binding of extracellular ATP either on P2X or P2Y receptors subtypes is a key step in the purinergic transmission. In fact, as previously discussed, the interaction of ATP with P2 receptors sub-family is implicated in many disorders and diseases (details are shown in tables 1.3, 1.4 and 1.5). Extracellular ATP is also susceptible to ectonucleotidases, which break down ATP in adenosine (Ado)³². This enzymatic degradation of ATP is one of the main ways of Ado production but represents also the tight link between P2 and P1 purinergic transmission since adenosine is the endogenous ligands of P1 receptors sub-family. P1 purinergic transmission and P1 receptor sub-family are discussed in more detail in the following section.

3.1 P1 Receptors

6-Amino-9-β-D-ribofuranosyl-9H-purine (Ado Fig.1.3) is an endogenous nucleoside, widespread in mammals. Ado is made up of a purine ring substituted in 6 position by a primary amino group and in 9 position by a D-ribose ring.

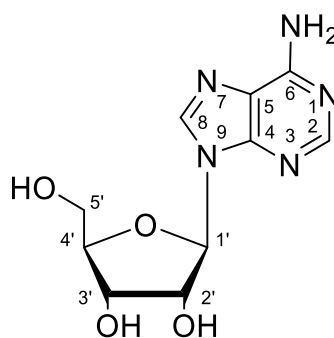


Figure 1.3: Chemical structure of Ado

Drury and Szent-Györgyi in the beginning of years 1900 were the first to outline the role of Ado as an extracellular messenger. In fact, they depicted the considerable vasodilatory potential of Ado³³. Consequently during the years 70s, Sattin and Rall exhibited a particular role of Ado in the central nervous system (CNS), showing that it was found to be implicated in the increase of 3',5'-cyclic Ado monophosphate (cAMP) in mammalian brain cuts. They also found that the cAMP formation was hindered by methylxanthines (for example caffeine and theophylline)³⁴. Later on, an inhibitory role of Ado was displayed in cortical neuron³⁵, cerebellar³⁶ and potential

synaptic excitatory cortical cuts and hippocampus³⁷. The inhibitory role of Ado on the discharge of acetylcholine³⁸, norepinephrine³⁹, amino acids, and excitatory serotonin^{40,41} was additionally demonstrated in different brain zones. Each single one of these effects was hindered by methylxanthines while expanded by Ado reuptake inhibitors, and related with an adjustment in cAMP levels. The experimental investigations that pursued these basic informations demonstrated the role of Ado in the homeostasis of the CNS as well as in the homeostasis of peripheral tissues.

Ado operates like a cytoprotective modulator under physiological and pathological conditions in response to oxidative stress in organs and tissues⁴². This defensive reaction may be expressed in the four following manner: by expanding the oxygen supply whenever required, securing against ischemic damage, activating inflammatory reactions, and stimulating angiogenesis⁴³. Therefore, it is conceivable to expect the presence of a guard system that permits the activation of different reactions important for the recovery of the cell work and an ordinary oxygen homeostasis.

Ado has characteristics very close to those of neurotransmitter. In fact, it exerts its function by binding to specific receptors known as adenosine receptors (ARs), it is metabolized in the synapses by the help of specific enzymes, and the fact that its functions can be obstructed by selective antagonists, by the reuptake system and its catabolism in the cytoplasm⁴⁴. Moreover, studies have demonstrated that Ado additionally is stored in synaptic vesicles and discharged by neurons in rat⁴⁵.

3.2 Synthesis, transport and metabolism of Ado

Ado is produced in physiological conditions at the intracellular and extracellular level. It is present in the cytoplasm mostly in its phosphorylated forms. For example Ado monophosphate (AMP), Ado diphosphate (ADP), and Ado triphosphate (ATP). Ado is present in low amount in the extracellular space in the range from 30 to 200 nanomolar (nM)⁴⁶. During ischemia or subsequently to an enormous tissue injury that induces cell necrosis, levels of extracellular Ado can achieve an amount of 30 micromolar (μ M)¹⁶.

Generation of cellular Ado (Fig. 1.4) relies upon the hydrolysis of AMP. Such hydrolysis is carried out by intracellular 5'-nucleotidase (cN-1), or by the activity of S-adenosylhomocysteine hydrolase on its substrate S-adenosylhomocysteine (SAH)⁴⁷. The intracellular Ado can be released into the extracellular space by the help of specific bidirectional transporters (equilibrative nucleoside transporters or ENTs). This movement of Ado out of the cell is crucial since it allows the balancing of the intra- and extracellular level of Ado (Fig. 1.4). ENT1 and

ENT2 are the two well documented among the four ENT isoforms which have been found to be encoded by the human genome (ENT1-4). The classification from 1-4 is determined by their sensibility to inhibition carried out by nitrobenzylthioinosine⁴⁸. These transporters, specifically ENT1, are widely expressed in the CNS⁴⁹.

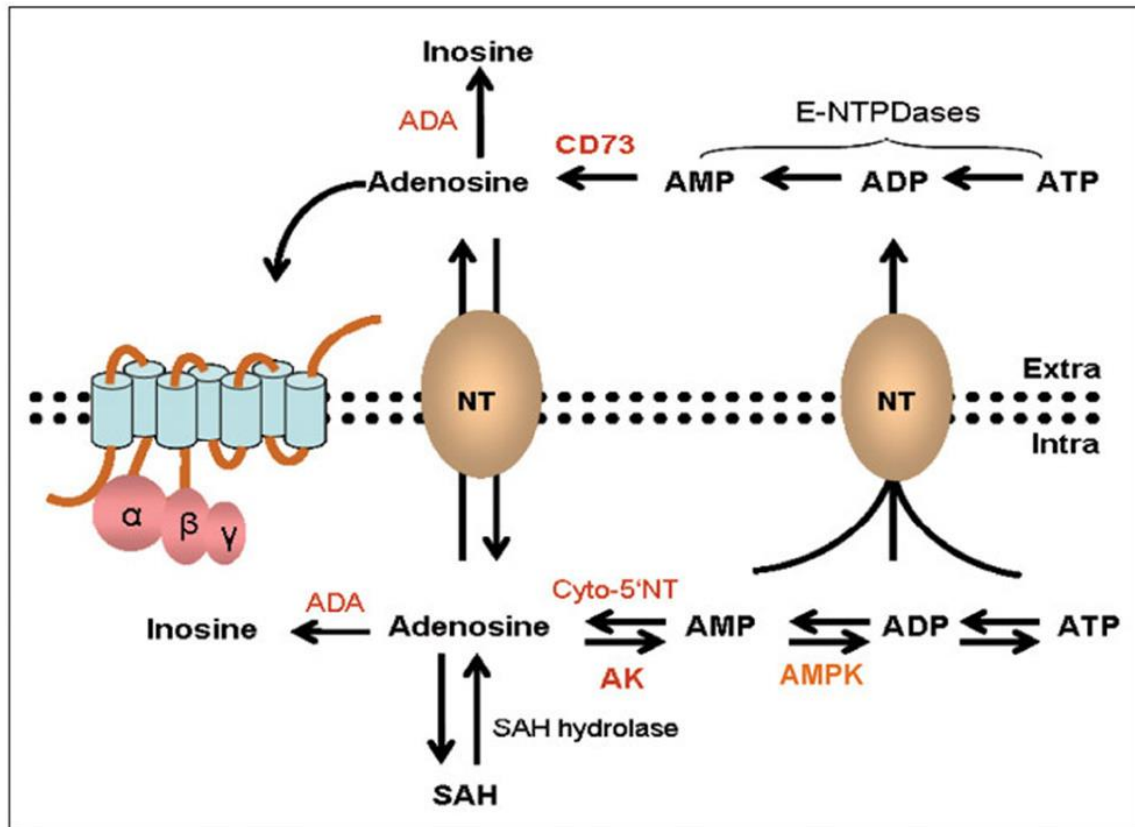


Figure 1.4: Ado synthesis, metabolism, and transport.

In addition to equilibrative transporter-proteins, a few tissues present Na^+ -dependent concentrative nucleoside transporters (CNTs), able to maintain high concentration of Ado by exchanging against gradient.⁵⁰ These transporter-proteins have been recognized in brain macrophages (microglia), thymocytes, liver, lung, choroid plexus, kidneys, and intestine.⁵¹ Their activity may vary upon interaction with medications or with decrease of body temperature⁵².

At the extracellular level, Ado is produced by consecutive dephosphorylation of adenine nucleotides, for example, ATP, mediated by a number of ectoenzymes, such as the apyrase (E-NTPDase1 or CD39) and the 5'- nucleotidase (CD73), found on the cell surface of numerous tissues. The CD73-mediated dephosphorylation which converts extracellular AMP to Ado is a rate restricting step of the nucleoside production⁵³. The whole catalytic pathway is achieved within a hundred milliseconds.

The metabolism of Ado is mostly controlled by two enzymes: Ado deaminase (ADA) and Ado kinase (AK). ADA works at high amount of substrate by converting Ado to inosine. ADA is found both in intra and extra cellular level where it is attached to the layer and takes part in the degradation mechanism of extracellular Ado⁵⁴. AK, at contrary, works at low amount of substrate changing Ado to AMP.

Because endogenous amount of Ado, as referenced above, is in the order of nanomolar, it is reasonable to access that certainly, under physiological conditions the fundamental catabolic pathway of Ado is the phosphorylation lead by AK, while the activity of ADA rise up in conditions inducing an increase of Ado, for example, during an ischemic episode⁵⁵.

3.3 Adenosine receptors

Ado achieves its functions by interfacing with specific membrane receptors coupled to G proteins (GPCR), known as ARs. ARs are classified as P1 purinergic receptor family. Up until now, four diverse receptor subtypes have been identified. According to their chronological discovery they are named A₁, A_{2A}, A_{2B}, and A₃ (Fig. 1.5).

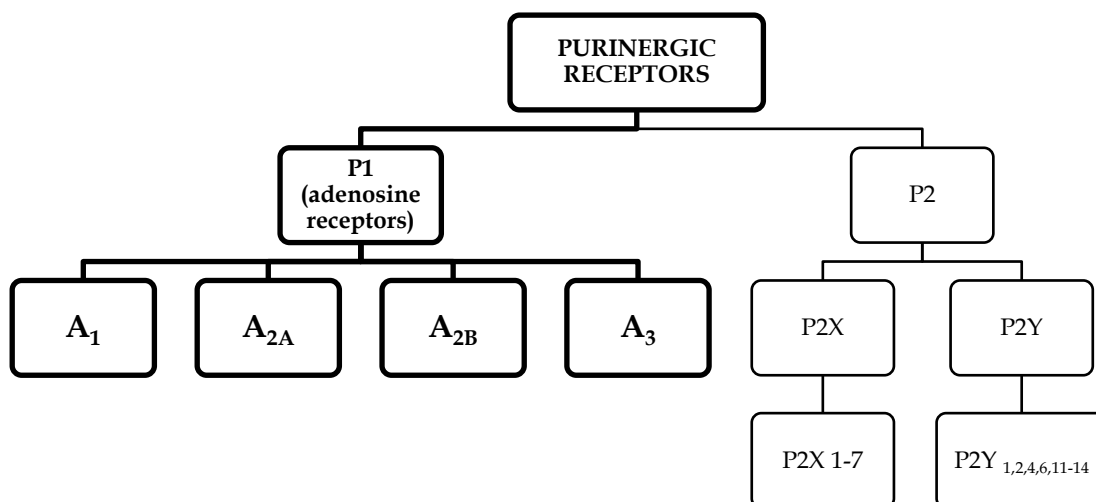


Figure 1.5: Classification of purinergic receptors.

P1 receptors were firstly divided only into A₁ and A₂ subtypes. This division was based on their capacity to repress or to activate the adenylate cyclase (AC)⁵⁶. Later on, the A₂ subtype was additionally studied and further characterized by Daly et al⁵⁷ describing them, on the base of

higher or lower affinity for Ado, in two subtypes: A_{2A}, which has higher affinity for the Ado (0.1-1.0 μM), and A_{2B}, having low affinity for the Ado (> 10 μM). A₃AR was the latest to be discovered in 1991 by recognizable proof of the rat cDNA sequences encoding a receptor coupled to regulatory proteins (G proteins) utilizing a polymerase chain reaction (PCR). Subsequently, Zhou and *et al*⁵⁸, reported that one of these sequence had high homology with AR subtypes A₁ and A_{2A}. However, unlike to others AR subtypes which have present high homology among the different species, the "newfound" receptor demonstrated a moderately low sequence homology between the rat and human subtypes⁵⁹. Furthermore, the "newfound" receptor demonstrated a difference binding with antagonists⁶⁰. The classification of P1 receptors has been affirmed with molecular cloning studies allowing the expression of the four receptor subtypes.⁴² ARs are found on the membrane of various cell types in the CNS, for example, neurons and glial cells⁶¹. At peripheral level they are found on the cells of the vascular smooth musculature, in platelets, lymphocytes, monocytes, macrophages, neutrophils, basophils, eosinophils, mast cells, lungs, heart, bladder and in immune tissues⁶².

3.4 Structure of the adenosine receptors

ARs are metabotropic receptors coupled to G proteins (Fig. 1.6). GPCRs are integral membrane proteins fundamentally made up of a single polypeptide chain that crosses 7 times the plasma membrane and having an extracellular N-terminal domain and an intracellular C-terminal domain. The seven transmembrane domains (TM1-7) are sorted out in an α -helix structures, each comprising from 20-27 hydrophobic amino acids, associated together by three intracellular loops (IL1-3) and three extracellular loops (EL1-3). Two cysteine amino acid residues (one interface TM3/EL1, and the other in EL2), forming a disulfide connect, are essential for the right folding of the protein⁶³.

ARs vary essentially in the domain length of the N-terminus, the C-terminus domain, as well as in the intra and extra cellular loops. Every one of these domain gives explicit properties to every AR subtype deciding explicit ligand selectivity profiles. The N-terminal area contains N-glycosylation sites having a key role in the right distribution of the receptor in the cell, whereas the C-terminal area has serine and threonine residues, phosphorylation sites for protein kinase implicated in the receptor desensitization⁶⁴.

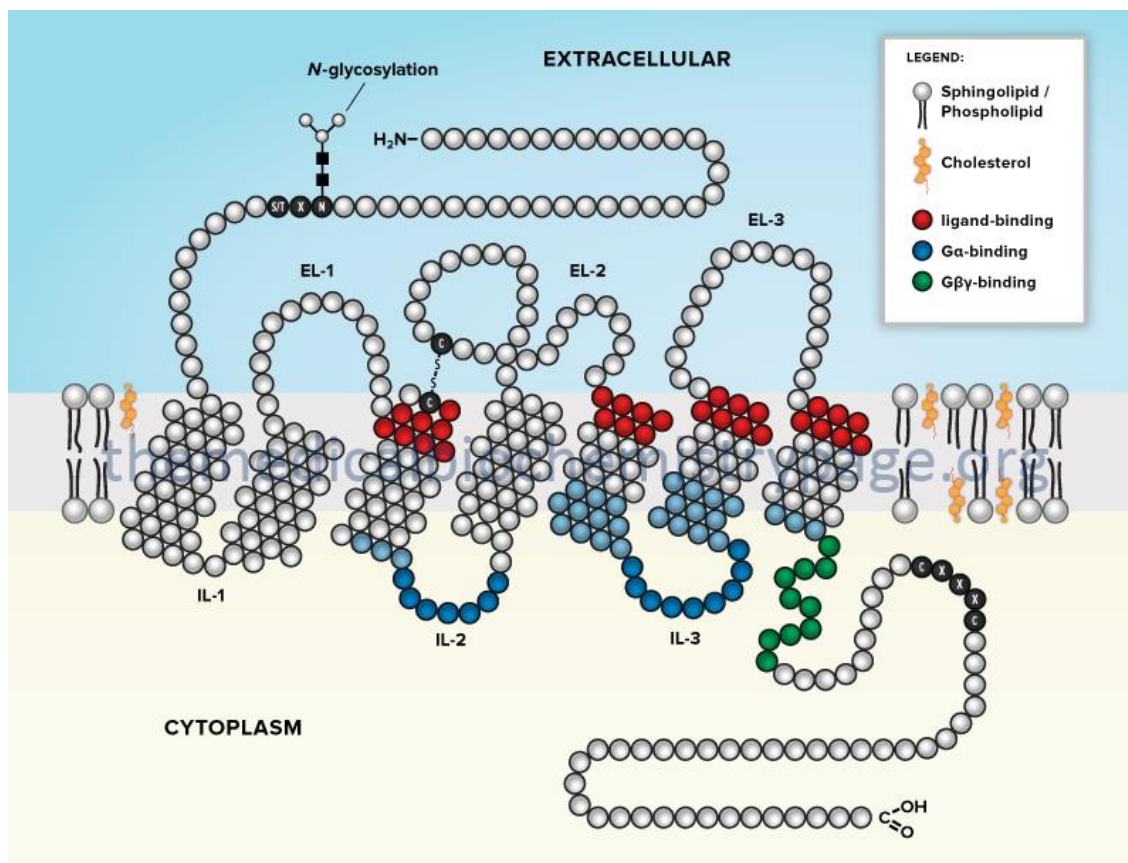


Figure 1.6: Structure of GPCRs.

The C-terminal tail of A₁, A_{2B}, and A₃ ARs has a conserved cysteine residue which might be a palmitoylation site, permitting the arrangement of a fourth IL. ARs are among the littlest members of the GPCR family. Human A₁, A_{2B}, and A₃ are made up of 326, 328, and 318 amino acids, respectively, while A_{2A} subtype with its 410 amino acids has a more extended C-terminal tail. The additional properties of this more extended C-terminal tail is that it contains the binding site of accessory proteins⁶⁵.

Additional information about the structure of A_{2A} subtype was provided in 2008 thanks to the crystal structure of the A_{2A} antagonist ZM241385 bound with A_{2A}AR⁶⁶ (Fig 1.7). In the following years A_{2A} subtype was also crystallized with A_{2A}AR agonists UK 432,097⁶⁷, 5'- N-ethylcarboxamidoAdo (NECA), CGS 21680⁶⁸ and Ado⁶⁹.

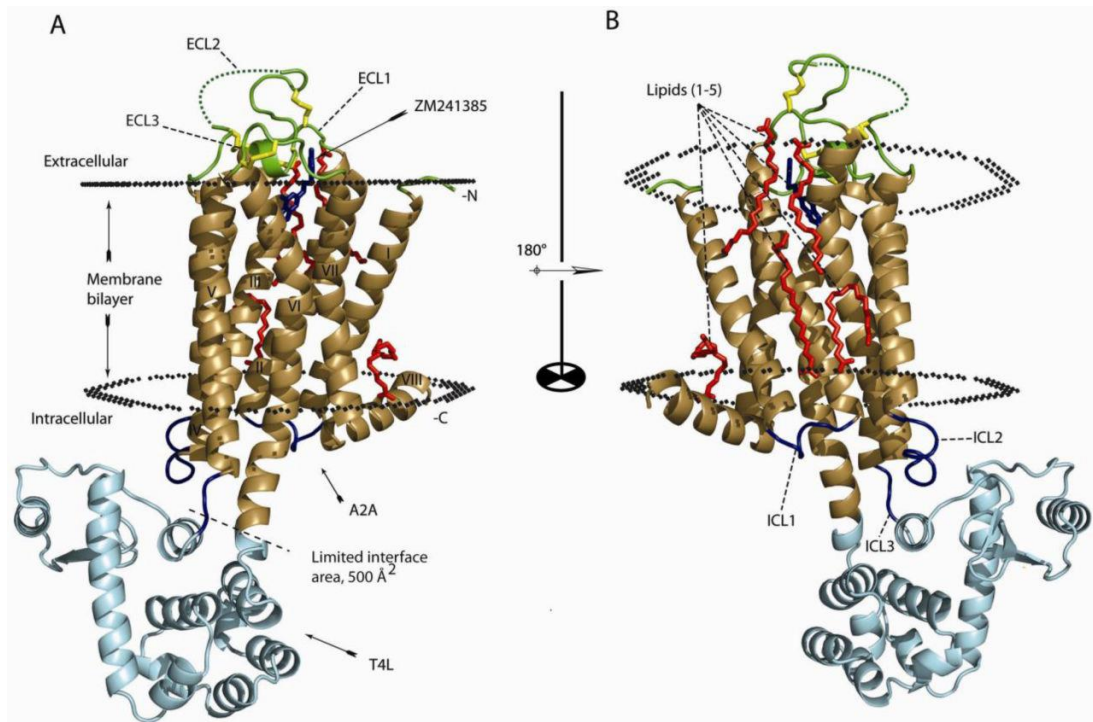


Figure 1.7: Structure of the antagonist ZM241385-bound A_{2A}AR.

Prior to the discovery of the crystal structure, the primary prediction strategy used for ARs was the homology modelling in which the receptor model was made according to the crystallographic structure of rhodopsin and mutagenesis studies.

The principle distinction of binding mode between AR agonists and AR antagonists reside on the ability of the agonist to establish hydrogen bonds between its hydroxyl groups of the ribosyl moiety with Ser277 (7.42) and His278 (7.43) residue of the AR (Fig. 1.8). In fact those hydrogen bonds allow the pulling of the extracellular end of TM3, TM5, and TM7, and this pulling has been suggested to be essential for the activation of the receptor. Moreover, because of the existence of hydrogen bond donors in the ribose moiety, amino acids Val84 (3.32) and Trp246 (6.48) could considerably move from their positions inducing like this a change that seems, critical for the accomplishment of the conformation vital for receptor activation.

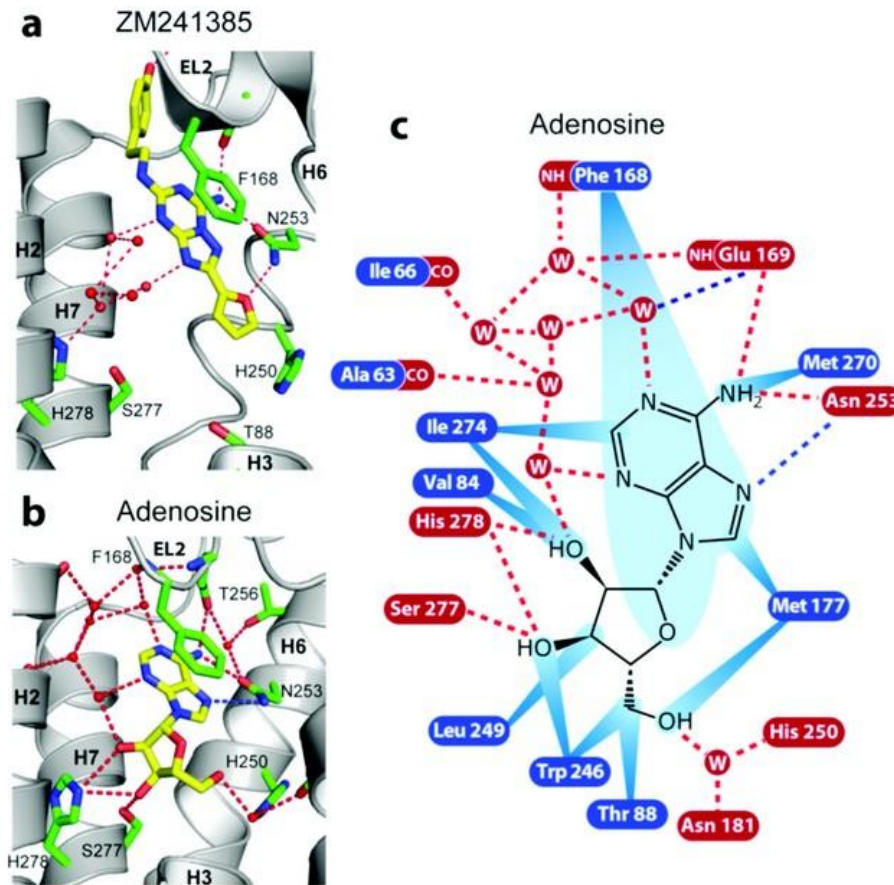


Figure 1.8: Interactions between the human A_{2A} AR and a) ZM 241385 and b) Ado. The interactions between the receptor and Ado c) are shown as red dotted lines (hydrogen bonds), blue dotted lines (polar interactions), and blue rays (van der Waals interactions).

3.4 Signal transduction

The presence of GPCRs on the outer part of the cell membrane, allows them to transduce many extracellular signals into the cells. This happens through the activation of at least one heterotrimeric G proteins situated on the cytoplasmic side of the membrane when an agonist binds to the extracellular domain of receptor followed by the interaction with different effector systems, for example, ion channels, phospholipase, and adenylyl cyclase (AC).

G proteins are made up of three subunits: α , β , and γ . At least 20 subtypes of the α subunits, 7 subtypes of the of β subunits and 12 subtypes of the γ subunits are known in humans. According to actions of the functional subunit α , we can recognize the following diverse G proteins: G_s (stimulating the AC), G_i (repressing AC), G_q (activating phospholipase C, PLC),.

A_1 and A_3 ARs are generally coupled to inhibitory G proteins (G_i) whereas A_{2A} and A_{2B} subtypes are coupled to stimulatory G protein (G_s) (Fig. 1.9).

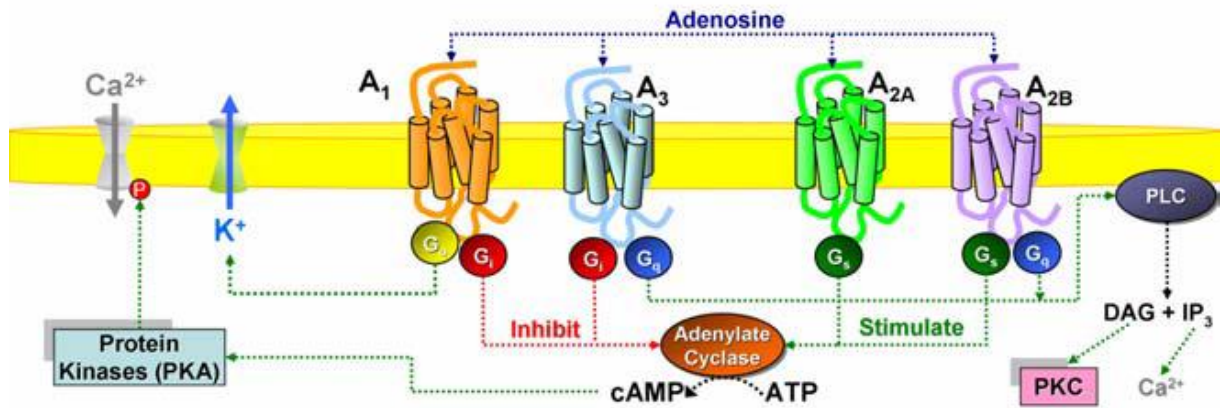


Figure 1.9: Schematic representation of the signal transduction pathways associated with ARs.

The G protein in the latent state is a trimer, with the α -subunit bound to guanosine diphosphate (GDP- $\alpha\beta\gamma$). When an agonist comes to interact and activates the receptor, there is a conformational change allowing the receptor to interact with the G protein. The conformational change is followed by the separation of GDP from $\alpha\beta\gamma$ allowing the formation of a vacuum transition state ($\alpha\beta\gamma$). Then transition state ($\alpha\beta\gamma$) interacts with guanosine triphosphate (GTP) to build up GTP- $\alpha\beta\gamma$. The complex GTP- $\alpha\beta\gamma$ triggers a conformational change which induces the activation and separation of the protein from the receptor. At this point the activated G protein separates into two components: the complex GTP- α and the dimer $\beta\gamma$, which activate the effectors of the signal transduction. The endogenous GTP-ase activity of the α -subunit, in the complex GTP- α , hydrolyses GTP to GDP. The hydrolysis results to reconstitution of the initial GDP- $\alpha\beta\gamma$ complex which can therefore interact with another GPCR when activated by an agonist (Fig. 1.10). Antagonists prevent the separation of GDP from the GDP- $\alpha\beta\gamma$ complex and by consequent they hamper the G protein activation.

The primary effectors in charge of the generation of second messengers are the two following enzymes: AC, in charge for the production of cAMP and PLC, the enzyme in charge of the production of inositol triphosphate (IP₃) and diacylglycerol (DAG).

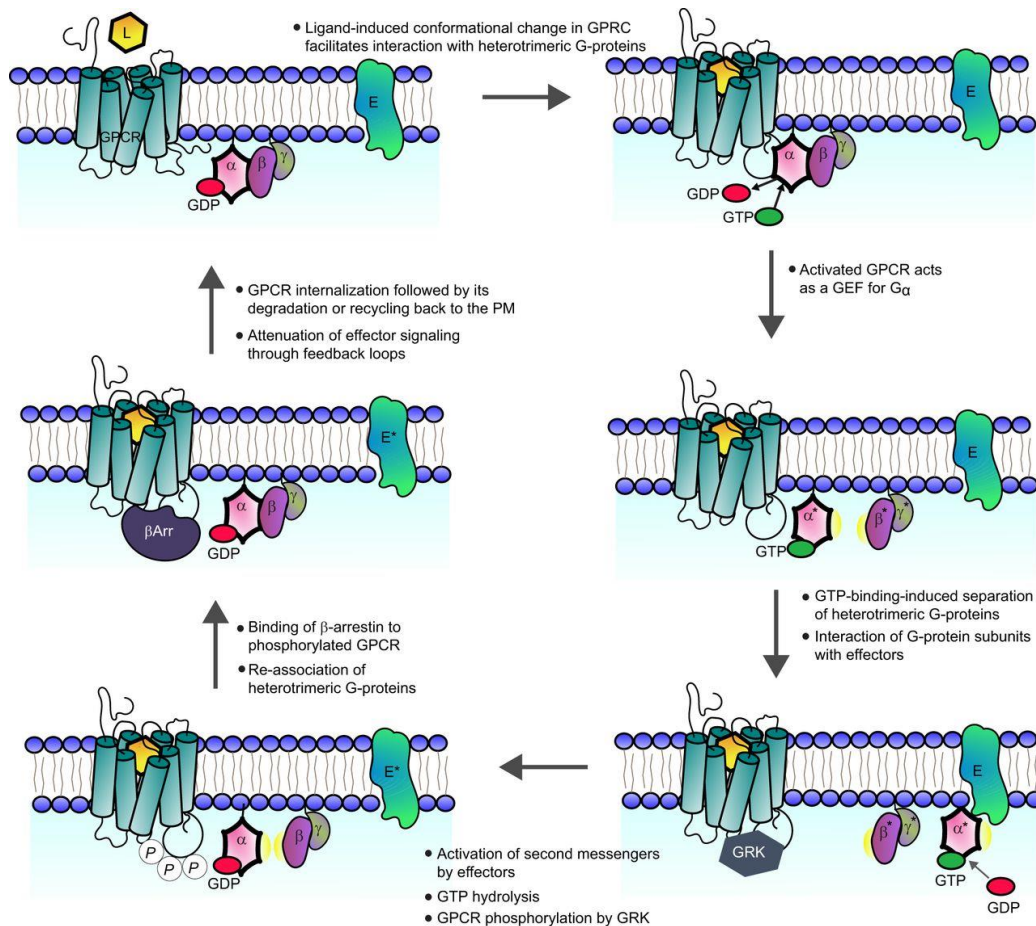


Figure 1.10: The activation mechanism of G proteins.

Even though the fundamental way of signal transduction for all ARs is through the interaction with G proteins, there are noticeable differences in signal transduction among the four ARs.

3.5 Adenosine receptor subtypes

3.5.1 A₁AR

The A₁AR subtype was purified, cloned and sequenced in various species including human species. Although there were featured contrasts in G protein-coupling as well as a species-dependent tissue distribution, a considerable homology has been found among the A₁AR subtypes of different species. The gene which guarantees the existence of the A₁AR subtype in human species is found on chromosome 1q32 and encodes a protein of 326 amino acids, with a molecular weight of about 36.7 kDa⁶³.

A₁AR subtype is generally distributed but mainly expressed in the CNS in pre-and postsynaptic sites on neuronal membranes. Large amounts of A₁ARs are expressed in the cerebral cortex,

hippocampus, cerebellum, thalamus, the spinal line and fat tissue. Moderate expression is found in skeletal muscle, liver, kidney, salivary organs, throat, colon, eyes, in the sinoatrial and atrioventricular hub of the heart, in the cave of the stomach and in the testicles. Relatively lower expression is notice in the lungs, ventricles and pancreas.⁷⁰

About the signal transduction, A₁ARs are essentially coupled to G proteins which belong to G_{i/q} family⁷¹ and many are the signal transduction pathways which have been attributed to this receptor subtype. Some of them are listed below:

- inhibition of AC with a subsequent decline of cAMP⁷² levels followed by phosphorylation of various target proteins by cAMP-dependent protein kinase (PKA)
- activation of PLC with a subsequent increment in the generation of IP₃, DAG, and accumulation of Ca²⁺ from intracellular stores contributing to the activation of protein kinase C (PKC), phospholipase A₂ (PLA₂), and nitric oxide synthase (NOS)⁷³ ;
- activation of various K⁺ channels through coupling with G proteins having a place in G_o family.

Through those signal transduction pathways, A₁ARs modulates many responses in various systems of the organism. Their stimulation causes:

- in the CNS: a decrease of transmitters release, sedation, anticonvulsant impacts, anxiety, locomotor-depressants⁷⁴;
- in metabolic systems: there is an antilipolytic effect and an increase insulin sensitivity⁷⁵;
- in the gastrointestinal tract: there is an inhibition of chloridric acid production;
- in the renal system: a decrease in glomerular filtration rate (GFR), an inhibition of renin release, an antidiuretic effect and a supply route vasoconstriction;
- in the cardiovascular system: a negative inotropic effect, negative chronotropic effects, negative dromotropic effects, negative bathmotropic effects and cardioprotection⁷⁶.

3.5.2. A_{2A}AR

The first in all crystallographic structure of A_{2A}AR was resolved in 2008.⁶⁶ The gene which guarantees the existence of this subtype in human species is found on chromosome 22 and encodes a protein of 410 amino acids⁷⁷ with a molecular weight of 45 kDa⁷⁸. The A_{2A}AR is found at central level in dopamine-rich regions, for example, in the striatum⁷⁹, nucleus accumbens, olfactory tubercle, and in the Purkinje cells of the cerebellum. At peripheral level they are plenty in endothelial cells, platelets, lymphocytes, monocytes, macrophages, neutrophils, basophils, eosinophils, pole cells, lungs, heart, bladder, and immune tissues^{33,80}.

A_{2A}AR is linked by the II and III intracytoplasmic loops to Gs proteins at the peripheral level and to Golf at the CNS level, both stimulating AC. The stimulation of AC induces an increase of intracellular amount of cAMP⁸¹. Then the high amount of intracellular cAMP induces the activation of PKA. The activated PKA can then activate different receptors, ion channels, phosphodiesterases and cAMP-managed phosphoprotein (CREB, cAMP responsive element binding protein), critical for numerous neuronal capacities. The activities of the A_{2A}AR are very huge because it is sometime co-localized or being sometime physically connected with other GPCRs, for example, the formation of heterodimers with the D₂ dopaminergic receptor (D₂/A_{2A}AR)⁸², with CB1 cannabinoid receptor (CB1/A_{2A}AR)⁸³, and with mGluR5 glutamate receptor (mGluR5/A_{2A}AR)⁸⁴, and heterotrimers (CB1/A_{2A}AR/D₂)⁸⁵.

The A_{2A}AR is particularly implicated in the modulation of vasodilation; it stimulates the synthesis of new blood vessels, and preserves tissues from collateral damage of inflammatory process. In the brain, A_{2A}AR indirectly impact the activity of the basal ganglia.

Additional mechanism mediated by A_{2A}AR includes:

- in the CNS: stimulation of the sensory nerve and synergistic repression of D₂;
- in the immune system: repression of polymorphonuclear leukocytes, repression of the discharge pro-inflammatory cytokines (TNF, IL-6, IL-8, and IL-12)⁸⁶, and activation of the discharge of inflammatory cytokines (IL-10);
- in the cardiovascular system: repression of platelet aggregation.

3.5.2.1 Interaction between A_{2A}AR and the dopamine D₂ receptor

Strong experimental proof shows that the A_{2A}AR subtypes interacts in an extremely broad way with dopaminergic receptors at the level of the basal ganglia. A_{2A}AR and D₂ receptors are co-localized in the membrane of the GABAergic striatopallidal neurons. This co-localization provides anatomical basis for the existence of functional association between these two receptors, moreover it has been broadly proved that activation of A_{2A}ARs enhance the functionality of striatopallidal neurons, due to the decrease of D₂ receptor activity⁸⁷. This co-expression of A_{2A}AR and D₂ receptors on neurons of the striatum and pallidum gives the anatomical premise to the presence of a practical association between these receptors. Furthermore, the impact of excitatory neurons in the striatum and pallidum applied by Ado upon A_{2A}AR is due somehow to their antagonistic effect on the activation of D₂ receptors by dopamin⁸⁸. Additional biochemical studies performed in rat striatal tissue, in human, and in various cell lines, have brought additional information about the A_{2A}AR/D₂ interaction since it

has been shown that activation of A_{2A} ARs diminishes the affinity of D_2 receptors for dopamine binding.⁸⁹ These impacts are related with the formation of heterodimeric complexes between the two receptors⁹⁰. The interaction existing between the A_{2A} AR and D_2 receptors is extended even at the second messenger level because, whereas the activation of D_2 receptors represses AC, the activation of A_{2A} ARs stimulates AC (Fig. 1.11)⁷³.

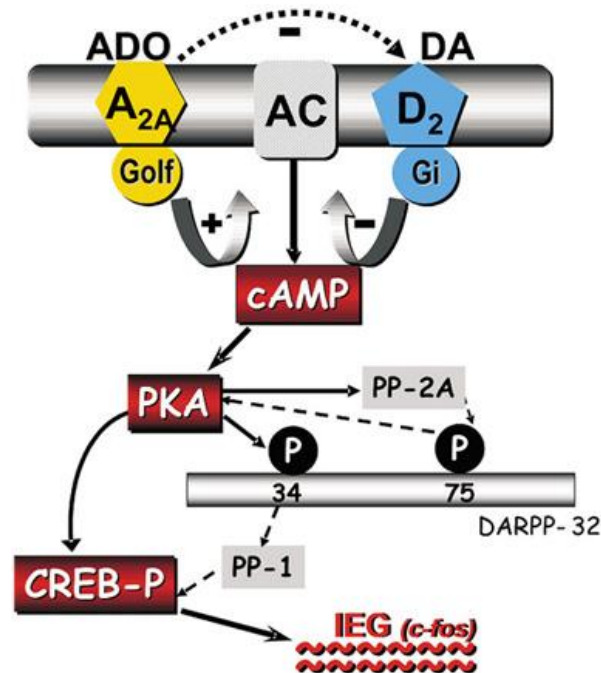


Figure 1.11: Interactions between A_{2A} AR and D_2 receptors. The two receptor subtypes exert opposite regulatory activity on the AC, which is inhibited by D_2 receptors and stimulated by A_{2A} AR.

Moreover, it has been demonstrated that the activation of A_{2A} AR can repress the Ca^{2+} -dependent reactions mediated by the D_2 receptor^{74, 90}.

It has been demonstrated also that A_{2A} ARs can influence the function of the D_1 receptors. Hence, it has been seen that administration of A_{2A} AR antagonists can enhance both the behavioral and neurochemical effects induced by iactivation D_1 receptor in the rat.⁹¹ Because A_{2A} AR and D_1 receptors are located on various neuronal populations,⁹² it is reasonable to suggest that, the interaction between these receptors happens via the side fibers of the striatum or via circuits that incorporate subthalamic-nigro-cortico striatal projections. In mice missing the dopamine D_2 receptors, activation or blockade of A_{2A} ARs generates behavioral as well as biochemical effects, supporting the theory that the activity of A_{2A} ARs might be autonomous of dopamine⁹³.

3.5.3 A_{2B}AR

The gene which guarantees the existence of the human A_{2B}AR is found on chromosome 17p11.2-p12 and encodes a protein of 328 amino acids, with molecular weight of about 37.0 kDa⁶³. A_{2B}AR signal transduction initiates with activation of AC via a direct coupling with Gs protein resulting to an increment of cAMP levels; then the increase of cAMP levels induces a stimulation of P type Ca²⁺ channels as well as the activation of PKA which phosphorylates protein residues, treonine and serine, and stimulates gene transcription. Moreover, A_{2B}AR is known to be couple through Gq protein family, to a phosphatidylinositol-lipase protein C (PI-PLC) system promoting an increase of DAG, which stimulates PKC, and IP3, assembling intracellular Ca²⁺.

At first, it was believed that the expression of the A_{2B}AR was limited to organs like the bladder, bowel, lung, epididymis, vas deferens, spine, and brain. However, they were found later to be also present in fibroblasts⁹⁴, hematopoietic cells⁹⁵, mast cells⁹⁶, cells of the myocardium⁹⁷, muscle cells⁹⁸, and endothelium⁹⁹.

Large amounts of the A_{2B}AR expression were found in various parts of the intestinal tract and their activity on gastric mucosal cells has been investigated¹⁰⁰. There are also proofs supporting that the presence of A_{2B}AR on mast cells is implicated in inflammatory processes, for example, asthma¹⁰¹. These A_{2B}ARs on mast cells activate the human mast cells MHC-I and stimulate the release of IL-8.

Numerous investigations associate A_{2B}ARs with cardiovascular effects since their activation can regulate fibroblast proliferation¹⁰², heart recoveries, and illness such as hypertension or myocardial infarction¹⁰³.

Among different effects mediated by A_{2B}AR there are:

- in CNS: inhibition of nerve transmission, stimulation of IL-6 production in astrocytes;
- in gastrointestinal system: stimulation of chloridric acid production into the intestinal lumen.

3.5.4 A₃AR

The gene which guarantee the existence of the human A₃AR is found on chromosome 1p13.3 and encodes for a protein of about 318 amino acids, with a molecular weight between 36.0 to 37.0 kDa⁶³. In contrast with other ARs, the A₃AR has huge differences in structure, function and tissues distribution among species¹⁰⁴. These differences make especially complex the A₃AR signalling physiology specifically among rodents and primates. The activation of A₃AR induces the inhibition of the AC via the coupling with Gi protein, with then decreases the levels of

cAMP. This activation stimulates also PLC and phospholipase D (PLD), via the coupling with the Gq protein¹⁰⁵, and finally stimulates the release of inflammatory mediators (for example histamine from mast cells)¹⁰⁶.

A₃ARs are found with high density in the lungs, liver, and immune system cells like neutrophils, eosinophils, and T lymphocytes, while it is present in low density in other tissues like brain, heart, testes, and many others.

Via interaction with A₃ARs, Ado has a cerebral protective role. Elevated amounts of A₃ARs were found in eosinophil cells in the lungs of rat, where they promote the inhibition of the degranulation and the discharge of free superoxide anion radicals¹⁰⁷.

Anticancer properties have been also assigned to A₃ARs: in fact, their activation seems to repress the tumor development by modulating the Wnt pathway and by regulating NF-κB¹⁰⁸. In addition, the ability of A₃AR antagonists to decrease intraocular pressure is under study as potential therapeutic agents in the treatment of glaucoma¹⁰⁹. Other effects promoted by A₃ARs are:

- in the CNS: neuroprotection, sedative-hypnotic, anticonvulsant and anxiolytic effects, inhibition of exocytosis;
- in the cardiovascular system: anticoagulant and hypotensive effects.

4. Adenosine

4.1 Overview

In chapter 1, the discussion was made around ATP as cell energy source and ATP as signal molecule for P2 purinergic signalling. In this chapter, the attention is focused on the Ado, P1 receptors sub-family and therapeutic potential of Ado receptor ligands.

Introduction

Previously, the two major metabolic pathways of extracellular ATP were described. Until recently, damaged or dying cells were considered as the only source of extracellular ATP. However, the release of ATP induced mechanically from healthy cells is now also accepted as a physiological mechanism¹¹⁰. A well-known example of physiological release of extracellular ATP is the co-release of ATP and noradrenaline found in sympathetic nerves¹¹¹. Once in the extracellular compartment, ATP follows two main pathways, which are the modulation of P2 purinergic signalling (details in the chapter one) and the production of Ado through cascade of enzymatic processes catalyzed by ectonucleotidases. In fact, both ATP and ADP are hydrolyzed to AMP by a subtype of ectonucleotidases known as ectonucleoside triphosphate diphosphohydrolase1 (NTPDase1), which is abbreviated CD39 for simplicity. The obtained AMP is further hydrolyzed to Ado by another subtype of ectonucleotidase known as ecto-5'-nucleotidase (5'NT) generally known as CD73³². Another important source of extracellular Ado is cAMP, which can be released from neurons and then converted into Ado in two steps: that is conversion of cAMP to AMP by extracellular phosphodiesterases followed by the conversion of AMP to Ado by CD73⁴². Extracellular Ado produced either from ATP or cAMP or constitutes the signal molecule for the P1 purinergic receptor signalling, which modulates several physiological and pathological conditions. In order to address the therapeutic potential of Ado, we will discuss in more details Ado, P1 purinergic receptors sub-family, and ligands for adenosine receptors (ARs) that are agonists, antagonists and allosteric modulators.

4.2 Production, metabolism and physiological role of adenosine

Ado (6-amino-9- β -D-ribofuranosyl-9H-purine) is an endogenous nucleoside ubiquitous in humans and other species. The structure of Ado is constituted from adenine and D-ribose, which are linked together with a N9 β -glycosidic bond (shown in figure 1.12). Ado plays a vital role in the body since it regulates the function of almost all tissues and constitutes a key component in the composition of many biomolecules such as ATP, RNA, NADH, etc¹¹².

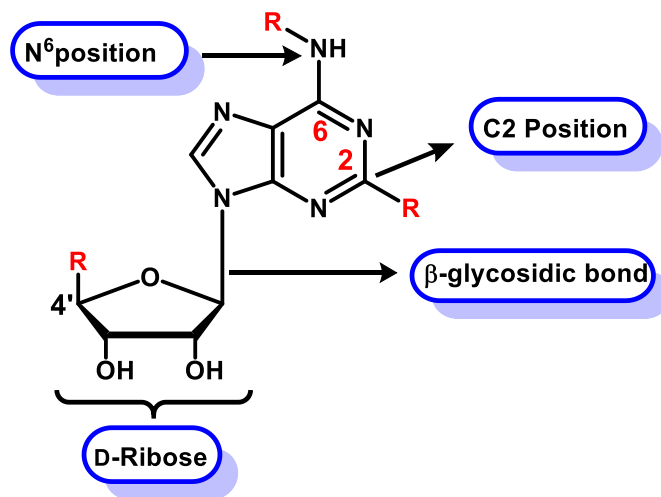


Figure 1.12: Structure of adenosine

4.2.1. Production

While extracellular Ado is produced by the enzymatic hydrolysis of ATP, the intracellular Ado is produced by the hydrolysis of adenine nucleotides¹¹³ and it can be also synthesized de novo during purine biosynthesis¹¹⁴.

4.2.2. Metabolism

Both intracellular and extracellular Ado are metabolized. In fact, after production, Ado modulates the function of many systems including CNS, cardiovascular system, immune system. Extracellular Ado is responsible for its physiological effects. Hence, to obtain a sufficient extracellular amount of Ado, intracellular Ado is transported across the cell membrane by the help of transporters¹¹⁵. After the extracellular Ado has achieved its modulator function, it is metabolized mainly in two pathways: the first one being the conversion to inosine by Ado deaminase. This catabolic process happens in erythrocytes and in vascular endothelial cell because they are the site where extracellular Ado is transported for metabolism and the second one the reuptake of extracellular Ado back into intracellular space where it is reconverted to AMP by adenosine kinase¹¹⁶. Figure 1.13 reports the production and metabolism of Ado.

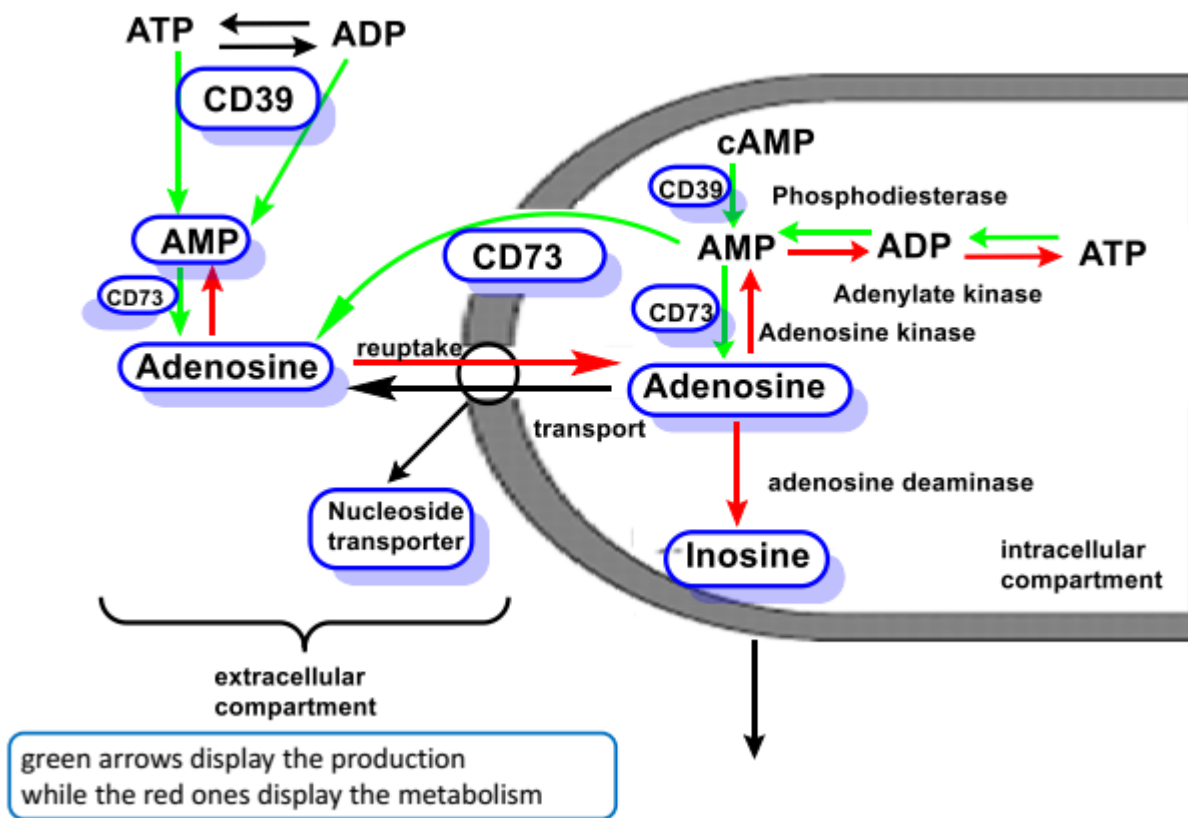


Figure 1.13: Production and Metabolism of Adenosine

4.2.3 Physiological role

The physiological role of Ado was reported for the first time early in the years 1900s by Drury and Szent-Györgyi who described the powerful vasodilator effect of Ado³³. From these preliminary evidences, subsequent studies were conducted by Sattin and Rall which later demonstrated that Ado was able to increase the formation of cAMP in the CNS³⁴. Thus following the same interest that is providing more understanding of Ado effects, many others studies have been carried out and Ado is now known to control and integrate a wide range of brain functions including regulation of sleep, locomotion, anxiety, cognition and memory¹¹⁷. The protective response of Ado during ischemia, hypoxia and inflammation has been also reported^{118,119,120,121}. These well described physiological effects are the results of the interaction of Ado with four receptors subtype belonging to P1 purinergic receptors sub-family, which are discussed in the next section.

5. Adenosine receptors

Ado is the only endogenous ligand for P1 purinergic receptors sub-family. In fact, P1 purinoreceptors are composed of four metabotropic receptor subtypes known as Ado receptors (ARs). The four subtypes of ARs have been identified and cloned from several species including rat, dog, mouse, and human. According to their chronological discovery, ARs are classified as A₁, A_{2A}, A_{2B} and A₃¹²². Table 1.6 described ARs more in details.

Table 1.6: ARs receptor subtypes.

Receptor Subtype	Localization	Signal transduction	Pharmacological implication
A₁AR	Neocortex, cerebellum, hippocampus, dorsal horn of the spinal cord, sinoatrial and atrioventricular node of the hear ¹²³	Inhibition of adenylate cyclase and also phospholipase C activation ¹²⁴	Heart diseases and neurodegenerative conditions ¹²⁵
A_{2A}AR	Pre and postsynaptic nerve terminals , on mast cells, airway smooth muscle and in circulating leukocytes ¹²⁶	Stimulation of A _{2A} AR leads to the activation of adenylate cyclase resulting to the elevation of intracellular cAMP ¹²⁶	Heart diseases, inflammatory conditions and neurodegenerative disorders e.g Parkinson's disease ¹²⁴
A_{2B}AR	Highly expressed in gastrointestinal tract, bladder, lungs and on mast cells ¹²³	Stimulation of adenylate cyclase and phospholipase C through activation of Gs and Gq proteins, respectively ¹²⁶	Possible role in the pathogenesis of inflammatory airways disease ¹²⁷
A₃AR	Kidney, testis, lung, mast cells, eosinophils, neutrophils, heart and the brain cortex ¹²⁷	Inhibition of adenylate cyclase and also stimulation of phospholipase C and D inducing a release of calcium ¹²⁸	linflammatory conditions including asthma ¹²⁷

6. Adenosine derivatives: agonists, antagonists and allosteric modulators.

6.1 Adenosine Receptor Agonists

The unselective action of Ado itself on ARs and its low half-life (~1s) and its limited the pharmacological use of it and forced the development of agonists with better profile⁴² (more stable and more selective). Most of the discovered AR agonists possess a structure similar to the endogenous ligand Ado. Structure–activity relationships (SARs) of them revealed that:

- substitution at the N⁶ position with certain alkyl, cycloalkyl, and arylalkyl groups increases selectivity for the A₁AR;
- substitution with an N⁶-benzyl group or substituted benzyl group increases selectivity for the A₃AR;
- substitution at the C2 position, especially with ethers, secondary amines, and alkynes, often results in high selectivity for the A_{2A}AR, but sometimes also for the A₃ARs.

Hence, most AR agonists are nucleoside derivatives similar to the natural ligand Ado, some exceptions have been reported to be represented by non-nucleoside structures consisting by substitute nitrogen heterocyclic derivatives¹²⁹. Among them Capadenoson (BAY 68–4986, Fig 1.14), a pyridine-3,5-dicarbonitrile derivative is in clinical trials for the oral treatment of stable angina. Its therapeutic potential is attributed to the selective activation of A₁AR^{130,131}.

Figure 1.14 discloses the structure of some ARs agonists.

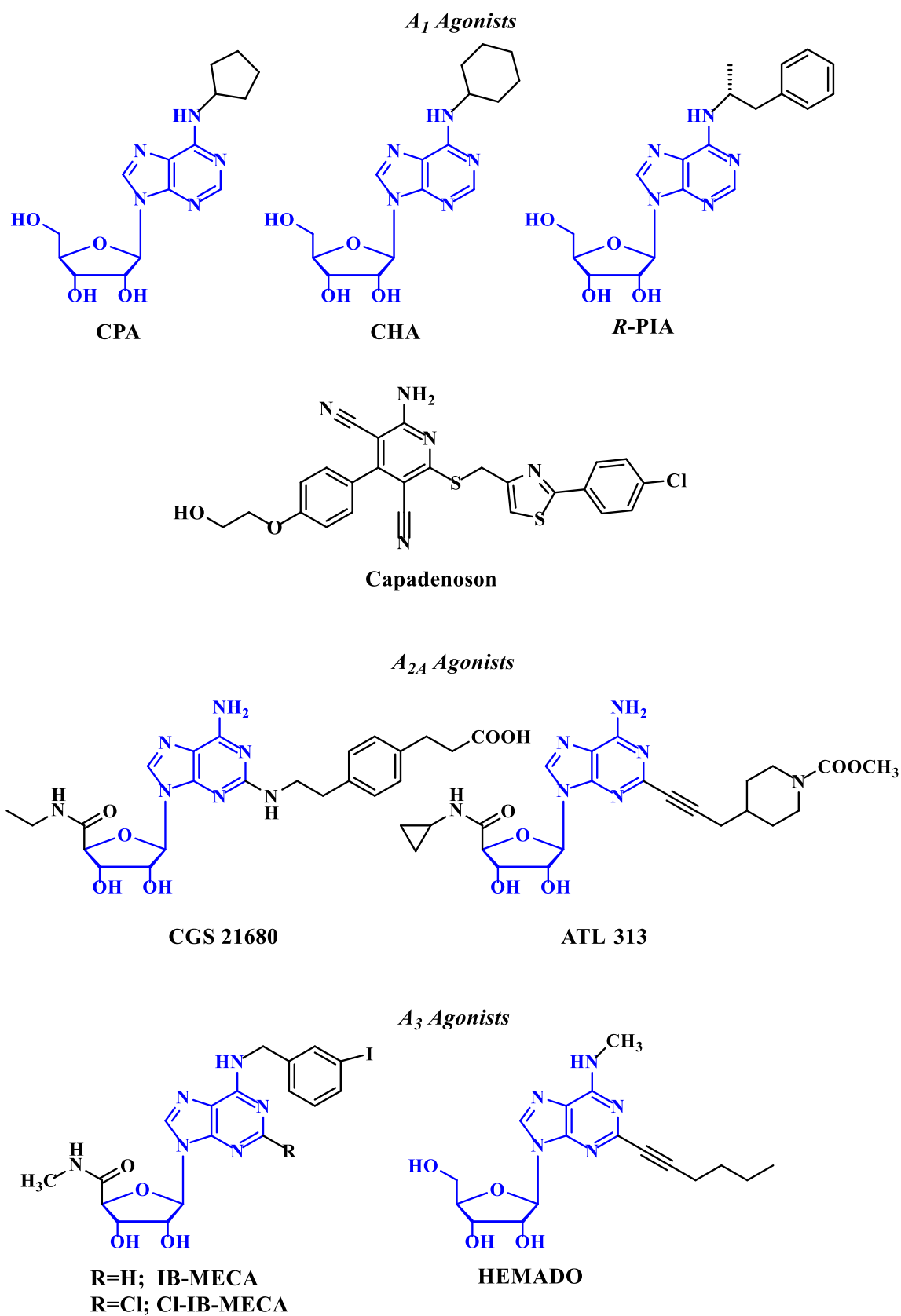


Figure 1.14: Example of Ado receptors agonists.

6.2 Adenosine Receptor Antagonists

The chemical structure of Ado receptor antagonists varies widely respect to that of agonists. Purine derivatives including both xanthine and adenine analogues, constitute the basic structure of almost all antagonists.

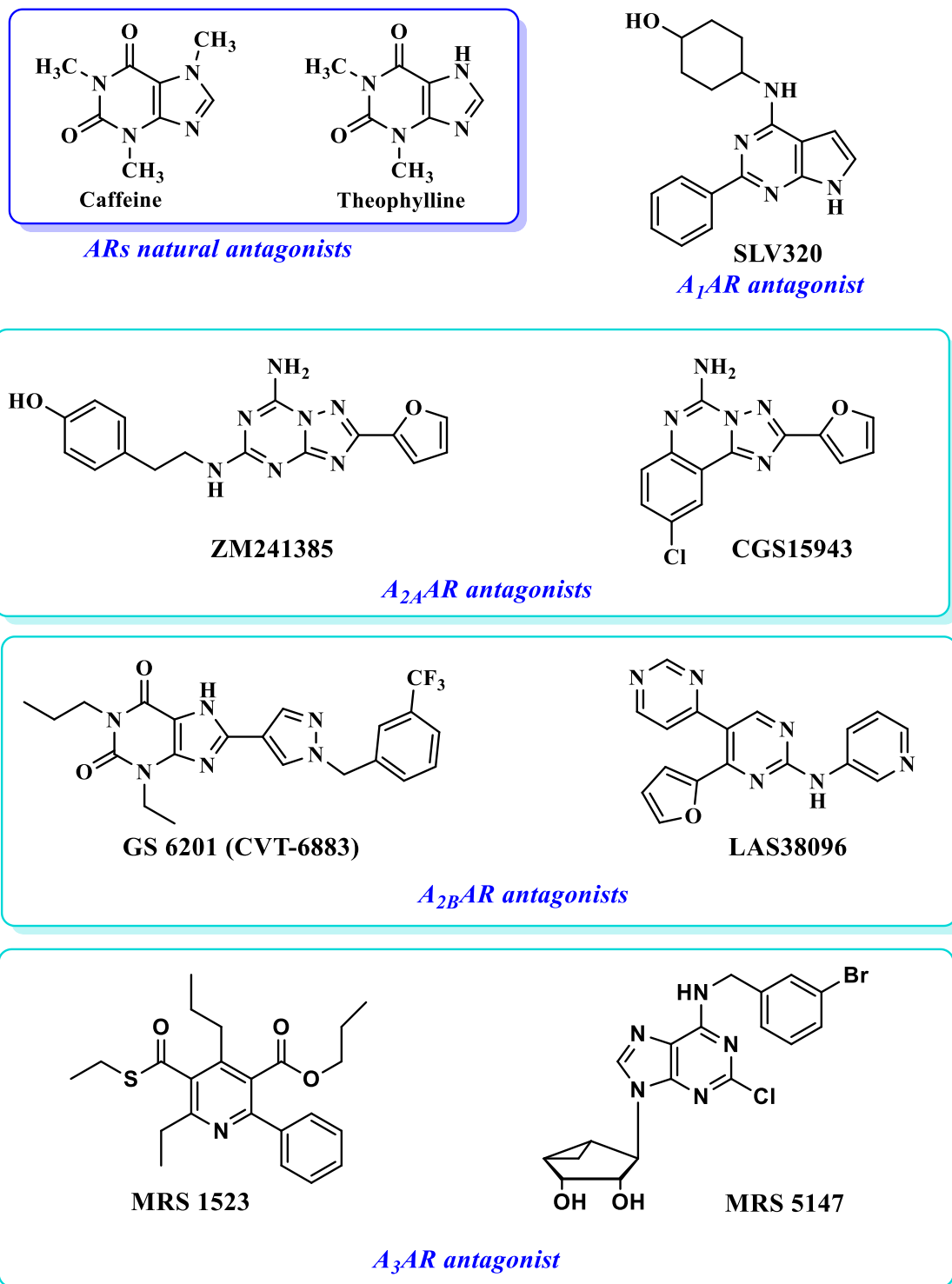


Figure 1.15: Example of Adenosine receptors antagonists¹³².

However in addition to xanthine and adenine analogues which have contributed a lot to the development of promising therapeutic candidates, different scaffolds are now commonly used for the synthesis of AR antagonists^{133, 134}. The compounds of these new series have a better selectivity profile and are chemically more diverse than the classical 1,3-dialkylxanthines, which have been used for long in pharmacology as AR antagonists⁵³. Figure 1.15 discloses the structure of some AR antagonists.

6.3 Allosteric modulators for adenosine receptors

Among the G-proteins coupled receptors (GPCRs), class A or rhodopsin-like receptors to which belong ARs (A_1 , A_{2A} , A_{2B} and A_3) are suggested to be allosterically modulated. Allosteric modulation indicates conformational changes of the receptor due to the binding of an allosteric agonist and which may affect the binding of the orthosteric ligand (which is either the endogenous ligand or the primary agonist). The allosteric agonist is a ligand able to mediate receptor activation on its own, by binding to a recognition domain on the receptor macromolecule distinct from the binding site of the orthosteric agonist or primary agonist. Although an allosteric modulator mediates receptor activation, it does not have any activity by itself, but it ‘needs’ the orthosteric ligand to show its action. Allosteric modulators can influence positively or negatively the action of orthosteric ligands¹³⁵. Historically, ARs are among the first GPCRs discovered to be allosterically regulated, thereby many lead compounds have been screened in order to identify allosteric modulators of all four subtype of ARs^{53, 136}. Some examples of allosteric modulators for ARs are discussed in the section below.

6.3.1 A_1 AR allosteric modulators

They were discovered during a screening of the library in a radioligand binding assay. In fact the authors observed that three of the screened molecules were increasing the binding of the agonist radioligand [3 H] N^6 -cyclohexyladenosine to A_1 AR in rat brain membranes. Further investigations about that enhancing characteristic were made and the results reported that, these three compounds were increasing agonist activity by slowing the dissociation of the agonist [3 H] N^6 -cyclohexyladenosine from the A_1 receptor. Therefore their mode of action was recognized as an allosteric mechanism of action. Interestingly the three compounds also appeared to behave as competitive antagonists at the same receptor. Therefore the concentration range within which the compounds enhance the effects of agonists was limited, in the 1–10 μ M range¹³⁷. Among these three compounds (PD 71,605, PD 81,723 and PD 117,975), PD 81,723 showed to be one of the

most potent, displaying the best ratio of enhancing antagonistic action. Hence PD 81,723 has been fully studied by many different research groups and represents today the reference allosteric modulator of A₁AR. PD 81,723 has been also extensively modified structurally by Baraldi *et al.* to afford analogues **2**, **4** and **6** which proved to be more potent than PD 81,723 and also has shown significant reduction of the cAMP content of CHO cells expressing human A₁AR^{138,139}. Figure 1.16 disclosures both the structure of the three PD compounds as well as the structure of PD 81,723 analogues.

6.3.2 A_{2A}AR allosteric modulators

Amiloride (Fig. 1.16) and analogues have been reported to allosterically inhibit A_{2A}AR antagonists. The mechanism of the allosteric inhibition of amiloride and analogues is the increasing of the dissociation rate of the antagonist from A_{2A}AR. An example of such class of molecules is the HMA, which has shown to increase the dissociation rate of [³H]ZM 241385 from the A_{2A}AR. Beside the HMA, which is one of the most potent A_{2A}AR allosteric inhibitors, recent studies carry out by Giorgi *et al.* have demonstrated that 1-[4-(9-benzyl-2-phenyl-9H-purin-6-ylamino)-phenyl]-3-phenyl-urea and 1-[4-(9-benzyl-2-phenyl-9H-8-azapurin-6-ylamino)-phenyl]-3-phenyl-urea (compound **29**, see Fig. 1.16) are allosteric enhancers on the A_{2A}AR antagonists since they slowed the dissociation of [³H] ZM241385 from the A_{2A}AR¹⁴⁰.

6.3.3 A_{2B}AR allosteric modulators

Allosteric modulators for A_{2B}AR have not been noted yet. In fact, till recently, no suitable commercial A_{2B}AR radioligands was available and thus the investigation of the allosteric modulator was not feasible. Today, even though the investigation of allosteric modulator for A_{2B}AR is now possible since the radiolabeled antagonist [3H] MRS1754 and other radioligands such as [3H]PSB603¹⁴¹ has been developed, no A_{2B}AR radiolabeled agonist is available and therefore development of allosteric enhancers of agonist is still hampered.

6.3.4 A_{3A}AR allosteric modulators

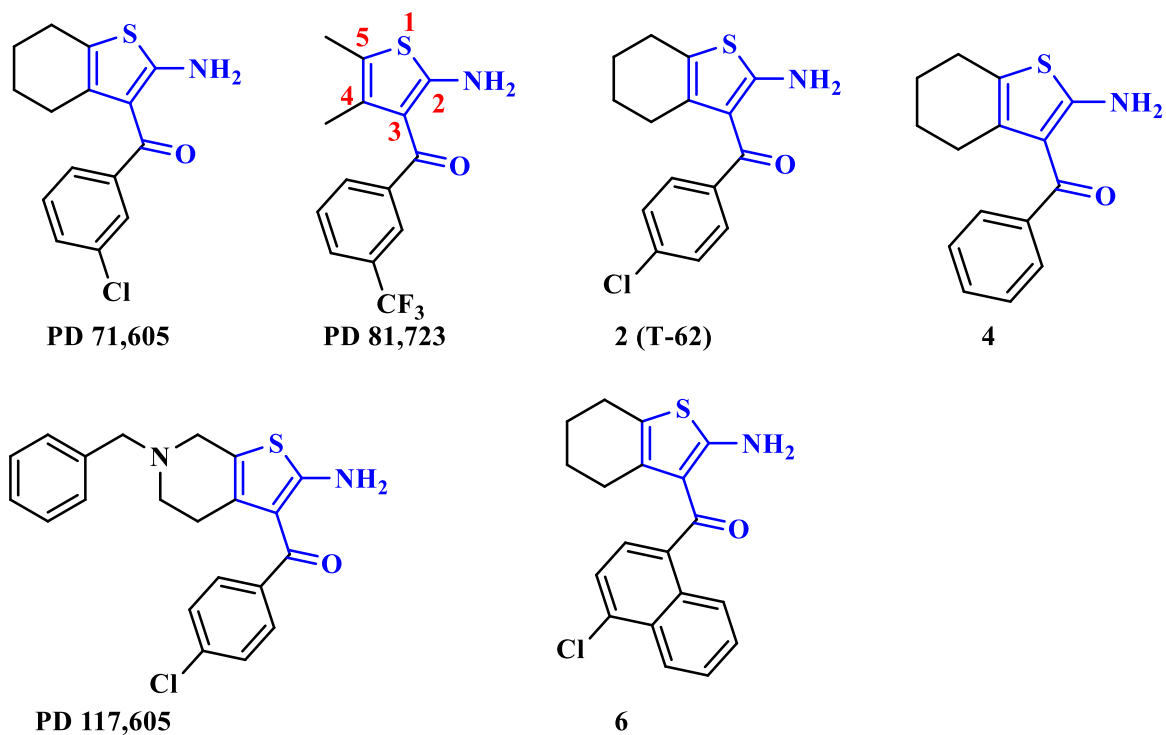
Development of allosteric modulators for A_{3A}AR faces the problem of selectivity since almost all current allosteric modulators for A_{3A}AR have also an allosteric modulator activity for A_{1A}AR. Therefore, despite the fact that numerous classes of allosteric modulators has been developed, the investigation of potential lead compounds whose modifications may result to selective allosteric modulators for A_{3A}AR remains an hot topic. Among such current classes, we have

HMA, an amiloride analogue which has shown to be an allosteric inhibitor of the antagonist binding of both A₃ and A₁ARs, but it is more potent at A₃AR receptors than on A₁AR.

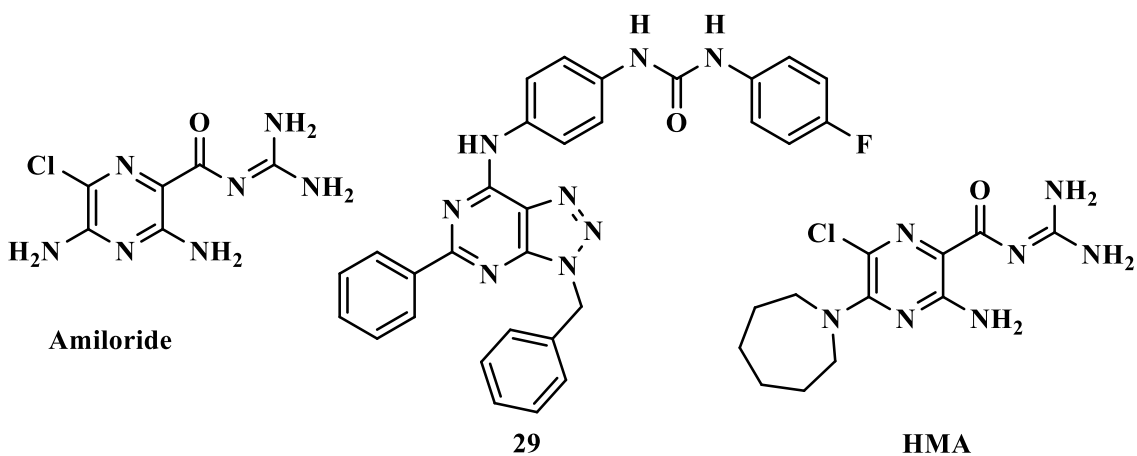
Beside allosteric inhibitors of the antagonist binding, there are a variety of allosteric enhancers for agonist binding. The first selective enhancer for A₃AR agonist was described by Gao *et al.*¹⁴² who reported that the compound VUF5455 was able to significantly enhance the effects of the reference A₃AR agonist CI-IB-MECA on forskolin induced cAMP formation¹⁴³.

Subsequently, 1*H*-imidazo-[4,5-*c*]quinolones derivatives, which have been described as non-xanthine ARs antagonists mainly active on A₁AR, were later considered¹⁴⁴. The compound DU124183, a member of this 1*H*-imidazo-[4,5-*c*]quinolones family, (Fig. 1.16) showed comparable activity with VUF5455 since it has shown to selectively enhance agonist binding on A₃AR. However, because DU124183 was reported to possess moderate orthosteric activity to human A₃AR (K_i = 820 nM), further structural modifications resulted to two optimized analogues. Among these two analogues 2-cyclopentyl-4-benzylamino and 2-cyclohexyl-4-(3,4-dichlorophenyl)amino, the 2-cyclohexyl-4-(3,4-dichlorophenyl)amino (LUF6000) analogue displayed the best activity enhancing the maximum efficacy of the agonist CI-IB-MECA by 45–50%¹³⁷.

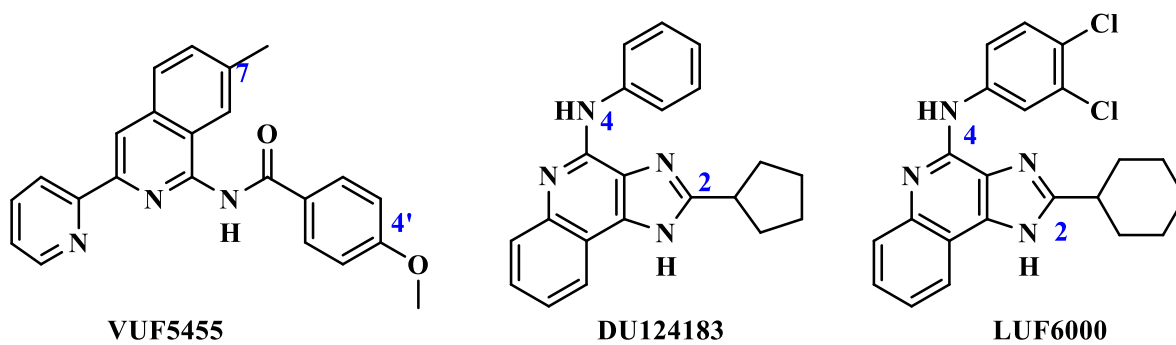
Cannabinoid ligands, investigated by Lane *et al.*, have shown to be potential modulators for human A₃AR. An example is illustrated by 2-arachidonylglycerol (2-AG), which has displayed considerable inhibition of the binding of the agonist [¹²⁵I]-AB-MECA at the human A₃AR¹⁴⁵. This inhibition was later shown to be the result of the increasing of the dissociation rate of [¹²⁵I]-AB-MECA in presence of 2-AG. Therefore 2-AG was known as a potential allosteric inhibitor of the agonist binding to hA₃AR¹³⁷. Figure 1.16 discloses the structure of allosteric modulators for ARs.



A₁AR allosteric modulators



A_{2A}AR allosteric modulators



A₃AR allosteric modulators

Figure 1.16: Structure of allosteric modulators for A₁AR, A_{2A}AR and A₃AR¹³⁷.

7. Therapeutic potential of Ado and adenosine receptor agonists.

The previous sections of this chapter have detailed the topic about Ado, AR subtypes and Ado ligands. The following final section reports how those knowledge all put together have allowed the use of Ado and Ado related compounds both in diagnosis and in therapy.

7.1 Uses of Ado receptor agonists in diagnosis and in therapy

Synthetic Ado for long time was the unique Ado agonist to be used in humans. Today, even if some others promising agonists have been developed, Ado remains on wide use. In fact Adenocard®, which is the synthetic Ado itself, remains the treatment of choice of paroxysmal supraventricular tachycardia and its therapeutic effect is due to the activation of A₁AR. Another Ado agonist is Adenoscan® (Astellas Pharma, Inc.), which is still a synthetic Ado but used for diagnostic purposes in myocardial perfusion imaging and its mode of action is based on the activation of A_{2A}AR leading to vasodilation¹³².

Beside synthetic Ado, which is metabolized quickly after systemic administration, various Ado analogues endowed with a better metabolic profile are under investigation both for therapy and diagnostic. The most promising are: the selective A₁AR agonist selodenoson (formerly known as DTI-0009, 8)¹⁴⁶ developed by Aderis Pharmaceuticals which has been in clinical trials both for tachycardia and diabetic foot ulcers treatment. Another promising A₁AR-selective agonist is the agonist BAY 68-4986 (Capadenoson)¹⁴⁷ which is under investigation for treatment of angina and atrial fibrillation.

Beside selective A₁AR agonists and Ado itself, the A_{2A}-selective agonist Regadenoson, also known as CVT-3146 or Lexiscan®, (Fig. 1.17), has been also approved and it is currently used for diagnostic purposes in cardiac imaging¹⁴⁸. Also Adenosine Therapeutics has developed two other selective A_{2A}AR agonists, which are currently in preclinical phase for acute inflammatory conditions (ATL-1222) and ophthalmic disease (ATL-313)¹⁴⁹.

Concerning A₃AR agonists, none has reached the market yet, however, CF101¹⁵⁰ and CI-IB-MECA (CF102), which are two selective A₃AR agonists are currently in clinical trials for autoimmune inflammatory disorders (CF101) and for liver cancer (CF-102)¹⁵¹, was recently reported to be efficacious in clinical trials of rheumatoid arthritis, psoriasis, and dry eye disease¹⁵². Figure 1.17 discloses the structure of Ado agonists with relevant therapeutic potential.

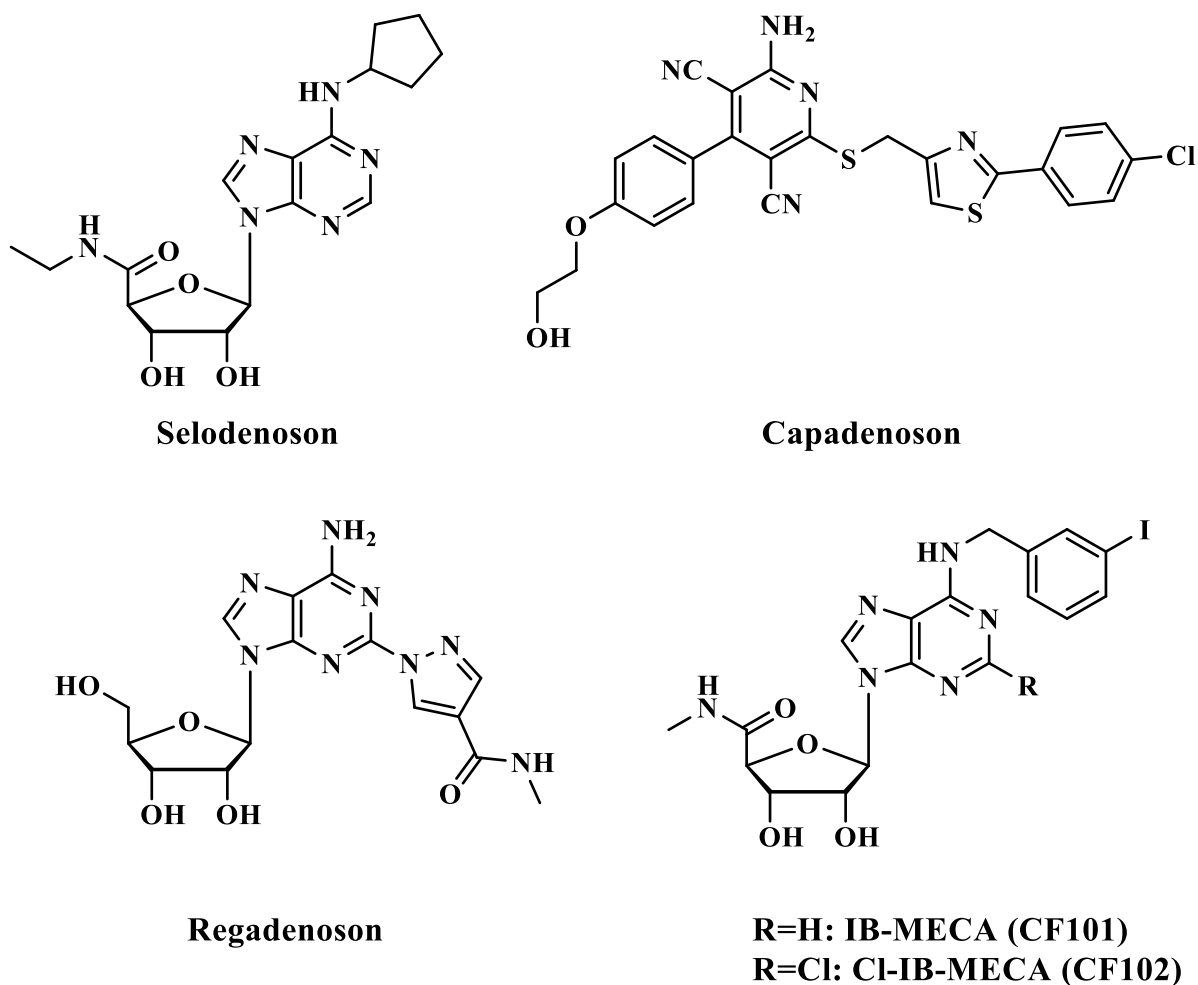


Figure 1.17: Structure of some AR agonists with promising therapeutic potential ¹³².

7.2 Uses of Ado receptor antagonists in diagnostic and in therapy

The methylxanthines (i.e. caffeine and theophylline)³⁴ were the first ARs antagonists to be recognized. This finding enlarges the use of methylxanthine in therapy. Some well documented cases are the use of caffeine in therapy for CNS stimulation to restore alertness and to counteract fatigue and for treatment of pain (e.g. headache, migraine) and the used of theophylline as second-line treatment of bronchial asthma and chronic obstructive pulmonary disease (COPD)¹⁵³. Despite the important therapeutic potential of methylxanthines, their use is now limited because of side effects both on the CNS and in the renal system. Even though the use in therapy has been reduced near to zero, methylxanthines remains molecules of great interest since the studies of their SAR allows the development of analogues which are more potent and selective for ARs. However, despite the fact that some of these analogues are very promising and are currently under investigation as kidney protective agents (A₁), antifibrotic (A_{2A}),

neuroprotective, antiasthmatic (A_{2B}), and antiglaucoma (A_3)^{153,154}, only one AR antagonist, istradefylline (Fig. 1.18), has been approved in Japan. Both figure 1.18 and table 1.7 gives additional knowledge on AR antagonists with promising therapeutic potential.

Table 1.7: description of AR antagonists with very good therapeutic potential.

Example of some promising ARs antagonists		
ARs antagonist subtype	Structure	Therapeutic potential
	L-97-1	Highly selective A_1 AR antagonist, in late preclinical development for the treatment of asthma and ¹⁵⁵
	Toponafylline	Preferable clinical candidates heart failure and renal function ¹⁵⁶
A_1AR antagonist		
A_{2A}AR antagonist	Istradefylline (KW6002)	It has been evaluated in clinical trials for the treatment of Parkinson's disease and in 2013 Kyowa Hakko Kirin pharmaceutical received the approval to develop istradefylline as the adjunctive treatment of PD ¹⁵⁷
A_{2B}AR antagonist	GS-6201	GS-6201 is a selective A_{2B} antagonist which has been clinically evaluated for the treatment of asthma ¹³⁴
A_3AR antagonist	KF26777	This compound has been explored by Kyowa Hakko Kirin pharmaceutical ¹³⁴

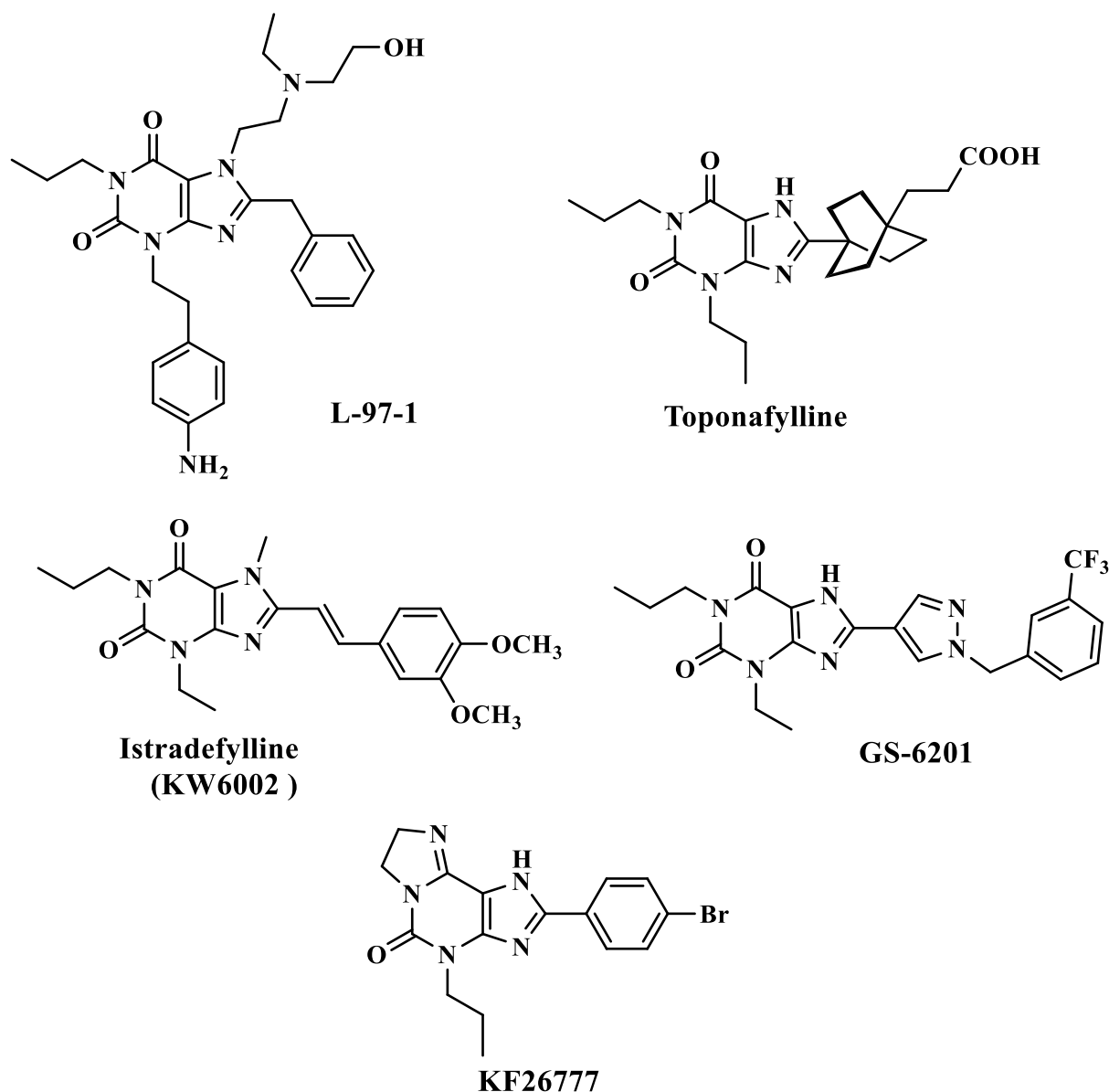


Figure 1.18: Structure of AR antagonists having a very good therapeutic potential ¹³².

Although Ado is present in virtually all cells, its levels are sufficient to activate ARs only where they are most abundant. As previously discussed, activation of ARs has the potential to be beneficial in the treatment of various inflammatory and autoimmune disorders, pain, arrhythmia as well as sleep and some metabolic disorders. During the last decades, specific agonists and antagonists of ARs have been synthesized. As a result, increasing numbers of clinical trials testing novel adenosine-based drugs in various indications have been initiated. However, to date, only few ligands have reached the market. In fact, given the wide-spread distribution of ARs, their ligands can have effects in most tissues and produce a variety of responses, which makes

them difficult to use. As a consequence, many clinical trials failed due to the appearance of serious side effects. Another problem of AR ligands is that, in most cases, they are nucleosides or nitrogen heterocyclic molecules that are characterized by poor water solubility, poor oral absorption and therefore poor bioavailability. These problems could be overcome by the development of highly selective ligands (which is the aim of the present thesis) that could be administered using vehicles like nanoparticles in order to overcome the limits of their scarce absorption.

CHAPTER 2: OBJECTIVES

The present work target the synthesis and biological evaluation of new ligands for the adenosine receptors. Especially the interest is focused on A_{2A} and A₃ receptors subtypes.

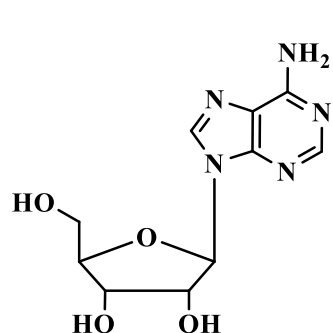
About A_{2A}AR subtype, the objectives of the work target the synthesis of new agonists. The particularity of the present work is that the author investigates a non-common modification upon the sugar moiety. In fact while the N-ethylcarboxamido (NECA) substituent has been well documented as a good 5'-modifacation conferring to the resulting nucleoside the good binding affinity and selectivity data for A_{2A} subtype, tetrazoyl moiety upon the sugar has been only fewer investigated. Hence, even though among the existing nucleosides bearing tetrazoyl moiety in 4'-position of the sugar, some have been reported to endow with better binding affinity and selectivity data respect the reference A_{2A} agonists NECA and CGS21680¹⁵⁸, no existing literature has investigated of whether or not the good binding affinity and selectivity data of those nucleosides bearing tetrazoyl analogue instead of NECA were related to the presence of the tetrazoyl moiety. Hence the originality of this work is properly the elucidation of whether or not the solely substitution of NECA with tetrazoyl upon the sugar may improve the binding affinity and selectivity of the resulting nucleoside for A_{2A} subtype. Another interesting aspect of this work is about the wound healing potential of the nucleosides that bears tetrazoyl moiety. Therefore, this work could be the first one reporting the wound healing potential of nucleoside bearing tetrazoyl moiety. The methodology, protocols and experiments used to reach those objectives are described in details in the following chapter 3 (see section below).

Another objective of this work is the synthesis of new antagonists for A₃AR subtype. Concerning the Ado receptors antagonists, the literature has well reported that the replacement of sugar moiety attached to the N-9 position of almost all Ado nucleosides induce loss of the agonistic properties¹⁵⁹. Hence in this work the N-9 position of the purine core is first substituted with a side chain different from the sugar moiety to assure the antagonistic properties of the resulting compounds. Then the author investigates different side chain in positions C-8, N-6 and C-2 of the purine cord in order to find a highly potent and selective A₃AR antagonist. The particularity of this research is the fact that the author perfectly combines in only one direction many previous and current findings of volpini *et al.* The methodology, protocols and experiments used to reach those objectives are described in details in the following chapter 4 (see section below).

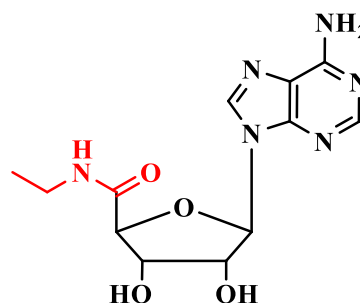
CHAPTER 3: Synthesis of new 4'-tetrazolyl adenosine derivatives as potential agents for wound healing

3.1 Aim of the research

The crystal structure of A_{2A} with agonist NECA highlighted the importance of 5'-modification. In fact A_{2A} agonist NECA (K_i $hA_{2A}AR = 20$ nM) differs from adenosine (K_i $hA_{2A}AR = 700$ nM) only with the 5'-modification (5'-N-ethylcarboxamido versus 5'-hydroxyl group)¹⁵⁹. From this evidence, the 5'-N-ethylcarboxamido rapidly became a worthy modification found in several new A_{2A} agonists (Figure 1.3). Some of the most famous and which have been well studied are CGS21680¹⁶⁰, Apadenoson¹⁶¹ and UK432097 which have been candidate for clinical trials^{162,163,67}. Contrary to the 5'-N-ethylcarboxamido which has been maintained unchanged all this while, the C-2 position has shown to be widely modified and in many cases, the C-2 side chain has shown to contribute a lot to the affinity and selectivity of the resulting compound toward A_{2A} .

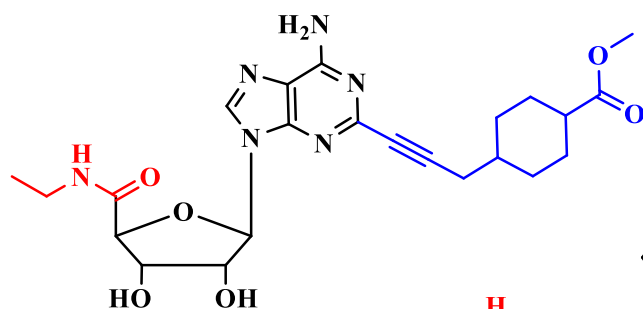


Adenosine (Ado, I)



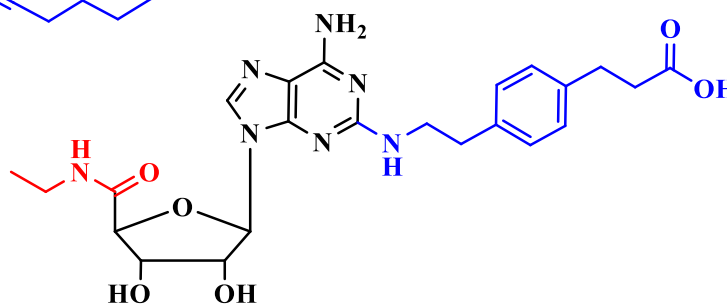
NECA (II)

K_i $hA_{2A} = 20$ nM



Apadenoson (ATL-146e, IV)

K_i $hA_{2A} = 0.5$ nM



CGS 21680 (III)

K_i $hA_{2A} = 27$ nM

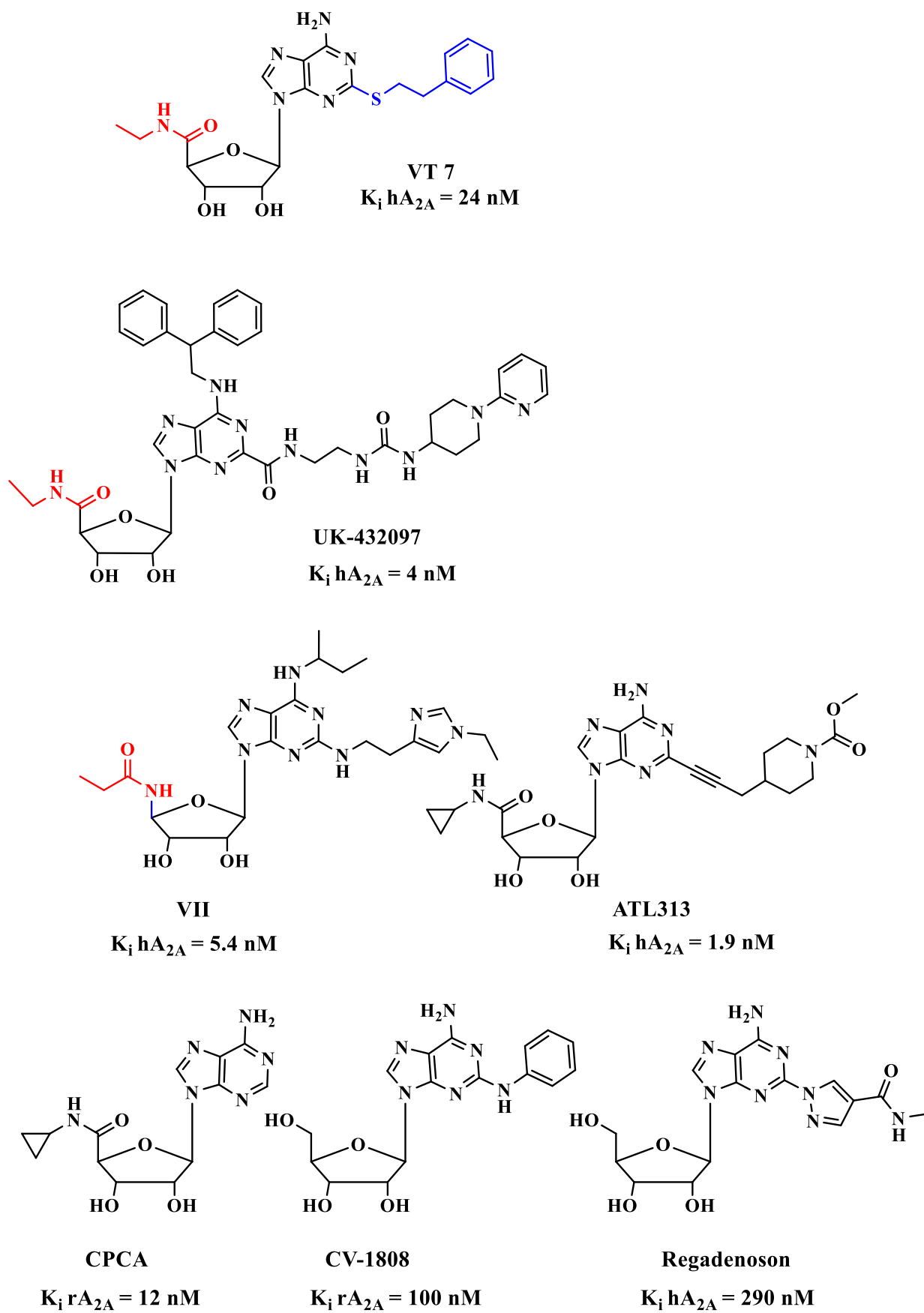
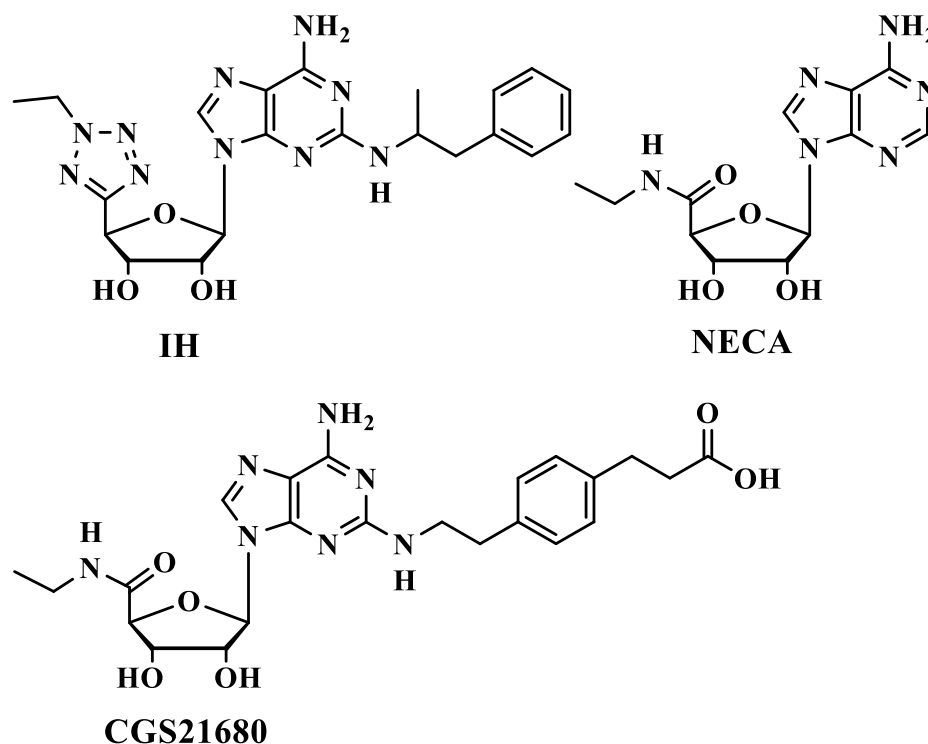


Figure 3.1: Some promising A_{2A} agonist.

Hence, until the year 2000 where new modification of 5'-position of ribose moiety started emerging, the development of A_{2A} agonist was mostly focused on the identification of the best C2 side chain with fixed 5'-N-ethylcarboxamido modification at the sugar moiety. In 2004, Bosh et al reported that 4'-N-ethyltetrazoyl moiety was well tolerated and above all seemed to improve the affinity and selectivity of the resulting compounds respect to NECA and CGS21680 known to be a reference A_{2A} agonist (Figure 3.2).



Cps ARs	A₁	A_{2A}	A_{2B}	A₃
I	356	1	2,780	100
NECA	14	20	330	6.2
CGS21680	290	27	361,000	67

Figure 3.2: Lead compounds used for the design of the AR ligands in this project.

Thus in this work the interest is focused on the investigation of the 4'-N-ethyltetrazoyl moiety with the aim to provide additional information or to confirm those reported already about the contribution of 4'-N-ethyltetrazoyl in the binding affinity and selectivity of A_{2A} agonist.

Taking the results obtained by the group of Prof Volpini, in which with VT 7 a good affinity and moderate selectivity versus the A_{2A} AR subtype was obtained, the synthesis of VT 7 analogues in which the 4'-N-ethylcarboxamido group was substituted by the tetrazolyl moiety used by Bosch was designed¹⁶⁴. Then the other side chains were also introduced in C-2 position in order to identify other potential good substituents or even better than phenylethylthio or which may be in the future combined both with other different 5'-modification and with some worthy N⁶ substituents. To end up the work, we investigate the displacement of the ethyl substituent from the N² to N¹ position of the tetrazole ring (Figure 3.3).

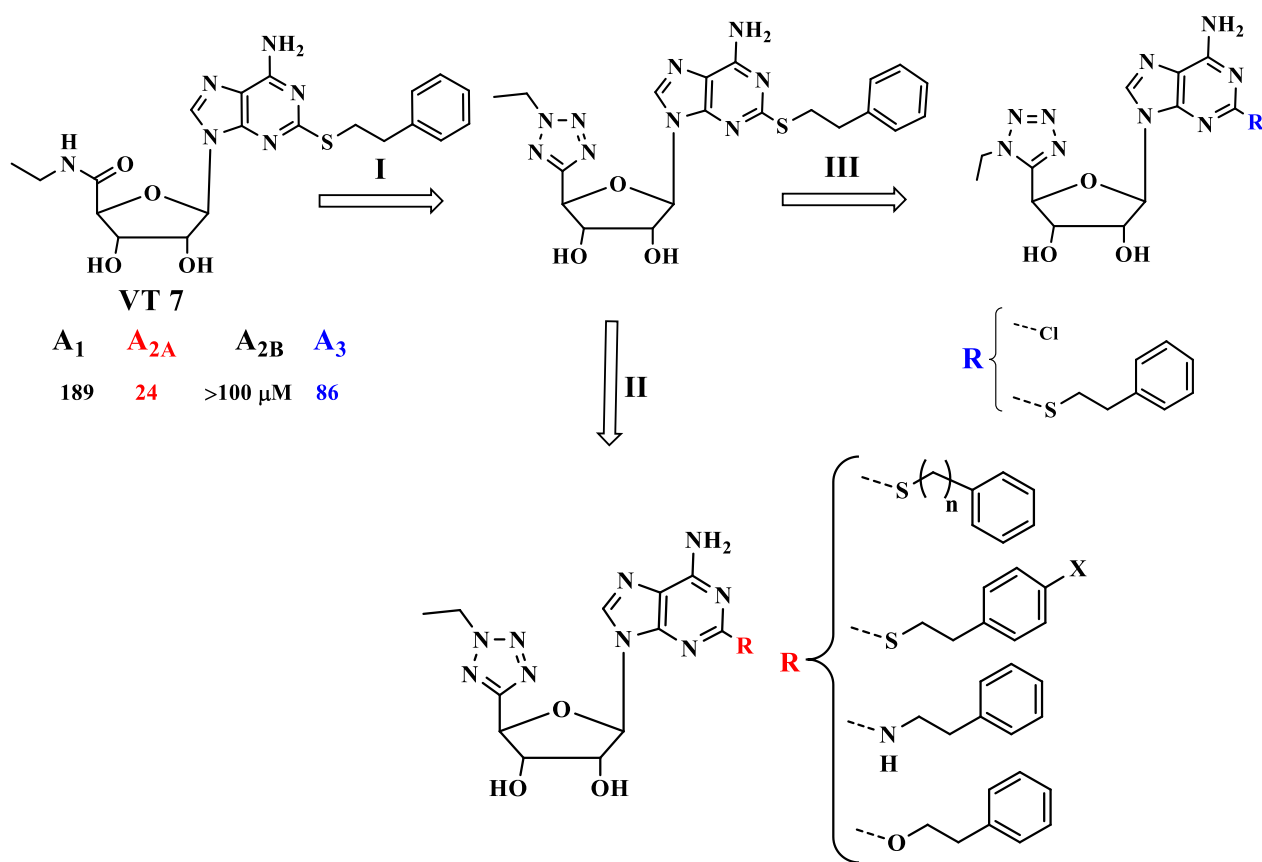


Figure 3.3: Plan of the designed research project.

3.2 Chemistry

Synthesis of desired nucleosides **2-23** was carried out by a divergent approach in which a suitable modified sugar was coupled with the appropriate heterocycle to get an intermediate nucleoside from which final compounds were obtained through several reactions.

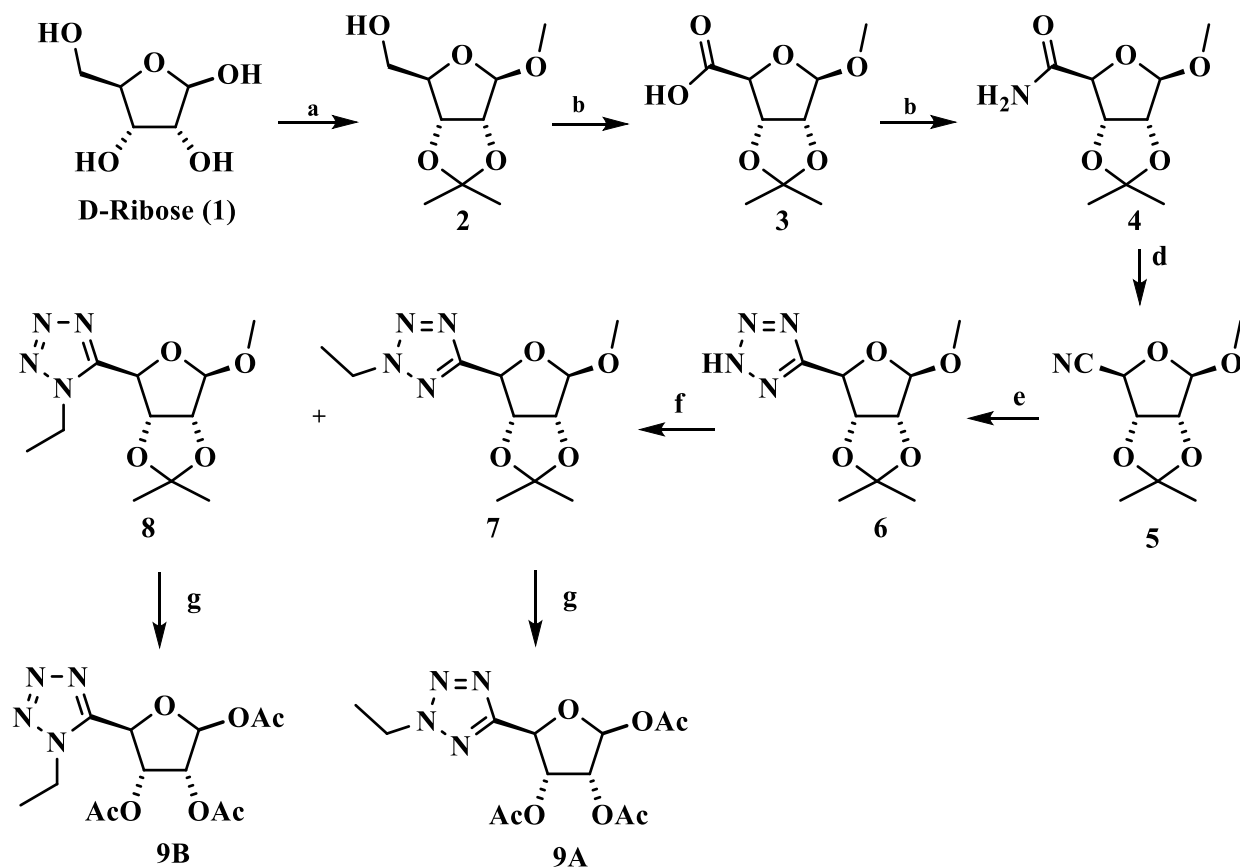
For the synthesis of our compounds we followed the following synthetic steps.

3.2.1 Synthesis of the modified sugar

For the synthesis of the tetrazolyl sugar moiety has been followed the procedure reported by Bosh *et al*¹⁵⁸. The protected ribose **2** was prepared from D-ribose (**1**) through the reaction with 2,2-dimethoxypropane in acetone in the presence of catalytic amount of perchloric acid and subsequent treatment of the reaction mixture with methanol (Scheme 3.1). Compound **2** was subsequently oxidized to the corresponding carboxylic acid **3** by treatment with 2,2,6,6-tetramethylpiperidinyloxy (TEMPO), in ethyl acetate (EtOAc), in the presence of NaHCO₃, KBr, and NaClO (commercial bleach), for the recovery of the TEMPO consumed during the reaction. Compound **3** was converted to the acyl chloride by reaction with thionyl chloride in dry EtOAc and then bubbling of gaseous ammonia (NH₃) in the reaction mixture converted the acyl chloride to the corresponding amide derivative **4**. The conversion of the amide **4** into the nitrile **5** has been obtained by treatment of a solution of **4** and triethylamine in EtOAc with phosphorous oxychloride in classical dehydration reaction conditions. The construction of the tetrazole ring at the 5-position of D-ribose was obtained by reaction of the nitrile **5** with sodium azide added portion wise in a mixture of **5** and ammonium chloride in dimethylformamide (DMF). The alkylation of compound **6**, obtained previously, was achieved with ethyl iodide with dry potassium carbonate as the catalyst in dry acetone. The later reaction provided a mixture of isomers due to the alkylation in N-1 or N-2 position of compounds **7** and **8** respectively, which were separated with flash column chromatography.

The N-2-ethyltetrazole isomer **7** was first hydrolyzed with trifluoroacetic acid and H₂O providing a crude which was co-evaporated with dry dichloromethane and freeze-dried overnight. The freeze-dried crude mixture obtained was dissolved in dry CH₂Cl₂ and fully acetylated with dry acetic anhydride to provide **9A** as an inseparable mixture of the α - and β -anomers. The presence of α - and β -anomers was confirmed by ¹H-NMR.

Scheme 3.1

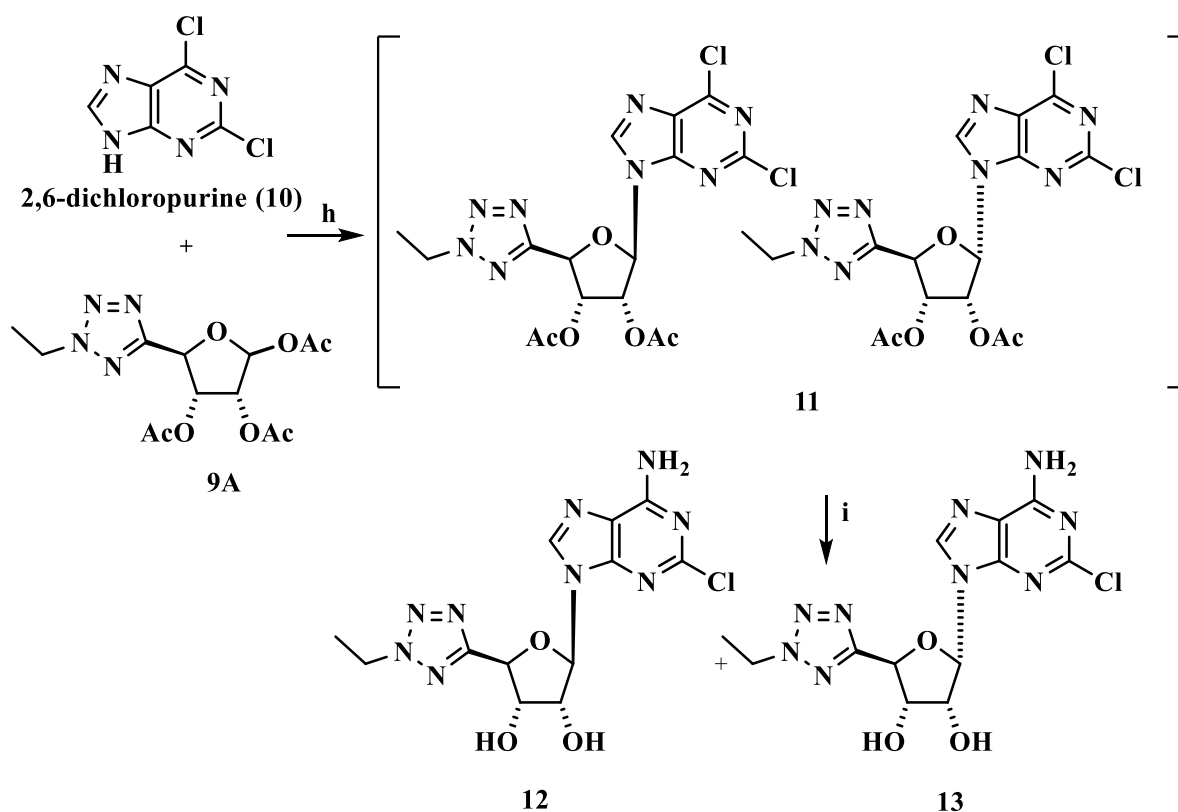


Reagents and conditions: (a) i. 2,2-Dimethoxypropane, HClO_4 , acetone, r.t., 4 h; ii. MeOH, acetone, r.t., 2 h 96%; (b) TEMPO, KBr, 6% NaHCO_3 aqueous solution, NaHCO_3 aqueous solution, 5% NaClO , EtOAc, r.t., 3 h, 79%; (c) SOCl_2 , EtOAc, gaseous NH_3 , 60°C, 3 h, 88%; (d) POCl_3 , Et_3N , EtOAc, 0°C, 2 h, 61%; (e) NaN_3 , NH_4Cl , DMF, 40-90°C, 3 h, 82%; (f) EtI, dry K_2CO_3 , acetone, 40°C, 3 h, 62%; (g) i. TFA, H_2O , 0°C, 6 h; ii. Ac_2O , Et_3N , DMAP, CH_2Cl_2 , r.t., 3 h, 64%.

3.2.2 Glycosylation reaction

Compound **9A** was coupled with commercial 2,6-dichloropurine (**10**) in the presence of 1,8-diazabicyclo[5.4.0]undec-7-ene (DBU) and trimethylsilyl triflate (TMSOTf) in dry acetonitrile to afford **11** as inseparable mixture of α - and β -nucleoside (Scheme 3.2). Amination of the anomer mixture **11** with gaseous NH_3 give mixture of **12** and **13** selectively aminated at the 6-position. The two anomers were separated with flash column chromatography to afford the β anomer compound **12** and the α anomer compound **13**, with 55 % and 35 % yield, respectively. Contrary to the reference paper by Bosch et al., in this case together with the beta anomer after glycosylation it was possible to isolate a sufficient amount of the alpha anomer which permitted to define the anomeric structure of the two intermediates obtained.

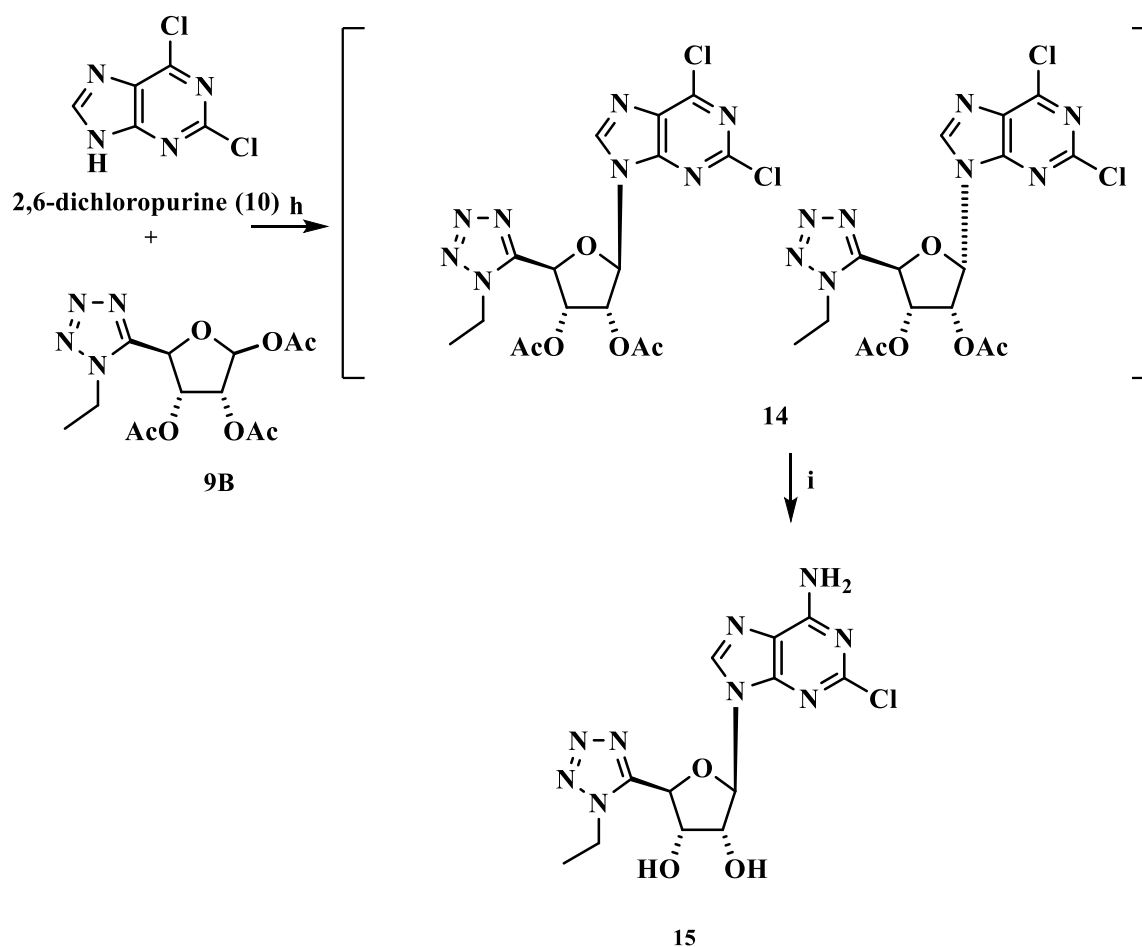
Scheme 3.2



Reagents and conditions: (h) 2,6-DCP, DBU, TMSOTf, dry acetonitrile, 0°C-r.t, 21 h, 90%; (i) gaseous NH₃, r.t., 6 h, **12**: 55%; **13**: 35%.

Furthermore, the synthesis of the *N*¹-ethyltetrazole nucleoside derivative has been carried out by glycosylation of the 2,6-dichloropurine (**10**) with the compound **9B**, to obtain nucleoside 15. The compound **9B** was obtained after a deprotection/protection reaction, in similar conditions used for **9A**, on the side product **8** (Scheme 3.1). The intermediate nucleoside **15** has been obtained, following similar steps of the synthesis that was previously utilized to obtain the *N*-2 isomer **12** (Scheme 3.3). After the glycosylation an inseparable mixture of the α and β -anomers were obtained. The conversion of the 2,6-dichloronucleosides **14** to the 6-amino derivatives, furnished after purification the β -anomer with 60% yield. The β -configuration was confirmed by ¹H-NMR. NOESY bidimensional, in fact, in the β configuration the hydrogens in position 1' and 4' are placed on the same side with respect to the plane of the sugar moiety and this conformation is detectable by using long-range coupling in the ¹H-NMR analysis. Hence, the saturation of H-1' of **12** resulted in NOEs of the H-4', whereas, the saturation of H-1' of **13** did not express NOEs of the H-4', confirming that **12** corresponds to the β anomer while **13** to the α anomer.

Scheme 3.3

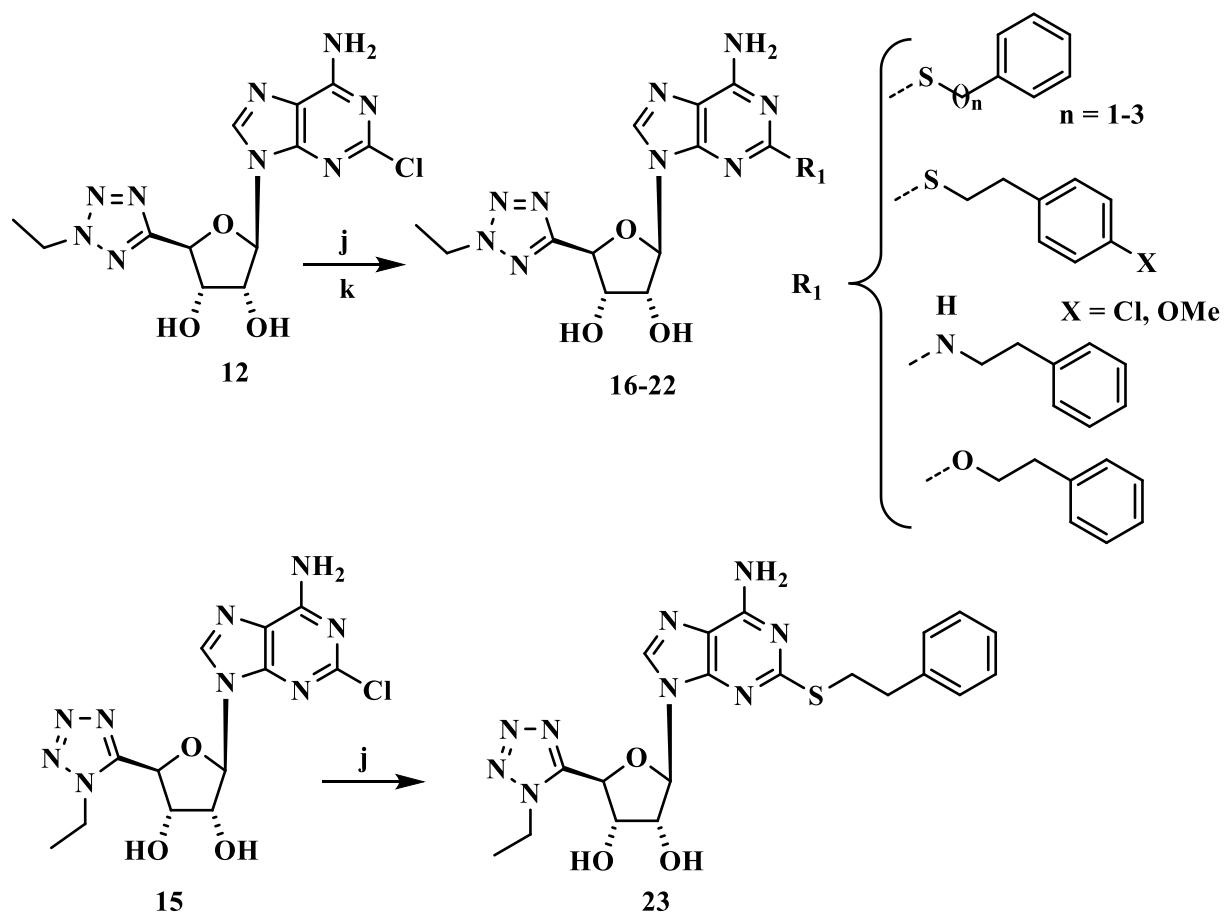


Reagents and conditions: (h) 2,6-DCP, DBU, TMSOTf, dry acetonitrile, 0°C-r.t., 21 h, 94%; (i) gaseous NH₃, r.t., 6 h, 90%.

3.2.3 Final compounds

Compounds **16-23** were prepared by addition of the corresponding arylalkylthiols or phenylethylamine, to a solution of **12** or **15** in dry DMF in the presence of dry K₂CO₃ to get the desired derivatives as pure compounds with yields ranging from 18 to 95% (Scheme 4.3). In the case of the synthesis of the C-2 alkoxy derivative, a different procedure was used. In fact, first the activation of the alcohol with metallic sodium has been carried out, then to the obtained suspension the suitable nucleoside **12** was added. The reaction was heated at 80 °C for 4 hours to get the designed final compound with 45% yield after chromatographic purification.

Scheme 3.4



Reagents and conditions: (j) R-SH or R-NH₂, K₂CO₃, DMF, 120°C, 24 h, 18-95%; (k) R-OH, Na, 80 °C, 4 h.

3.3 Results and discussion

The newly synthesized derivatives were tested in binding and functional studies by the research group of Professor Marucci G., at human A₁, A_{2A}, and A₃ ARs cloned and transfected in CHO cells. For the binding studies the [³H]-N⁶-cyclopentyl-2-chloroAdo ([³H]-CCPA), the [³H]-NECA, and the [³H]-2-hexynyl-N⁶-methylAdo ([³H]-HEMADO) radioligands for the A₁, A_{2A}, and A₃ AR subtypes, respectively, were used. At A_{2B} subtype a functional study evaluating the adenylyl cyclase activity assay was performed by measuring the cAMP levels in CHO cells.

Moreover, selected compounds showing high hA_{2A} AR affinity and selectivity were studied by evaluating their effect on cAMP production in CHO cells, stably expressing A₁, A_{2A}, and A₃ receptor subtypes in order to assess their ability to inhibit or stimulate adenylyl cyclase activity coupled with the activation of the receptor.

Results are shown in Table **3.1** and Table **3.2**, with the *K_i* and EC₅₀ or IC₅₀ expressed as nM. The compound 6-amino-2-(phenethylthio)-5'-N-ethylcarboxamidoadenosine (**VT 7**) has been used as reference compound.

The binding studies at A₁, A_{2A}, and A₃ receptors showed that compounds are endowed with binding affinity in the nanomolar range having the better binding affinity versus the A₃ subtype. Evaluation at A_{2B} subtype showed that the analyzed compounds are not endowed with affinity for this receptors behaving, in general, EC₅₀ value > 30,000 nM.

The comparison of the activity of the reference compound **VT 7** and its analogue compound **17** modified at the sugar moiety with a N²-ethyltetrazolyl group in 4'-position indicate that this modification improve affinity of the resulting compound for all the AR subtypes (**17**: *K_i* hA₁R = 35 nM; *K_i* hA_{2A}R = 5.8 nM; *K_i* hA₃R = 1.2 nM; versus **VT 7**: *K_i* hA₁R = 189 nM; *K_i* hA_{2A}R = 24 nM; *K_i* hA₃R = 86 nM). These results shows that compound **17** is approximately 4 times selective for A₃AR respect to A_{2A}AR (**17**: selectivity A₁/A₃ = 29; selectivity A_{2A}/A₃ = 5).

Table 3.1: Binding studies at human A₁, A_{2A}, and A₃ ARs cloned and transfected in CHO cells and functional activity at A_{2B}AR cloned and transfected in CHO cells. K_i, for data at A₁, A_{2A}, and A₃ ARs, and EC₅₀, for data at A_{2B}AR, are expressed as nM.

Cps	R	^a hA ₁ AR	^b hA _{2A} AR	^c hA _{2B} AR	^d hA ₃ AR
4'-N²-ethyltetrazoyl derivatives					
VT 7 ¹⁶⁴		189	24	>100,000	86
12	Cl	1.0±0.18	19±4	5,900±1,250	0.23±0.06
16	S-CH₂-Ph	208±47	165±37	> 30,000	1.4±0.24
17	S-(CH₂)₂-Ph	35±8.5	5.8±0.78	> 30,000	1.2±0.17
18	S-(CH₂)₃-Ph	165±38	188±47	> 30,000	2.6±0.45
19	S-(CH₂)₂-<i>p</i>-Cl-Ph	51±21	21±3.5	> 30,000	4.0±0.75
20	S-(CH₂)₂-<i>p</i>-CH₃O-Ph	96±21	7.9±1.5	> 30,000	5.1±1.0
21	NH-(CH₂)₂-Ph	49±11	11±2.5	> 30,000	1.3±0.3
22	O-(CH₂)₂-Ph	0.45±0.08	0.91±0.03	> 30,000	0.08±0.02
4'-N¹-ethyltetrazoyl derivatives					
15	Cl	> 30,000	> 30,000	> 30,000	417±68
23	S-(CH₂)₂-Ph	> 30,000	> 30,000	> 30,000	251±33

^aDisplacement of specific [³H]-CCPA binding at human A₁R expressed in CHO cells. ^bDisplacement of specific [³H]-NECA binding at human A_{2A}R expressed in CHO cells. ^cValue obtained from cAMP quantification. ^dDisplacement of specific [³H]-HEMADO binding at human A₃R expressed in CHO cells. Data are expressed as means ± SE.

The capacity of compound **17** to interact with good affinity both with A_{2A}AR and A₃AR is in agreement with the study of Bosch et al which reported “the dual effect of 4'-N²-ethyltetrazoyl analogues”¹⁵⁸. Another interesting aspect of the results obtained is the binding affinity data of compounds **16** and **18**. In fact, the replacement of the ethyl chain in 2-position, of the adenine core, in these two compounds with a shorter methylene or a longer propylene chain brought to a

lower affinity both for A₁ and A_{2A} subtypes maintaining their ability to bind to the A₃ AR being more selective for this subtype (**16**: K_i hA₃R = 2.6 nM; **18**: K_i hA₃R = 1.4 nM ; **16**: selectivity A₁/A₃ = 148, A_{2A}/A₃ = 117; **18**: selectivity A₁/A₃ = 63, A_{2A}/A₃ = 72)

So, even if such compounds **16** and **18** were not further investigated due their lower affinity for A_{2A}, their affinity and selectivity data for A₃ open widely their evaluation as A₃ ligands.

Compounds **19** and **20** bearing a substitution in *para* position of the phenyl ring disclosed a slightly decreased affinity for A₁, A_{2A}, and A₃ ARs. However, while the *para*-methoxy substituent is better tolerated by A_{2A}AR (**20**: K_i hA_{2A}R = 7.9 nM versus **17**: K_i hA_{2A}R = 5.8 nM) the *para*-chloro substitution resulted detrimental for such subtype reducing affinity more than 4 times (**19**: K_i hA_{2A}R = 21 nM versus **17**: K_i hA_{2A}R = 5.8 nM).

Considering the substitution of the sulfur atom with the isosteric amino group or oxygen it is possible to outline that the first substitution seems to affect more A_{2A} subtype since affinity has decreased twice (**21**: K_i hA_{2A}R = 11 nM versus **17**: K_i hA_{2A}R = 5.8 nM) while the affinity for the other receptor was almost unchanged. On the other hand, in the case of the substitution of the sulfur atom with oxygen a great improvement of affinity for A₁, A_{2A} and A₃ ARs was obtained (**22**: K_i hA₁R = 0.45 nM; K_i hA_{2A}R = 0.91 nM; K_i hA₃R = 0.08 nM) with a subnanomolar affinity of the compound at all the adenosine receptors excepting A_{2B} subtype. Also in this case the selectivity is maintained for the A₃ subtype (**22**: selectivity A₁/A₃ = 5, A_{2A}/A₃ = 11) but the selectivity versus the A_{2A} and A₃ receptors it worse than the other compounds.

Some selected compounds were analyzed in functional studies at human A₁, A_{2A}, and A₃ ARs transfected in CHO cells by evaluating the ability of the compounds to affect cAMP levels associated with AC activity coupled with the receptor. In particular, the technique of the GloSensor cAMP assay in which the cAMP production was detected through a luciferase-based biosensor was used: the binding of the produced cAMP to the biosensor leads to a conformational change which promotes a luminescence activity which is proportional to the concentration of the second messenger. The technology permits to perform the evaluation on live cells. NECA was used as a reference agonist, and the compounds that are being studied, were added to the preparation at different concentration to draw a curve concentration-effect. When compounds were unable to stimulate the cAMP production or to inhibit cAMP production stimulated by forskolin in the case of receptors coupled to Gi, they were studied as antagonists. In particular, the antagonist profile was evaluated by assessing the ability of these compounds to counteract NECA-induced increase of cAMP accumulation. The cells were incubated in the

reaction medium with different understudy derivative concentrations and then treated with NECA.

In Table 3.1 have been also reported the results of the binding affinity of compounds **15** and **23** which are 4'- N^1 -ethyltetrazoyl derivatives. The displacement of the ethyl group from the N^2 to N^1 position resulted to be not tolerated for affinity at A_1 and A_{2A} while it is tolerated at the A_3 subtype. These compounds showed a K_i at hA_3AR equal to 451 and 217 nM, respectively. The inability to bind the A_1 and A_{2A} ARs resulted in an increased selectivity of **15** and **23** for A_3AR , compared to the 4'- N^2 -ethyltetrazoyl derivatives (Table 3.1). However, even though the displacement of ethyl really improved selectivity for A_3 , the binding affinity was reduced for more than 1000 time for compounds bearing the chlorine atom in 2 position (**12**: $hK_iA_3 = 0.23$ nM and **15**: $hK_iA_3 = 417$ nM,) and more than 200 time for compounds bearing the 2-phenylethylthio chain in 2 position (**17**: $hK_iA_3 = 1.16$ and **23**: $hK_iA_3 = 251$ nM); these results did not allow further investigation with the evaluation of different C2 substituents.

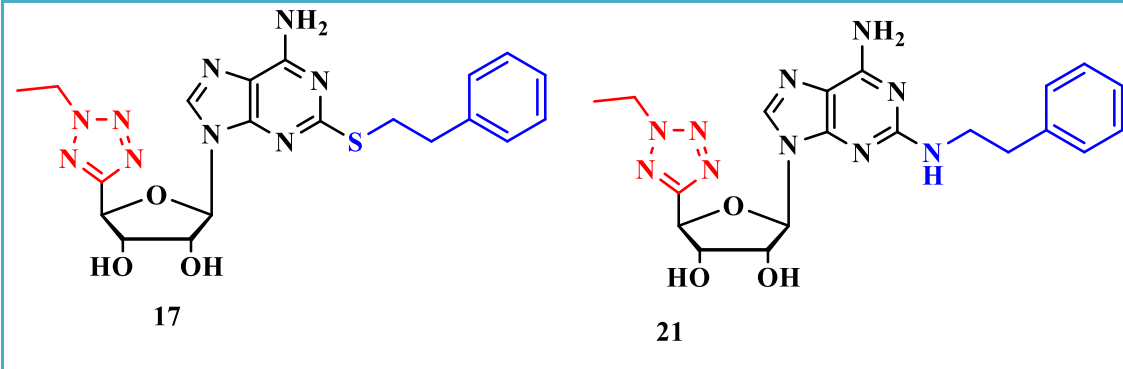
So even though this investigation was not done before and it may require more investigations or even different orientations, it is obvious that the displacement of ethyl from N^2 to N^1 is detrimental for the development of AR ligands.

Functional studies data are shown in Table 3.2. The results of functional studies agreed with our expectations since they effectively confirmed the dual behavior of the N^2 -ethyltetrazoyl derivatives tested which showed to activate A_1 , A_{2A} , A_{2B} ARs and at the same time to inhibit the A_3 subtype (Table 3.2).

Compounds **17** and **21** showed a comparable activity at all the receptors with EC_{50}/IC_{50} in the nanomolar range (**17**: $EC_{50} hA_1R = 790$ nM; $EC_{50} hA_{2A}R = 160$ nM; $IC_{50} hA_3R = 79$ nM; **21**: $EC_{50} hA_1R = 630$ nM; $EC_{50} hA_{2A}R = 98$ nM; $IC_{50} hA_3R = 40$ nM; Table **3.2**). The functional assay confirmed a low preference of these compounds for the A_3 receptors, and, in this case, compound **21** resulted faintly more active than **17** (Table 3.2).

Thus, even though only compound **17** and **21** were investigated in functional studies, it is reasonable to assume that all the compounds (**12-22**) are endowed with the dual effect. Furthermore, it is difficult to establish a border line to differentiate such compounds as being A_{2A} or A_3 ligands and it is possible to argue that they could be used in conditions in which the A_{2A} agonism is not well-suited with the activation of the A_3AR .

Table 2.3: Functional studies on chosen candidates at human A₁, A_{2A}, A_{2B}, and A₃ ARs cloned and transfected in CHO cells. The activities, EC₅₀ or IC₅₀, are expressed as nM.



Cpds	hA ₁ AR (EC ₅₀) ^a	hA _{2A} AR (EC ₅₀) ^b	hA ₃ AR (IC ₅₀)
17	790±120	160±90	79±14
21	630±110	98±27	40±10

^aEC₅₀ values of the inhibition of forskolin-stimulated adenylyl cyclase activity in CHO cells expressing hA₁AR. ^bEC₅₀ values of the stimulation of adenylyl cyclase activity in CHO cells expressing hA_{2A}AR. ^cIC₅₀ values of the inhibition of NECA-effect on adenylyl cyclase activity in CHO cells expressing hA₃AR.

Those binding affinity and functional studies results are in agreement and support the previous observation of Volpini et al¹⁶⁴ which reported that 2-phenylethylthio was a promising C-2 side chain and should be further investigated in the development of new A_{2A}R agonist.

In conclusion, the results are in agreement with the previous observation of Bosch et al who described the dual effect of 4'-N-ethyltetrazolyl analogue¹⁵⁸. Also such results clearly reports that the improvement of the affinity for A_{2A} of 4'-N-ethyltetrazolyl analogue respect to NECA and CGS21680 observed by Bosh et al¹⁵⁸ was due to presence of 4'-N-ethyltetrazolyl moiety since compound **17** which differs from **VT 7** only with the 4'-N-ethyltetrazolyl moiety is endowed with better affinity for A_{2A} compared to **VT 7**. Those results are also in agreement with the previous observation of Volpini et al¹⁶⁴ which reported that phenylethylthio is a promising C-2 side chain and should get particular interest in the development of new A_{2A} agonists. The reason which may explain why 4'-N-ethyltetrazolyl moiety improve A_{2A} binding affinity respect to 5'-NECA is that 4'-N-ethyltetrazolyl moiety could establish additional interaction with A_{2A} respect to 5'-NECA. This hypothesis received a great support from a paper published in 2015 by Bosh et al where it was reported that, probably 4'-N-ethyltetrazolyl moiety allows additional interaction with histine 6.52 respect to NECA (Figure 3.4).

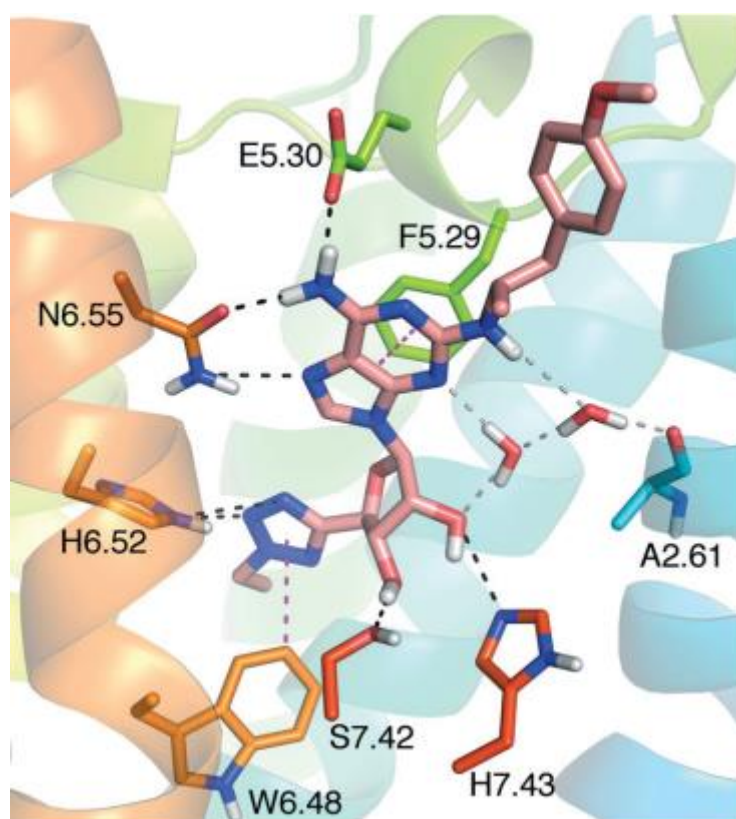


Figure 3.4: NECA and 4'-N-ethyltetrazolyl Ado derivative in the A_{2A} AR binding pocket with their respective interactions highlighting the additional 4'-N-ethyltetrazolyl group interaction with histine 6.52 respect to the 4'-N-ethyl group¹⁶⁵.

Although those results have shown that 4'-N-ethyltetrazolyl can be an alternative 5'-modification respect to the well-known 5'-NECA, there is still a lot to study on the contribution of 4'-N-ethyltetrazolyl in the binding affinity of the resulting compound for ARs. In this case, some compounds, such as compound **16** (selectivity of human $A_1/A_3=148$ and selectivity of $hA_{2A}/A_3=117$; see table 3.1) and compound **18** (selectivity of human $A_1/A_3=63$ and selectivity of $hA_{2A}/A_3=72$; see table 3.1) resulted A_3 ligands with a certain selectivity respect to the other receptors. Also a recent paper of Petrelli et al also reported that, combining 4'-N-ethyltetrazolyl moiety with some N^6 -modification resulted to compounds endowed with dual effect of being A_1 agonist and A_3 antagonist¹⁶⁶. Thus, to access for which AR subtype 4'-N-ethyltetrazolyl moiety specifically improve binding affinity or how the C-2 side chain or the N^6 modification can improve or shift the binding affinity of a 4'-N-ethyltetrazolyl analogue for an AR subtype respect to another is still not yet well understood.

3.4 Wound healing assay

It has been reported that Ado acts as one of the factor that modulate wound healing and some $A_{2A}AR$ agonists have been tested for their ability to repair damaged skin behaving as tools for the treatment of pathologies which involve skin damage: some compounds have been tested in clinical studies for the treatment of diabetic foot ulcers^{95,96}.

In order to understand the ability of new synthesized compounds **16-22** and also of the intermediate **12**, which showed affinity at $A_{2A}AR$ in the nanomolar range, in the mechanism of fibroblast migration and hence their ability to modulate wound healing, they were tested in the scratched wound assay.

The scratched wound assay is a standard in vitro technique developed to study directional cell migration in two dimensions and it allows the study of compounds as potential wound healing agents. This method mimics cell migration during wound healing in vivo. The basic steps involve creating a "wound" in a cell monolayer, capturing the images at the beginning and at regular intervals during cell migration to close the wound, and comparing the images to quantify the migration rate of the cells which led to the reparation of the wound. As example, in Figure 8 are reported images of the scratched areas at different time points of the control, of compound **12** at the concentration of 200 nM, and also of the positive control EGF.

This assay is particularly suitable for studies on the effects of cell-matrix and cell-cell interactions on cell migration^{97,98} For the assay, epidermal growth factor (EGF) is used as positive control, at 10 nM, to promote the stimulation of growth, while CGS21680 was used as reference $A_{2A}AR$ agonist and the migration was evaluated by measuring the reduction in wound area (%) at specific time point after 6, 12, and 24 hrs after the treatment with the compounds at 3 different concentrations.

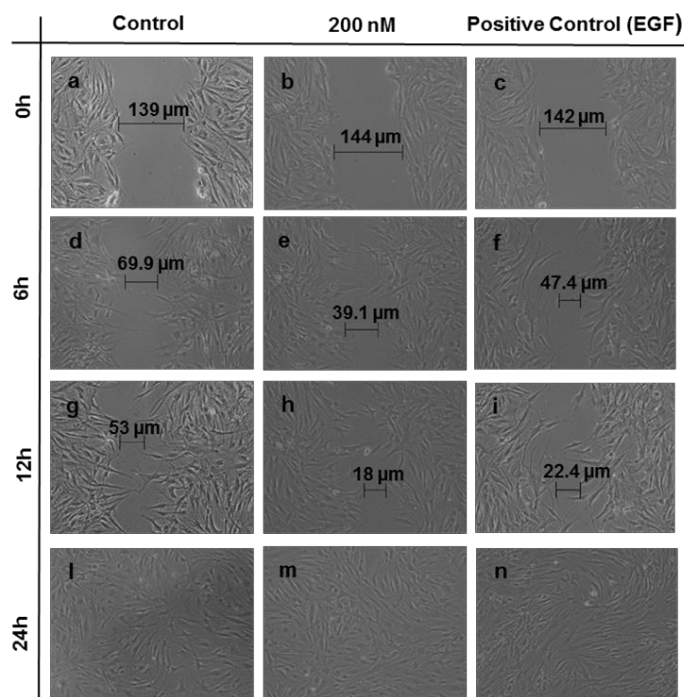


Figure 3.5: Example of the scratched wound assay in which it is showed the effect of compound **12** on the migration of human fibroblasts in comparison with control and EGF (10 nM). In each picture is showed, as example, the scratch-width after 0, 6, 12, and 24 hrs.

In Table 3.3 all the data of compounds **12**, **16-22** are reported at the different concentration tested at time 6, 12, and 24 has *versus* activity of control and EGF at the same time points, while in Figures 3.6-3.7 are reported graphics of the activity of reference compounds CGS21680 and VT 7, respectively.

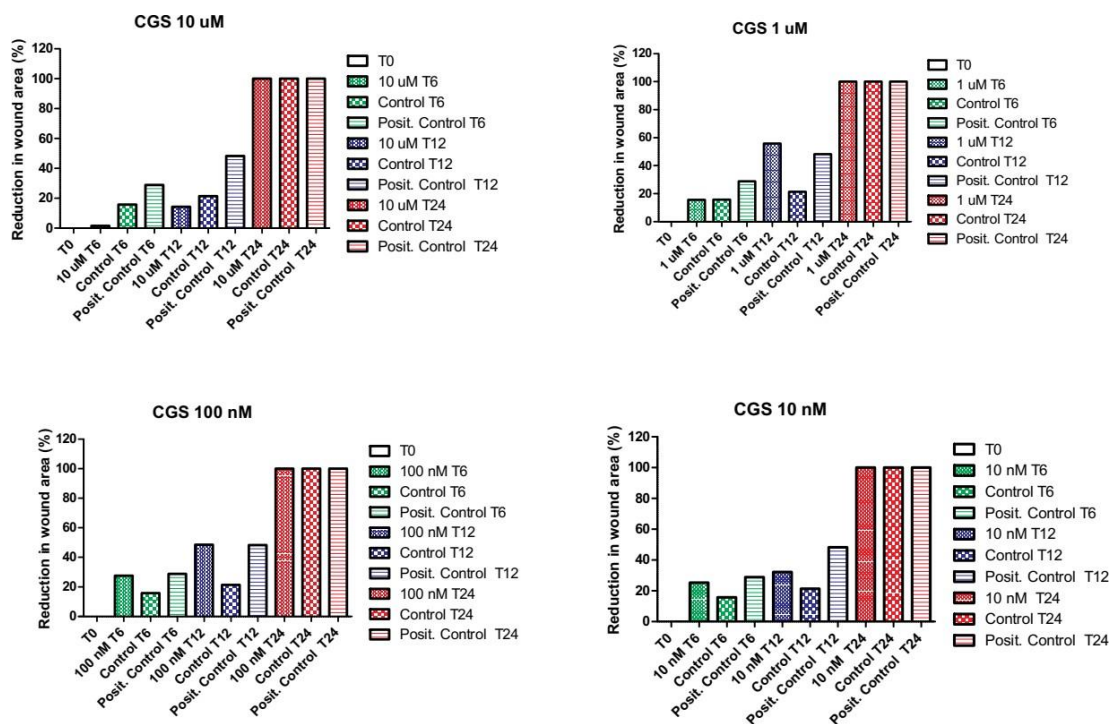


Figure 3.6: Effect of CGS21680 on wound healing assay at 10, 100, 1000, 10000 nM at 0, 6, 12, and 24 hrs. The results represent the average of three independent experiments.

The lowest concentration tested was set close to the K_i of the compound under evaluation, at the $A_{2A}AR$, while the other 2 concentrations have been set at higher levels in order to understand how efficiency change with concentration. Each experiment was conducted in comparison with the control, untreated sample, and with the positive control (EGF 10 nM).

As shown is Figure 3.6, CGS21680 induces an higher repair of the wound thorough the migration of fibroblasts after 6 and 12 hrs at 10 and 100 nM concentration respect to the control even if it remains less or equal potent than the positive control: at 100 nM at 12 hrs CGS and EGF show the same effect.

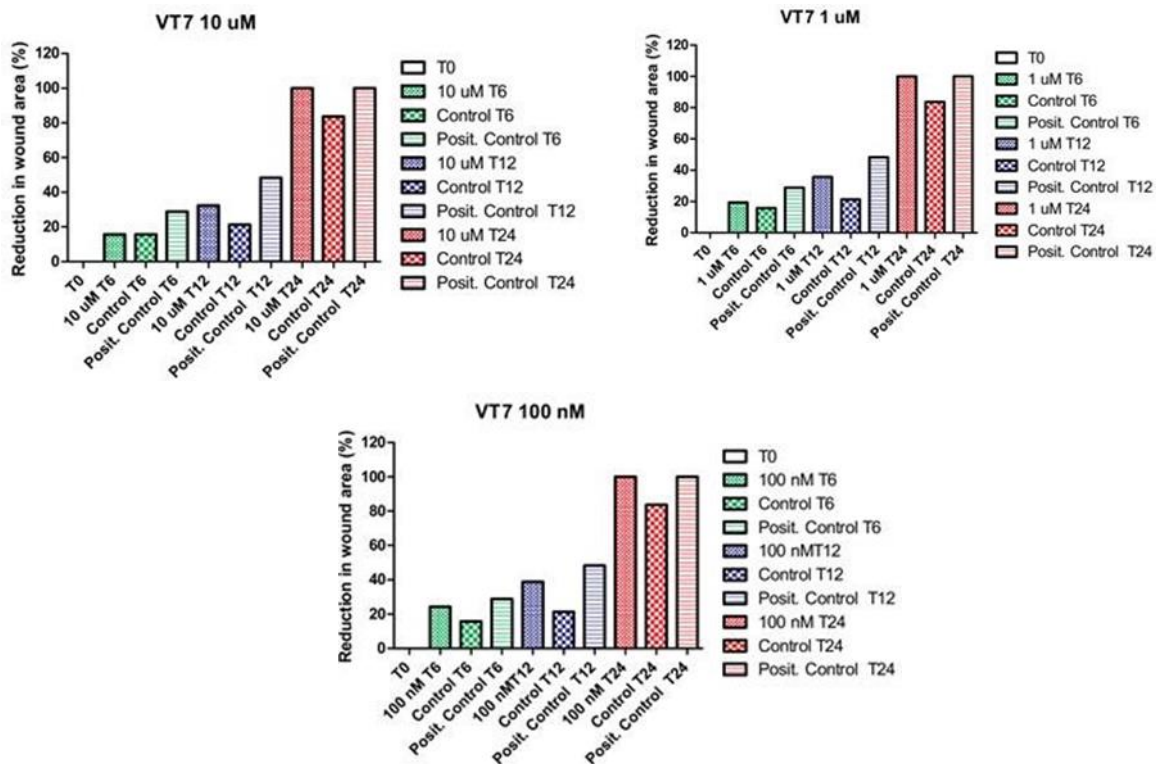


Figure 3.7: Effect of VT 7 on wound healing assay at 100, 1000, 10000 nM at 0, 6, 12, and 24 hrs. The results represent the average of three independent experiments.

At 24 hrs there is no difference between CGS21680, control, and positive control: this is an expected result since the assay is done with live cells having ability of self-growth. This result allows us to conclude that CGS21680 is able to stimulate the growth of fibroblasts and, even if these data are already known, they show that the assay used here is efficient and correct⁹⁶. At 10 μ M the loss of the ability of CGS21680 to stimulate cell growth is probably due to a toxic effect at this concentration and CGS21680 became lethal for cells.

The results on the scratch wound assay of VT 7 (Figure 3.7) showed that, at 100 nM the maximum effect has been obtained. The higher reparation of the scratched area respect to the control, at T6 and also at T12, demonstrates an effect on the fibroblasts migration respect to the untreated batch, even if it did not reach the effect of EGF. Also in this case the percentage of repair decreases at higher concentrations probably due to a toxic effect.

Table 3.3: Activity of tested compounds **12**, **16-22** at different concentrations and at different time points in comparison with EGF (positive control) and control, in the wound-healing assay.

Cpd	Conc. (nM)	% repair at time point (h)			Normalized effect to the control at time point (h)		
		T6	T12	T24	T6	T12	T24
CGS	10	25.28	32.12	100.00	1.60	1.50	1.00
"	100	27.53	48.50	100.00	1.74	2.27	1.00
"	1000	15.69	55.85	100.00	0.99	2.61	1.00
"	10000	1.46	14.21	100.00	0.09	0.66	1.00
EGF		28.88	48.20	100.00	1.83	2.25	1.00
Control		15.79	21.40	100.00	1.00	1.00	1.00
VT 7	100	24.26	38.88	87.00	1.54	1.82	1.04
"	1000	19.33	35.72	91.00	1.22	1.67	1.09
"	10000	15.65	32.33	100.00	0.99	1.51	1.19
EGF		28.88	48.20	100.00	1.83	2.25	1.19
Control		15.79	21.40	83.73	1.00	1.00	1.00
12	50	33.25	52.39	100.00	1.20	1.15	1.00
"	200	54.97	85.87	100.00	1.98	1.89	1.00
"	1000	42.38	57.99	100.00	1.53	1.23	1.00
EGF		40.86	56.69	100.00	1.47	1.25	1.00
Control		27.71	45.44	100.00	1.00	1.00	1.00
16	500	21.06	35.60	87.00	1.19	1.34	1.18
"	1500	31.04	65.79	91.00	1.76	2.48	1.23
"	3000	27.05	48.20	100.00	1.53	1.81	1.35
EGF		20.90	41.16	100.00	1.18	1.55	1.35
Control		17.67	26.58	74.00	1.00	1.00	1.00
17	10	39.20	60.19	100.00	1.93	1.53	1.00
"	60	42.55	69.58	100.00	2.09	1.77	1.00
"	300	14.49	53.83	100.00	0.71	1.37	1.00
EGF		34.27	71.49	100.00	1.69	1.82	1.00
Control		20.30	39.28	100.00	1.00	1.00	1.00
18	500	17.83	30.15	82.53	1.11	1.23	1.14
"	2000	28.21	37.37	82.97	1.76	1.52	1.14
"	10000	10.26	12.33	25.50	0.64	0.50	0.35
EGF		18.99	39.51	100.00	1.18	1.61	1.38
Control		16.05	24.57	72.67	1.00	1.00	1.00
19	50	30.25	50.39	100.00	0.98	1.10	1.00
"	200	57.97	80.26	100.00	1.88	1.76	1.00
"	800	40.38	52.99	100.00	1.31	1.16	1.00
EGF		38.86	52.47	100.00	1.26	1.15	1.00
Control		30.83	45.67	100.00	1.00	1.00	1.00
20	20	39.47	74.09	100.00	0.84	0.97	1.00
"	100	55.58	83.72	100.00	1.18	1.09	1.00
"	200	86.69	95.75	100.00	1.85	1.27	1.00
EGF		75.40	100.00	100.00	1.61	1.31	1.00
Control		46.76	76.40	100.00	1.00	1.00	1.00
21	20	30.83	73.15	100.00	1.80	1.19	1.00
"	100	42.72	74.26	100.00	2.48	1.21	1.00
"	500	40.24	75.17	100.00	2.34	1.22	1.00
EGF		29.56	70.67	100.00	1.72	1.15	1.00
Control		17.19	61.31	100.00	1.00	1.00	1.00
22	2	44.39	75.05	100.00	0.94	0.98	1.00
"	10	53.63	81.04	100.00	1.15	1.06	1.00
"	50	87.58	93.87	100.00	1.87	1.23	1.00
EGF		75.40	100.00	100.00	1.61	1.31	1.00
Control		46.76	76.40	100.00	1.00	1.00	1.00

There is a noticeable variability of the repairing effect both for the control and for EGF (compare the % of repair and control in table 3 left part). In fact, in any case both at T6 and at T12 the growth rate of fibroblasts, expressed in percentage change according to preparation, ranged 15.79-46.76% repaired area at T6, 21.40 – 76.40% at T12 for the control; 18.99—75.40 at T6 and 41.16 – 100% at T12 for EGF, although the preparations were evaluated at the same conditions (concentration in the case of EGF). These data demonstrated a great variability of the self-reparative ability of the fibroblasts and hence a great variability of the capacity of compounds and EGF to modulate the wound-healing. On the other hand, almost all the preparations showed complete reparation of the wound at T24.

The great variability for control at T6 and T12 required an elaboration of the data obtained through a normalization of the repaired area of the tested compound and EGF respect to the effect of the control in order to remove the divergence for the better interpretation of the effect of the tested compounds in the single preparation (Table 3.3, blue part).

The values reported on the blue side were computed based on the effect of each single tested compound. To do such calculations it was considered the control as reference point and it was evaluated the efficacy of each tested compound according to the control. Hence, the growth rate percentage induced by each compound was divided by the growth rate value of the control allowing to have the proportion of the effect on the repairing ability of the compounds respect to the growth rate of each preparation. In this way, the growth rate induced by each compound was converted into the same scale taking in consideration the growth rate of each preparation. The calculations were made at T6, T12, and T24 for each of the tested compound at the different concentrations and also for EGF.

However at certain highest concentrations a lower effect was reported. This experimental observation was hypothesized as being the result of a toxic effect. Most of the tested compounds an ability to repair the wound superior than to that of the control. In fact, the effect at the different time, T6 and T12, the normalized effect is higher than 1 which is the value of the control, demonstrating their effectiveness in wound-healing.

Some of the new compounds showed an ability to increase fibroblasts migration higher respect to the positive control EGF. In fact, at the concentration of 200 nM compound **12** showed a doubled effect respect to the control (1.98 at T6 and 1.89 at T12 versus 1.00 of the control). The same compound resulted also more effective than EGF (1.47 at T6, 1.25 at T12).

The same results have been observed for compound **16** at both concentrations 1.5 and 3 μM with the normalized effect of 1.76 and 1.53 at T6, and 2.48, 1.81 at T12 versus that of EGF (1.18 at T6 and 1.55 at T12).

Compounds **17**, **18**, and **19** resulted more active respect to the positive control only at specific concentration and at T6, generally (**17**: effect 2.09 at 60 nM versus EGF 1.69; **18**: effect 1.76 at 2 μM versus EGF 1.18; **19**: effect 1.88 at 200 nM versus EGF 1.26).

It is worthwhile to note that, compound **21** bearing a phenylethylamino chain in 2-position of the tetrazolynucleoside, resulted, in general, more active of the positive control at all the three tested concentrations at T6 and also at T12 (**21**: 1.80, 2.48, 2.34 at 20, 100, 500 nM, respectively, at T6; 1.19, 1.21, 1.22, at the same concentration, at T12; versus EGF 1.72 and 1.15 at T6 and T12, respectively). This compound **21** showed a comparable activity as compound **16** but in this case the activity was obtained at higher concentrations (**16**: 1.98 and 1.53 at 1500 nM, respectively, versus **21**: 1.80, 2.48 and 2.34 at 20, 100, 500 nM, respectively). This showed the higher activity among the new compounds. Furthermore, it is possible to argue that the thioalkyl chain in 2-position did not favor the activity of the corresponding nucleosides respective to the arylalkylamino chain.

The activity of this compounds, in the present assay, demonstrated that their $A_3\text{AR}$ antagonist behavior do not interfere with their ability to stimulate fibroblasts migration. Other experiments are necessary to demonstrate if the $A_3\text{AR}$ antagonist activity could be beneficial in the wound healing.

3.5 Conclusion

In general, in the wound–healing assay compounds **12**, **16-22** showed an agonist effect justified by their growth stimulating effect on fibroblasts which is dependent to their binding affinity. In fact, compound **17**, which showed a good binding affinity, at the $A_{2A}\text{AR}$ showed also a good behavior at the scratched wound test. On the other hand, compounds **16** and **18** described as compounds with low $A_{2A}\text{AR}$ affinity showed a low activity as fibroblasts migration stimulatory agents.

Moreover this promising effect supports the fact that wound healing effect resulting from $A_{2A}\text{AR}$ activation is not affected by simultaneous blockage of A_3 .

Moreover, at high doses, some compounds showed to inhibit wound healing showing a percentage of repair lower than the untreated batch. This result could be explained with a toxic effect obtained at these concentrations.

The evaluation of the ability of such compound to revert wound demonstrate they are suitable for the use in the repair of skin and possibly to be used for pathologies as diabetic foot ulcers.

3.6 Experimental section

3.6.1 Materials and methods

Thin layer chromatography (TLC)

The reactions were monitored by thin layer chromatography (TLC), using TLC plates pre-coated with silica gel 60 (F254, Merck); the thickness of the silica layer is 0.25 mm. The products were visualized by UV radiation ($\lambda = 254$ nm) and iodine vapours.

Column chromatography

For flash chromatography, it was used Fluka silica gel 230-400 mesh. When the reaction mixture was not soluble in the eluent, it was prepared out a dry-load.

Nuclear magnetic resonance (NMR)

All products reported showed an ^1H NMR spectrum in agreement with the assigned structure. The ^1H NMR spectra were obtained with a Varian Mercury 400 MHz spectrometer; δ in ppm, J in Hz. All exchangeable protons were confirmed by addition of D_2O .

Mass spectroscopy (MS)

Mass spectroscopic analyses were performed by ESI-mass with single quadrupole analyser (HP 1100 MSD).

Melting point

The melting points were determined with a Büchi apparatus and have not been modified.

3.6.2 Chemistry

2',3'-O-isopropylidene-1-O-methyl-D-ribose¹⁵⁸ (2): 2,2-Dimethoxypropane (20.5 mL, 166.53 mmol), and 70% HClO₄ (4.0 mL) were added to a suspension of D-ribose (**1**) (10.0 g, 66.61 mmol) in acetone (80 mL). The mixture was stirred at room temperature for 4 h, and MeOH (13.3 mL) was then added and further stirred for 2 h more. The mixture was cooled on an ice bath, and a 30% Na₂CO₃ solution (30 mL) was slowly added and the pH was checked to be basic. The precipitate was filtered and washed with EtOAc (3 x 15 mL). The filtrate was concentrated and diluted with a mixture of EtOAc (100 mL) and water (50 mL). The phases were decanted, and the aqueous one was extracted with EtOAc (2 x 60 mL). The organic phases were washed with brine, dried over anhydrous NaSO₄, and filtered. The filtrate was dried under vacuum to afford **2** (13.047 g, 63.89 mmol) as a yellow oil. This was used in the next step without further purification. Yield: 96%; ¹H-NMR (DMSO-d₆) δ: 1.23 (s, 3H, CH₃), 1.35 (s, 3H, CH₃), 3.18 (s, 3H, OCH₃), 3.30 (m, 1H, HCH-5'), 3.35 (m, 1H, HCH-5'), 3.98 (q, *J*=6.0 Hz, 1H, H-4'), 4.51 (app d, *J*=6.0 Hz, 1H, H-3'), 4.65 (app d, *J*=6.0 Hz, 1H, H-2'), 4.84 (t, *J* = 5.6 Hz, 1H, OH), 4.85 ppm (app s, 1H, H-1').

5'-Carboxyl-2',3'-O-isopropylidene-1-O-methyl-D-ribose¹⁵⁸ (3): **2** (13.05 g, 63.89 mmol) was dissolved in EtOAc (104 mL) and a 6% NaHCO₃ aqueous solution (44.7 mL, 31.95 mmol), KBr (684 mg), and TEMPO (50 mg) were added. The mixture was cooled to 0 °C, and then, a solution of NaHCO₃ (1.932 g, 23.00 mmol) in 5% NaClO (commercial bleach, 232 mL) was slowly added. When the addition was complete, the reaction was stirred at room temperature for 3 h. Then, a saturated aqueous solution of NaHCO₃ (10 mL) and water (10 mL) were added, the phases separated, and the aqueous one was acidified to pH 3 with 3 M HCl and extracted with EtOAc (3 x 150 mL). The organic phase was dried over anhydrous Na₂SO₄, filtered, and concentrated to provide a residue, which was washed with cold hexane (3 x 30 mL). After drying under vacuum, **3** (10.250 g, 46.97 mmol) was obtained as a white crystalline solid, which was directly used in the next step. Yield: 73%. M. p.: 118-121 °C; ¹H-NMR (DMSO-d₆) δ: 1.24 (s, 3H, CH₃), 1.36 (s, 3H, CH₃), 3.26 (s, 3H, OCH₃), 4.48 (app d, *J* = 5.6 Hz, 1H, H-2'), 4.51 (app s, 1H, H-3'), 4.95 (app s, 1H, H-4'), 5.08 (d, *J* = 6.0 Hz, 1H, H-1'), 12.9 ppm (br s, 1H, COOH).

5'-Carboxamide-2',3'-O-isopropylidene-1-O-methyl-D-ribose¹⁵⁸ (4): The acid **3** (5.737 g, 26.29 mmol) was dissolved in dry EtOAc and SOCl₂ (27 mL, 37.07 mmol) was added. The reaction mixture was warmed to 60 °C for 3 h and then cooled to room temperature. Dry NH₃ was bubbled into the mixture maintaining the temperature between 0 °C and 10 °C for 15 min. Water (15 mL) and EtOAc (15 mL) were added, the aqueous phase was separated and washed with

EtOAc (2 x 15 mL). The organic layers were washed with brine, dried over anhydrous Na₂SO₄, filtered, and evaporated to dryness. The residue was recrystallized from a 1:4 mixture of diethylether and *n*-hexane to afford **4** (4.659 g, 21.45 mmol) as an off-white solid. Yield: 82%. M. p.: 127–130 °C; ¹H-NMR (DMSO-d₆) δ: 1.24 (s, 3H, CH₃), 1.37 (s, 3H, CH₃), 3.32 (s, 3H, OCH₃), 4.36 (app s, 1H, H-3'), 4.48 (app d, *J* = 6.0 Hz, 1H, H-2'), 4.99 (app s, 1H, H-4'), 5.07 (d, *J* = 5.6 Hz, 1H, H-1'), 7.11 (br s, 1H, HNHCO) 7.29 ppm (br s, 1H, HNHCO).

4'-Nitril-2',3'-O-isopropylidene-1-O-methyl-D-ribose¹⁵⁸ (**5**): POCl₃ (7.0 mL, 75.35 mmol) was added drop wise to a solution of **4** (3.254 g, 14.98 mmol) in EtOAc (39.4 mL), DMF (6.4 mL), and Et₃N (10.9 mL, 78.05 mmol) cooled to 0 °C. The reaction was stirred for 2 h at 0 °C and quenched by the addition of NaHCO₃ saturated aqueous solution (6.5 mL). The layers were separated, the aqueous phase was extracted with EtOAc (2 x 10 mL), and the combined organic layers were washed with NaHCO₃ saturated aqueous solution (2 x 15 mL) and brine. The organic layer was dried over anhydrous Na₂SO₄, filtered, and evaporated to dryness. The residue was purified over a flash column eluting with *n*-hexane/EtOAc 99:1 to 98:2 to obtain a yellow gum, which was thoroughly dried under vacuum to obtain **5** (1.827 g, 9.17 mmol) as yellow vitreous solid. Yield: 61%. ¹H-NMR (DMSO-d₆) δ: 1.25 (s, 3H, CH₃), 1.35 (s, 3H, CH₃), 3.31 (s, 3H, OCH₃), 4.68 (app d, *J* = 5.6 Hz, 1H, H-3'), 5.12 (app d, *J* = 6.0 Hz, 1H, H-2'), 5.15 (app s, 1H, H-4'), 5.18 ppm (app s, 1H, H-1').

4'-(2-H-tetrazolyl)-2',3'-O-isopropylidene-1-O-methyl-D-ribose¹⁵⁸ (**6**): NaN₃ (948 mg, 14.85 mmol) was added portion wise to a mixture of **5** (1.450 g, 7.28 mmol) and NH₄Cl (833 mg, 15.58 mmol) in DMF (37 mL) cooled to 0 °C. The reaction mixture was then stirred for 5 min at 0 °C, 15 min at r.t., 1 h at 40 °C, slowly increased to 90 °C over 3 h, and then at 90 °C for 2 h. The mixture was then left to cool to r.t. and placed in an ice bath. It was quenched by the addition of 6% aqueous solution of NaNO₂ (2.5 mL) and water (7 mL) and the mixture was stirred at 0 °C for 2 h. the pH was adjusted to 2 with 2M H₂SO₄ and extracted with EtOAc (3 x 20 mL). The combined organic layer was washed with water (5 x 30 mL), dried over anhydrous Na₂SO₄, filtered, and concentrated to give a yellow gum, which was thoroughly dried to give **6** (1.327 g, 5.48 mmol) as a yellow amorphous solid. Yield: 75%. M. p.: 119 - 121 °C; ¹H-NMR (DMSO-d₆) δ: 1.31 (s, 3H, CH₃), 1.43 (s, 3H, CH₃), 3.01 (s, 3H, OCH₃), 4.63 (app d, *J*=5.6 Hz, 1H, H-3'), 5.07 (app s, 1H, H-2'), 5.50 (app s, 1H, H-4'), 5.53 ppm (d, *J* = 6.0 Hz, 1H, H-1').

4'-(2-Ethyl-tetrazolyl)-2',3'-O-isopropylidene-1-O-methyl-D-ribose¹⁵⁸ (**7**), **4'-(1-ethyl-tetrazolyl)-2',3'-O-isopropylidene-1-O-methyl-D-ribose**¹⁵⁸ (**8**): Dry K₂CO₃ (908 mg, 6.57 mmol) was added to a stirred solution of **6** (1.223 g, 5.09 mmol) and ethyliodide (528 μL, 6.57

mmol) in dry acetone (8.5 mL). The reaction was stirred at 40 °C for 3 h and then cooled to r.t. Cyclohexane was added, and the precipitate was separated and further washed with more cyclohexane (thoroughly washed till there was no more product in it). The filtrate was concentrated under vacuum and the residue was made into slurry and purified over a flash column. The column was eluted with *n*-hexane/EtOAc 94:6 to obtain **7** (865 mg, 3.17 mmol) as a colourless oil and then with *n*-hexane/EtOAc 92:8 – 90:10 to get **8** (427 mg, 1.58 mmol) as a white solid. Yields: **7** (62%), **8** (31%), overall (93%); **7**: m. p.: n.d.; ¹H-NMR (DMSO-d₆) δ: 1.31 (s, 3H, CH₃), 1.43 (s, 3H, CH₃), 1.47 (t, *J*=7.2 Hz, 3H, CH₃), 2.98 (s, 3H, OCH₃), 4.66 (m, 3H, H-3' & CH₂), 5.03 (app s, 1H, H-2'), 5.35 (app s, 1H, H-4'), 5.45 ppm (d, *J* = 6.0 Hz, 1H, H-1').

8: m. p.: 111–113 °C; ¹H-NMR (DMSO-d₆) δ: 1.33 (s, 3H, CH₃), 1.44 (s, 3H, CH₃), 1.47 (t, *J*=7.2 Hz, 3H, CH₃), 2.90 (s, 3H, OCH₃), 4.48 (q, *J*=7.2 Hz, 2H, CH₂), 4.71 (app d, *J* = 6.0 Hz, 1H, H-3'), 5.06 (app s, 1H, H-2'), 5.62 (app s, 1H, H-4'), 5.66 ppm (d, *J* = 5.6 Hz, 1H, H-1').

4'-(2-Ethyl-tetrazolyl)-1',2',3'-O-tetracethyl-D-ribose¹⁵⁸ (**9A**): A solution of **7** (856 mg, 3.17 mmol) in TFA (2 mL, 26.12 mmol) and H₂O (218 μL, 12.11 mmol) was stirred at r.t. for 6 h. The mixture was evaporated to dryness under reduced pressure and the residue was co-evaporated with dry CH₂Cl₂ (3 x 5 mL). The residue was freeze-dried overnight and then dissolved in CH₂Cl₂ (11.1 mL), and DMAP (23 mg, 0.19 mmol) was added. The solution was cooled to 0 °C and dry Et₃N (1.6 mL, 11.19 mmol) and Ac₂O (1.8 mL, 18.64 mmol) were added. The reaction mixture was stirred at r.t. for 3 h. After the removal of all volatiles under vacuum, the residue was made into slurry and purified over a flash column (*n*-hexane/EtOAc 88:12 to 80:20) to afford an inseparable mixture of the α- and β-anomers of **9A** (697 mg, 2.04 mmol) as a slightly yellow transparent oil. Yield: 65%.

9A (α-anomer) - ¹H-NMR (DMSO-d₆) δ: 1.50 (t, *J* = 7.2 Hz, 3H, CH₃), 2.06 (s, 3H, CH₃), 2.08 (s, 3H, CH₃), 2.10 (s, 3H, CH₃), 4.71 (q, *J* = 7.2 Hz, 2H, CH₂), 5.48 (m, 2H, H-3' and H-2'), 5.58 (m, 1H, H-4'), 6.43 ppm (d, *J* = 4.8 Hz, 1H, H-1').

9A (β-anomer) - ¹H-NMR (DMSO-d₆) δ: 1.50 (t, *J*=7.2 Hz, 3H, CH₃), 2.00 (s, 3H, CH₃), 2.01 (s, 3H, CH₃), 2.12 (s, 3H, CH₃), 4.71 (q, *J*=7.2 Hz, 2H, CH₂), 5.43 (m, 2H, H-3' & H-2'), 5.78 (m, 1H, H-4'), 6.15 ppm (s, 1H, H-1').

4'-(1-Ethyl-tetrazolyl)-1',2',3'-O-tetracethyl-D-ribose¹⁵⁸ (**9B**): A solution of **8** (1.5g, 5.55 mmol) in TFA (3.5 mL, 45.7 mmol) and H₂O (0.38 mL, 21.2 mmol) was stirred at r.t. for 6 h. The mixture was evaporated to dryness under reduced pressure and the residue was co-evaporated with dry CH₂Cl₂ (3 x 5 mL). The residue was freeze-dried overnight and then dissolved in

CH₂Cl₂ (11.1 mL), and DMAP (39.6 mg, 0,32 mmol) was added. The solution was cooled to 0 °C and dry Et₃N (2.7 mL, 19.4 mmol) and Ac₂O (3.1 mL, 32.6 mmol) were added. The reaction mixture was stirred at r.t. for 3 h. After the removal of all volatiles under vacuum, the residue was made into slurry and purified over a flash column (*n*-hexane/EtOAc 88:12 to 80:20) to afford an **9B** (968 mg, 2.83 mmol) as a slightly yellow transparent oil. Yield: 55%. ¹H-NMR (DMSO-d₆) δ: 1.53 (t, *J* = 7.2 Hz, 3H, CH₃), 1.95 (s, 3H, CH₃), 2.08 (s, 3H, CH₃), 2.12 (s, 3H, CH₃), 4.02 (q, *J* = 7.2 Hz, 2H, CH₂), 5.45 (m, 2H, H-3' & H-2'), 5.68 (m, 1H, H-4'), 6.17 ppm (s, 1H, H-1').

2,6-Dichloro-N9-[4'-(2-ethyl-tetrazolyl)]-2',3'-O-diacethyl-purinoriboside (11): Trimethylsilyl triflate (635 μL, 3.51 mmol) was added dropwise to a suspension of 2,6-dichloropurine (**10**) (478 mg, 2.53 mmol), **9A** (660 mg, 1.93 mmol), and DBU (435 μL, 2.91 mmol) in dry acetonitrile (8.6 mL) cooled at 0 °C. The final solution was stirred at room temperature for 21 h and quenched by the addition of H₂O (10 ml). The product was extracted with EtOAc (3 x 20 ml). The combined organic layers were dried over anhydrous Na₂SO₄, filtered, and concentrated under vacuum. The residue was made into slurry and purified over flash column eluting with *n*-hex/CHCl₃/MeOH 90:8:2 to afford **11** as a mixture of both α and β anomer that was not possible to separate.

2-Chloro-4'-(2-ethyl-tetrazolyl)-Ado (β-anomer)¹⁵⁸ (12) and 2-chloro-4'-(2-ethyl-tetrazolyl)-Ado α-anomer (13): NH₃ was condensed into a steel vessel at -78 °C and **11** (400 mg, 0.85 mmol) was added. The steel vessel was tightly closed and left to react at r.t. for 6 h. The content was then transferred into a flask by solvent and co-evaporated with MeOH (5 x 10 mL). The residue was further dried on an oil pump to eliminate all NH₄Cl. It was then recrystallized from MeOH to afford **12** as a white powder in 55% yield and **13** in 35% yield. **12**: m. P.: 214–216 °C; ¹H-NMR (DMSO-d₆) δ: 1.52 (t, *J* = 7.2 Hz, 3H, CH₃), 4.54 (q, *J* = 4.4 Hz, 1H, H-3'), 4.71 (q, *J* = 7.2 Hz, 2H, CH₂), 4.77 (q, *J* = 5.2 Hz, 1H, H-2'), 5.20 (d, *J* = 4.4 Hz, 1H, H-4'), 5.79 (d, *J* = 6.8 Hz, 1H, OH), 5.82 (d, *J* = 6.8 Hz, 1H, OH), 6.02 (d, *J* = 5.2 Hz, 1H, H-1'), 7.85 (br s, 2H, NH₂), 8.40 ppm (s, 1H, H-8). ESI-MS: positive mode *m/z* 367.9 [M+H]⁺, 389.8 [M+Na]⁺, 756.9 [2M+Na]⁺. **13**: ¹H-NMR (DMSO-d₆) δ: 1.50 (t, *J* = 7.6 Hz, 3H, CH₃), 4.41 (q, *J* = 4.4 Hz, 1H, H-3'), 4.54 (q, *J* = 7.2 Hz, 1H, H-2'), 4.70 (q, *J* = 5.6 Hz, 2H, CH₂), 5.32 (d, *J* = 4.4 Hz, 1H, H-4'), 5.85 (d, *J* = 6.0 Hz, 1H, OH), 6.02 (d, *J* = 6.0 Hz, 1H, OH), 6.15 (d, *J* = 5.6 Hz, 1H, H-1'), 7.39 (br s, 2H, NH₂), 8.61 ppm (s, 1H, H-8).

2-(Methylthiophenyl)-4'-(2-ethyl-tetrazolyl)-Ado (16): A mixture of **12** (50 mg, 0.14 mmol), benzyl mercaptan (82 μL, 0.70 mmol), and K₂CO₃ (39 mg, 0.28 mmol) in dry DMF (1.4 mL)

was heated in a steel vessel at 120 °C for 24 h. After the removal of volatiles under vacuum, the residue was made into slurry and purified over a flash column, eluting with CH₂Cl₂/MeOH 99:1 to 97:3. The correct fractions were pooled and evaporated to dryness. The obtained solid was recrystallized from isopropanol to afford **16** (58 mg, 0.13 mmol) as a white powder. Yield: 93 %. M. p.: 102-105 °C; ¹H-NMR (DMSO-*d*₆) δ: 1.50 (t, *J*=7.2 Hz, 3H, CH₃), 4.34 (s, 2H, CH₂), 4.60 (app s, 1H, H-3'), 4.68 (q, *J*=7.2 Hz, 2H, CH₂), 4.80 (app s, 1H, H-2'), 5.18 (d, *J*=4.8 Hz, 1H, H-4'), 5.88 (app s, 1H, OH), 5.91 (app s, 1H, OH), 6.08 (d, *J*=5.2 Hz, 1H, H-1'), 7.20 (m, 1H, Ph), 7.27 (m, 2H, Ph), 7.43 (m, 4H, Ph and NH₂), 8.27 ppm (s, 1H, H-8). ¹³C-NMR (DMSO-*d*₆, 75 MHz) δ: 14.77, 35.04, 48.92, 73.94, 74.31, 77.57, 88.41, 117.34, 127.55, 129.01, 129.77, 138.89, 139.26, 150.86, 156.05, 164.22, 164.81 ppm. ESI-MS: positive mode *m/z* 455.9 [M+H]⁺, 477.8 [M+Na]⁺.

2-(2-Phenyl-ethylthio)-4'-(2-ethyl-tetrazolyl)-Ado (17): A mixture of **12** (150 mg, 0.41 mmol), phenylethanthiol (275 μL, 2.05 mmol), and K₂CO₃ (113 mg, 0.82 mmol) in dry DMF (4.1 mL) was heated in a steel vessel at 120 °C for 24 h. After the removal of volatiles under vacuum, the residue was made into slurry and purified over a flash column, eluting with CHCl₃/MeOH 99.5:0.5. The correct fractions were pooled and evaporated to dryness. The obtained solid was recrystallized from isopropanol to afford **17** (148 mg, 0.32 mmol) as light yellowish crystals. Yield: 78%. M. p.: 158-160 °C; ¹H-NMR (DMSO-*d*₆) δ: 1.50 (t, *J* = 7.2 Hz, 3H, CH₃), 2.96 (t, *J* = 6.8 Hz, 2H, CH₂), 3.26 (m, 2H, CH₂), 4.59 (q, *J* = 5.2 Hz, 1H, H-3'), 4.68 (q, *J* = 7.2 Hz, 2H, CH₂), 4.87 (q, *J* = 5.6 Hz, 1H, H-2'), 5.20 (d, *J* = 4.4 Hz, 1H, H-4'), 5.80 (m, 2H, OH x 2), 6.10 (d, *J* = 5.2 Hz, 1H, H-1'), 7.21 (m, 1H, Ph), 7.31 (m, 4H, Ph), 7.41 (br.s, 2H, NH₂), 8.28 ppm (s, 1H, H-8). ¹³C-NMR (DMSO-*d*₆, 75 MHz) δ: 14.77, 32.42, 36.18, 48.92, 73.81, 74.38, 77.75, 88.07, 117.26, 126.85, 129.06, 129.41, 138.80, 141.27, 151.07, 156.12, 164.56, 164.84 ppm. ESI-MS: positive mode *m/z* 469.8 [M+H]⁺, 491.8 [M+Na]⁺.

2-(3-Phenyl-propylthio)-4'-(2-ethyl-tetrazolyl)-Ado (18): A mixture of **12** (50 mg, 0.14 mmol), phenylpropanethiol (107 μL, 0.70 mmol), and K₂CO₃ (39 mg, 0.28 mmol) in dry DMF (1.4 mL) was heated in a steel vessel at 120 °C for 24 h. After the removal of volatiles under vacuum, the residue was made into slurry and purified over a flash column, eluting with CH₂Cl₂/MeOH 98:2 to 96:4. The correct fractions were pooled and evaporated to dryness. The obtained solid was recrystallized from an EtOAc/*n*-Hexane 1:9 mixture to afford **18** (42 mg, 0.09 mmol) as a white powder. Yield: 64%. M. p.: 87-90 °C; ¹H-NMR (DMSO-*d*₆) δ: 1.49 (t, *J* = 7.2 Hz, 3H, CH₃), 1.94 (quint., *J* = 6.4 Hz, 2H, CH₂), 2.70 (t, *J* = 7.2 Hz, 2H, CH₂), 3.02 (m, 1H, H-CH), 3.10 (m, 1H, H-CH), 4.67 (m, 3H, H-3' and CH₂), 4.85 (app s, 1H, H-2'), 5.17 (d, *J* = 4.8 Hz, 1H, H-4'), 5.78

(app s, 1H, OH), 5.85 (app s, 1H, OH), 6.03 (d, $J = 4.4$ Hz, 1H, H-1'), 7.16 (m, 1H, Ph), 7.23 (m, 4H, Ph), 7.37 (br s, 2H, NH₂), 8.26 ppm (s, 1H, H-8). ¹³C-NMR (DMSO-d₆, 75 MHz) δ : 14.77, 30.36, 31.81, 35.01, 48.89, 73.71, 74.33, 77.51, 88.54, 117.31, 126.47, 129.02, 129.04, 139.06, 142.18, 150.88, 156.06, 164.65, 164.78 ppm. ESI-MS: positive mode m/z 484.3 [M+H]⁺, 506.2[M+Na]⁺.

2-(2-*p*-Chloro-phenyl-ethylthio)-4'-(2-ethyl-tetrazolyl)-Ado (19): A mixture of **12** (50 mg, 0.14 mmol), 4-chlorophenylethyl mercaptan (121 mg, 0.70 mmol), and K₂CO₃ (39 mg, 0.28 mmol) in dry DMF (1.4 mL) was heated in a steel vessel at 120 °C for 24 h. After the removal of volatiles under vacuum, the residue was made into slurry and purified over a flash column, eluting with CH₂Cl₂/MeOH 99:1 to 98:2. The correct fractions were pooled and evaporated to dryness. The obtained solid was recrystallized from methanol to afford **19** (43 mg, 0.085 mmol) as a white powder. Yield: 61 %. M. p.: 176-178 °C; ¹H-NMR (DMSO-d₆) δ : 1.50 (t, $J = 7.2$ Hz, 3H, CH₃), 2.95 (t, $J = 7.2$ Hz, 2H, CH₂), 3.25 (m, 2H, CH₂), 4.57 (q, $J = 4.0$ Hz, 1H, H-3'), 4.68 (q, $J = 7.2$ Hz, 2H, CH₂), 4.86 (q, $J = 4.8$ Hz, 1H, H-2'), 5.20 (d, $J = 3.6$ Hz, 1H, H-4'), 5.82 (m, 2H, OH x 2), 6.10 (d, $J = 5.6$ Hz, 1H, H-1'), 7.35 (app s, 4H, Ph), 7.43 (br.s, 2H, NH₂), 8.28 ppm (s, 1H, H-8). ¹³C-NMR (DMSO-d₆, 75 MHz) δ : 14.77, 32.20, 35.48, 48.91, 73.84, 74.40, 77.75, 88.01, 117.27, 128.95, 131.35, 131.46, 138.74, 140.30, 151.05, 156.14, 164.38, 164.85 ppm. ESI-MS: positive mode m/z 504.2 [M+H]⁺, 526.2 [M+Na]⁺.

2-(2-*p*-Methoxy-phenyl-ethylthio)-4'-(2-ethyl-tetrazolyl)-Ado (20): A mixture of **12** (50 mg, 0.14 mmol), 4-methoxyphenylethyl mercaptan (118 mg, 0.70 mmol), and K₂CO₃ (39 mg, 0.28 mmol) in dry DMF (1.4 mL) was heated in a steel vessel at 120 °C for 24 h. After the removal of volatiles under vacuum, the residue was made into slurry and purified over a flash column, eluting with CH₂Cl₂/MeOH 99:1 to 98:2. The correct fractions were pooled and evaporated to dryness. The obtained solid was recrystallized from an EtOAc/*n*-Hexane 1:9 mixture to afford **20** (13 mg, 0.026 mmol) as a white powder. Yield: 19%; M. p.: 174-176 °C; ¹H-NMR (DMSO-d₆) δ : 1.50 (t, $J = 7.6$ Hz, 3H, CH₃), 2.87 (m, 2H, CH₂), 3.22 (m, 2H, CH₂), 3.71 (s, 3H, OCH₃), 4.58 (m, 1H, H-3'), 4.68 (q, $J = 7.2$ Hz, 2H, CH₂), 4.86 (m, 1H, H-2'), 5.19 (app s, 1H, H-4'), 5.85 (app br.s, 2H, OH x2), 6.10 (d, $J = 4.0$ Hz, 1H, H-1'), 6.85 (d, $J = 7.6$ Hz, 2H, Ph), 7.23 (d, $J = 8.0$ Hz, 2H, Ph), 7.40 (br.s, 2H, NH₂), 8.27 ppm (s, 1H, H-8). ¹³C-NMR (DMSO-d₆, 75 MHz) δ : 14.75, 32.69, 35.28, 48.92, 55.64, 73.77, 74.37, 77.75, 88.02, 114.43, 117.18, 130.39, 133.21, 138.80, 151.05, 156.06, 158.36, 164.66, 164.82 ppm. ESI-MS: positive mode m/z 500.3 [M+H]⁺, 522.3 [M+Na]⁺.

2-(2-Phenyl-ethylamino)-4'-(2-ethyl-tetrazolyl)-Ado (21): A mixture of **12** (50 mg, 0.14 mmol) and phenylethylamine (2 mL) was heated in a steel vessel at 120 °C for 16 h. The reaction mixture was directly made into slurry and purified over a flash column, eluting with CH₂Cl₂/*c*-Hexane 90:10 to remove the excess phenylethylamine and then with CH₂Cl₂/MeOH 99:1 to 97:3. The correct fractions were pooled and evaporated to dryness. The obtained solid was recrystallized from an EtOAc/*n*-Hexane 1:9 mixture to afford **21** (17 mg, 0.038 mmol) as a white solid. Yield: 27%. M. p.: 92-95 °C; ¹H-NMR (DMSO-d₆) δ: 1.48 (t, *J* = 7.2 Hz, 3H, CH₃), 2.82 (t, *J* = 7.2 Hz, 2H, CH₂), 3.42 (q, *J* = 8.4 Hz, 2H, CH₂), 4.62 (m, 1H, H-3'), 4.66 (q, *J* = 7.6 Hz, 2H, CH₂), 4.79 (m, 1H, H-2'), 5.13 (d, *J* = 4.8 Hz, 1H, H-4'), 5.69 (d, *J* = 5.6 Hz, 1H, OH), 5.76 (d, *J* = 5.2 Hz, 1H, OH), 5.96 (d, *J* = 5.2 Hz, 1H, H-1'), 6.32 (t, *J* = 5.2 Hz, 1H, NH), 6.74 (br s, 2H, NH₂), 7.17 (m, 1H, Ph), 7.25 (m, 4H, Ph), 7.94 ppm (s, 1H, H-8). ¹³C-NMR (DMSO-d₆, 75 MHz) δ: 14.78, 36.02, 37.75, 43.49, 48.86, 73.74, 74.35, 77.22, 87.85, 126.56, 128.94, 129.44, 136.17, 140.83, 152.46, 156.56, 160.06, 164.93 ppm. ESI-MS: positive mode *m/z* 452.9 [M+H]⁺, 474.9 [M+Na]⁺, 927.1 [2M+Na]⁺.

2-(2-Phenyl-ethylalchoxy)-4'-(2-ethyl-tetrazolyl)-Ado (22): In a round bottom flask, the 2-phenyl-ethanol (1 ml, 8.35 mmol) was first activated with sodium metallic (30 mg, 1.3 mmol) in oil bath at 100 °C under stirring until the total consumption of sodium, then the solution was cooled at room temperature and **12** was then added under N₂ flow. The mixture was heated at 80 °C in oil bath and was left to react. After 4 h the reaction was complete, cooled and evaporated to dryness, made into slurry and purified on flash chromatography eluting with CH₂Cl₂/MeOH 99:1 to 97:3. Compound **22** was obtained as with solid (42 mg, 0.096 mmol). Yield: 45%. M. p.: 156-162 °C; ¹H-NMR (DMSO-d₆) δ: 1.52 (t, *J* = 7.3 Hz, 3H, CH₃), 3.02 (t, *J* = 6.8 Hz, 2H, CH₂), 4.41 (t, *J* = 6.7 Hz, 2H, CH₂), 4.65 (t, 1H, H-3'), 4.70 (q, *J* = 7.3 Hz, 2H, CH₂), 4.82 (m, 1H, H-2'), 5.18 (d, *J* = 4.4 Hz, 1H, H-4'), 5.78 (br s, 2H, 2xOH), 6.01 (d, *J* = 4.9 Hz, 1H, H-1'), 7.23 (m, 1H, Ph), 7.32 (m, 6H, NH₂+Ph), 8.19 (s, 1H, H-8) ppm. ESI-MS: positive mode *m/z* 454.0 [M+H]⁺, 476.0 [M+Na]⁺, 929.3 [2M+Na]⁺; negative mode *m/z* 488.1 [M-H]⁻.

2,6-Dichloro-N9-[4'-(1-ethyl-tetrazolyl)]-2',3'-O-diacethyl-purine (14): Trimethylsilyl triflate (635 µl, 3.51 mmol) was added dropwise to a suspension of 2,6-dichloropurine (**10**) (478 mg, 2.53 mmol), **9B** (660 mg, 1.93 mmol), and DBU (435 µl, 2.91 mmol) in dry acetonitrile (8.6 ml) cooled at 0 °C. The final solution was stirred at room temperature for 21 h and quenched by the addition of H₂O (10 ml). The product was extracted with EtOAc (3 x 20 ml). The combined organic layers were dried over anhydrous Na₂SO₄, filtered, and concentrated under vacuum. The

residue was made into slurry and purified over flash column eluting with *c*-hex/CHCl₃/MeOH 90:8:2 to afford **14** as a mixture of α and β anomer.

2-Chloro-4'-(1-ethyl-tetrazolyl)-Ado (15): NH₃ was condensed into a steel vessel at -78 °C and **14** (501 mg, 1,06 mmol) was added. The steel vessel was tightly closed and left to react at r.t. for 6 h. The content was then transferred into a flask by solvent and co-evaporated with MeOH (5 x 10 mL). The residue was further dried on an oil pump to eliminate all NH₄Cl. It was then recrystallized from MeOH to afford **15** (167 mg, 0.45 mmol) as a white powder. Yield: 43%. M. p.: 134-138 °C; ¹H NMR (DMSO-d₆) δ : 1.31 (t, *J* = 7.17 Hz, 3H, CH₃), 4.40 (q, *J* = 7.06 Hz, 1H, H-3'), 4.79 (d, *J* = 3.45 Hz, 2H, CH₂), 4.83 (t, *J* = 5.07 Hz, 1H, H-2'), 5.40 (d, *J* = 2.95 Hz, 1H, H-4'), 5.87 (d, *J* = 5.40 Hz, 1H, OH), 5.94 (d, *J* = 4.60 Hz, 1H, OH), 6.05 (d, *J* = 5.60 Hz, 1H, H-1'), 7.86 (br s, 2H, NH₂), 8.39 (s, 1H, H-8). ESI-MS: positive mode *m/z* 367.9 [M+H]⁺, 389.9 [M+Na]⁺, 756.9 [2M+Na]⁺; negative mode *m/z* 365.9 [M-H]⁻, 401.9 [M-H]⁻, 733.0 [2M-H]⁻.

2-(2-Phenyl-ethylthio)-4'-(1-ethyl-tetrazolyl)-Ado (23): **15** (78 mg, 0,21 mmol), phenylethanethiol (0.28 mL, 2.1 mmol), and K₂CO₃ (58.05 mg, 0.42 mmol) in dry DMF (2.1 mL) was heated in a steel vessel at 120 °C for 24 h. After the removal of volatiles under vacuum, the residue was made into slurry and purified over a flash column, eluting with CHCl₃/MeOH 99.5:0.5. The correct fractions were collected and evaporated to dryness. The obtained solid was recrystallized from isopropanol to afford **23** (12 mg, 0.025 mmol) as light yellowish crystals. Yield: 12%. M. p.: 98-102 °C; ¹H-NMR (DMSO-d₆) δ : 1.31 (t, *J* = 7.50 Hz, 3H, CH₃), 2.95 (m, 2H, CH₂Ph), 3.20 (m, 2H, CH₂S), 4.41 (q, *J* = 7.30 Hz, 2H, CH₂), 4.81 (q, *J* = 4.0 Hz, 1H, H-2'), 4.92 (q, *J* = 5.10 Hz, 1H, H-3'), 5.39 (d, *J* = 3.65 Hz, 1H, H-4'), 5.86 (d, *J* = 5.70 Hz, 1H, OH), 5.93 (d, *J* = 5.00 Hz, 1 H, OH), 6.12 (d, *J* = 5.00 Hz, 1 H, H-1), 7.22 (m, 1H, H-Ph), 7.33 (m, 4H, H-Ph), 7.42 (br s, 2H, NH₂), 8.25 (s, 1H, H-8). ESI-MS: positive mode *m/z* 469.9 [M+H]⁺, 491.8 [M+Na]⁺; negative mode *m/z* 468.0 [M-H]⁻, 937.2 [2M-H]⁻.

3.7 Biological assay

3.7.1 Cell culture

The Chinese hamster ovary cells (CHO) stably transfected with the desired ARs were grown in DMEM / F12 medium containing 10% FBS (fetal bovine serum), 100 U / ml penicillin, 100 μ g / ml streptomycin, 2.5 μ g / ml amphotericin B, 1 mM sodium pyruvate, 0.1 mg / ml genetecina (G418) and incubated at 37 °C in a gaseous mixture of 5% CO₂: 95% O₂.

3.7.2 Preparation of membranes

Cell membranes for binding assays were prepared mechanically detaching the cells from the petri and suspending them in a cold hypotonic buffer (5 mM Tris / HCl, 2 mM EDTA, pH 7.4). The cell suspension was homogenized (Ultra-Turrax, 2 x 15 sec at maximum speed) and the homogenate centrifuged for 10 min (4 °C) to 1000 g. The supernatant was subsequently centrifuged for 30 min (4 °C) at 100,000 g and the pellet containing the membrane proteins was resuspended in specific buffer for each receptor subtype (A₁: 50 mM Tris / HCl, pH 7.4; A_{2A}: 50 mM Tris / HCl, 10 mM MgCl₂, pH 7.4; A₃: 50 mM Tris / HCl, 10 mM MgCl₂, 1 mM EDTA, pH 8.25). The amount of the protein suspension was determined according to the Bradford method using the BCA Protein Assay Kit (Pierce), frozen in liquid nitrogen and stored at - 80 °C.

3.7.3 Binding assays

The dissociation constants of the radioligand (*K_D*) were calculated through saturation assays, while the dissociation constants of the compounds under study (*K_i*) were determined by competition experiments. All binding data were calculated by nonlinear regression curves using the software GraphPad Prism 5 (GraphPad Software, San Diego, CA, USA). For the increasing concentrations of radioligand saturation binding ([³H]-CCPA for the A₁ receptor subtype, [³H]-NECA for the A_{2A} receptor subtype and [³H]-HEMADO for the A₃ receptor) subtype were incubated in a total volume of 250 μL containing 0.2 U / ml of Ado deaminase (ADA) and 12 micrograms of membrane proteins in the specific buffer. In competition experiments for the A₁ receptor subtype wells containing 1 nM of [³H]-CCPA and the compound to be tested at increasing concentrations to a final volume of 200μL. The samples were left to incubate for 3 h at room temperature, filtered in a filter 96-well plate (UniFilter GF / C, Perkin-Elmer Life and Analytical Science, Boston, MA) using the FilterMate Cell Harvester (Perkin-Elmer) and washed 3 times with cold distilled water. After drying the filter plate at 40 °C for 30', they were added 20 μl of scintillating liquid (Microscint-20, Perkin-Elmer) to each well, and then the radioactivity was quantized with the MicroBeta2 Plate Counter (Perkin-Elmer). The conditions for binding experiments at A_{2A} and A₃ receptor subtypes were essentially the same as for the A₁AR using [³H]-NECA (*N*-ethylcarboxyamidoAdo) at a concentration of 10 nM and [³H]-HEMADO (2-(1-hexyne)-*N*⁶-methylAdo) at a concentration of 1 nM, respectively, as radioligands. The samples were incubated with 12 micrograms of protein for 3 h at room temperature and filtered as described above.

The non-specific binding was determined in the presence of 1 mM theophylline for the A₁ receptor, or 100 μM R-PIA (*N*⁶-(1-methyl-2-phenylethyl)Ado) for the A_{2A} and A₃ receptors.

3.7.4 GloSensor cAMP Assay

Cells, stably expressing the human A₁, A_{2A}, A_{2B}, or A₃ ARs and transiently the biosensor, were harvested in CO₂-independent medium and were counted in a Neubauer chamber. The desired number of cells was incubated in equilibration medium containing a 3% v/v GloSensor cAMP reagent stock solution, 10% *foetal* bovine serum (FBS), and 87% CO₂ independent medium. After 2 h of incubation at r.t., the cells were dispensed in the wells of a 384-well plate and, when a steady-state basal signal was obtained, agonists under study (or the reference agonist NECA), at different concentrations, were added. After 10 minutes various luminescence reads were performed at different incubation times^{167,168}.

The desired cell number was incubated in equilibration medium containing a 3% v/v GloSensor cAMP reagent stock solution, 10% *foetal* bovine serum (FBS), and 87% CO₂ independent medium. After 2 h of incubation, the cells were dispensed in wells of 384-well plate and, when a steady-state basal signal was obtained, agonists under study (or the reference agonist NECA), at different concentrations, were added. After 10 minutes various luminescence reads were performed at different incubation times.

3.7.5 Wound healing-migration assay

Five hundred thousand fibroblast cells were seeded on a 6-well plate. The day after the medium was aspirated and fresh 2% FBS medium with or without several concentrations of methanolic or aqueous extract was added. To create an artificial wound (0.5–1 mm) the cells were scratched once per well with a P10 pipette tip and the wound was allowed to heal for 24 h. After the scratch, fibroblasts were treated with the suitable concentration of compounds under study and they were examined at 0, 6, 12, and 24 h after treatment.

Untreated control and positive control (10 nM Epidermal Growth Factor, EGF) were also maintained. The average extent of wound closure was evaluated by measuring the area of the wound. The extent of cell migration into the wound area was photographed at the same location and measured using Image J as Image analysing software¹⁶⁹. Each experiment was performed in triplicate.

**CHAPTER 4: SYNTHESIS OF NEW ADENINE DERIVATIVES AS POTENT
ANTAGONIST OF THE HUMAN A₃AR**

4.1 Aim of the work

A₃AR subtype has been reported as an important therapeutic target in cancer and inflammatory diseases. Therefore for such purposes development of new ligands has been the target of many efforts and researches activities.

In particular, Volpini *et al.* reported in many papers the design and synthesis of new A₃AR antagonists consisting in substituted adenine derivatives and their structure activity relationship¹⁷⁰. In particular, they reported that the substitution of the bromine atom in C-8 position of the 8-bromo-9-ethyladenine (K_i hA₁AR = 280 nM, K_i hA_{2A}AR = 52 nM, K_i hA_{2B}AR = 840 nM, K_i hA₃AR = 28,000 nM; Fig. 4.1) with a phenylethynyl chain shifts the preference of the resulting compound 9-ethyl-8-phenylethynyladenine (K_i hA₁AR = 1,300 nM, K_i hA_{2A}AR = 600 nM, K_i hA_{2B}AR \geq 30,000 nM, K_i hA₃AR = 86 nM) from the A_{2A}AR to the A₃AR subtype.

Moreover, the substitution of the ethyl group of 9-ethyl-8-phenylethynyladenine with a cyclopentyl ring improved affinity of the resulting 9-cyclopentyl-8-phenylethynyladenine for A₃AR (K_i hA₃AR: 86 nM and 30 nM, respectively; Fig. 4.1)¹⁷⁰.

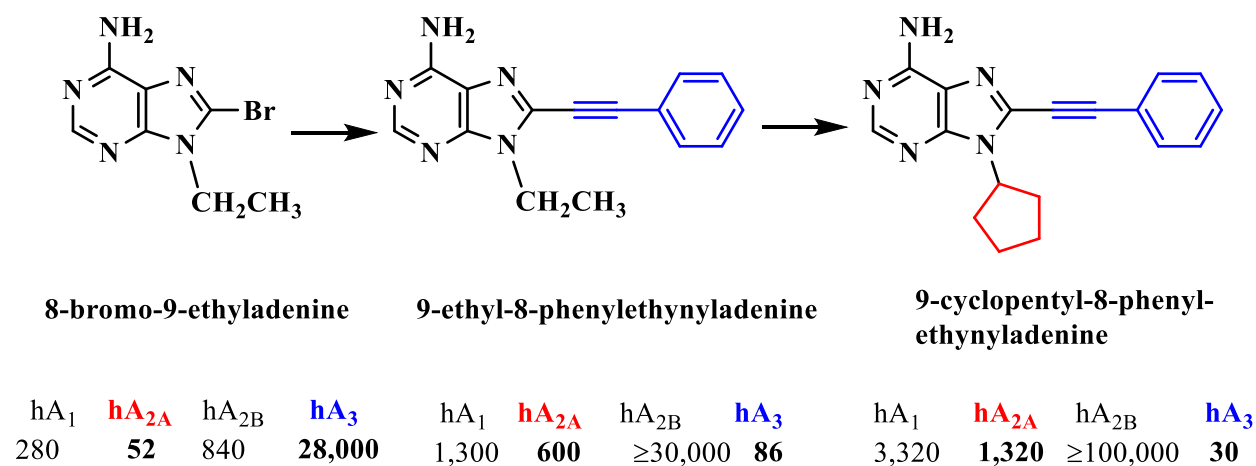


Figure 4.1: previously synthesized compounds and their AR binding affinity as rational for the design of new antagonists for the A₃AR subtype.

Hence, the present work focused attention first on the substitution of cyclopentyl in 9 position of 9-cyclopentyl-8-phenylethynyladenine with other side chains in order to identify the better 9-substituent (first series). The chains were chosen on the base of previous findings which showed that a propanol or phenethyl chain in 9-position of adenine derivatives proved to increase affinity/selectivity for the A₃AR subtype. Furthermore, while a longer chain was not tested

before, also 3-propylphenyl group in 9-position of the adenine was introduced in order to test its influence on the binding of the resulted compound ¹⁷¹. Then, in the second series, the 9-substituents which improve the binding A₃AR profile, were selected and combined with a substituted aromatic group at the alkynyl chain in C-8 position. In particular chlorine, methyl, and methoxy groups were introduced at the ortho, meta, and para position of the phenyl ring. Furthermore the phenyl was replaced by the pyridine.

The third series of compounds derived from the combination of most promising chains in 9-position, the best C-8 arylalkynyl substituent, and a 2-chlorine atom together with different alkyl groups in N⁶-position.

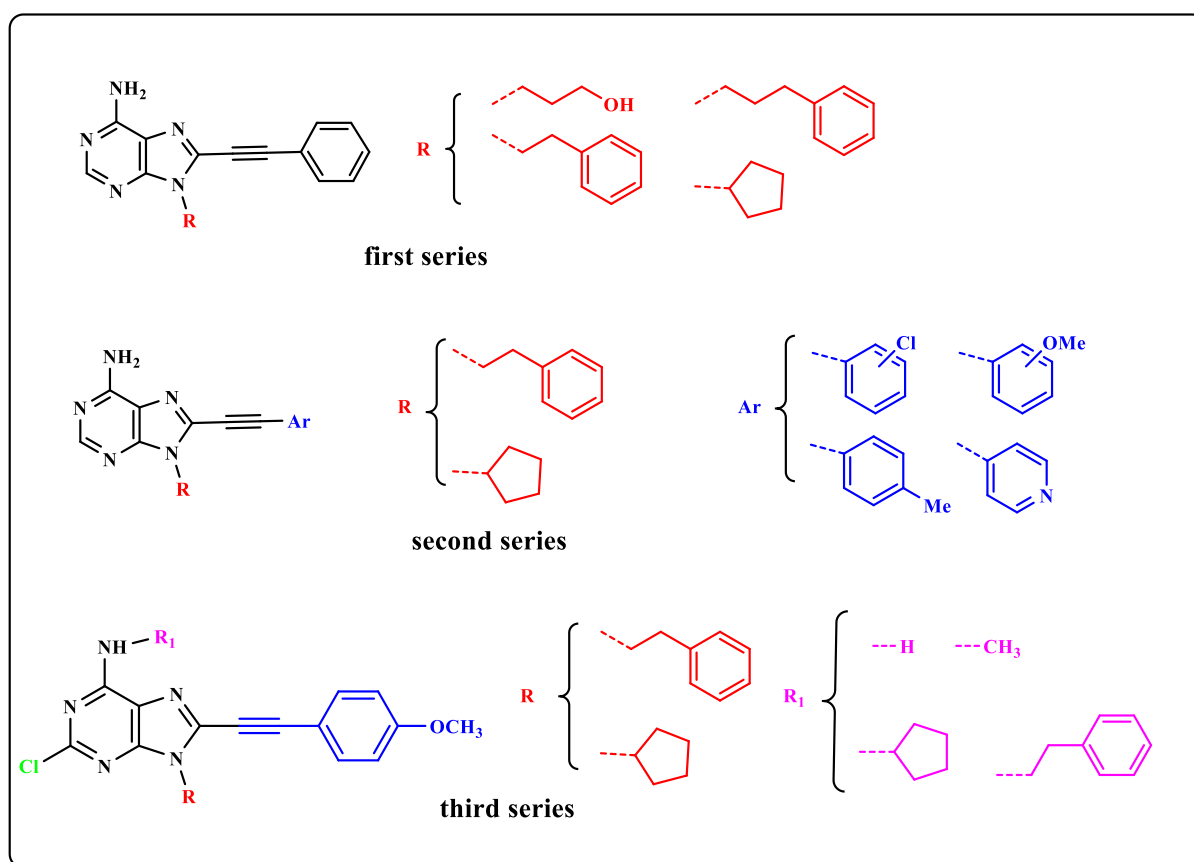


Figure 4.2: structure of designed compounds.

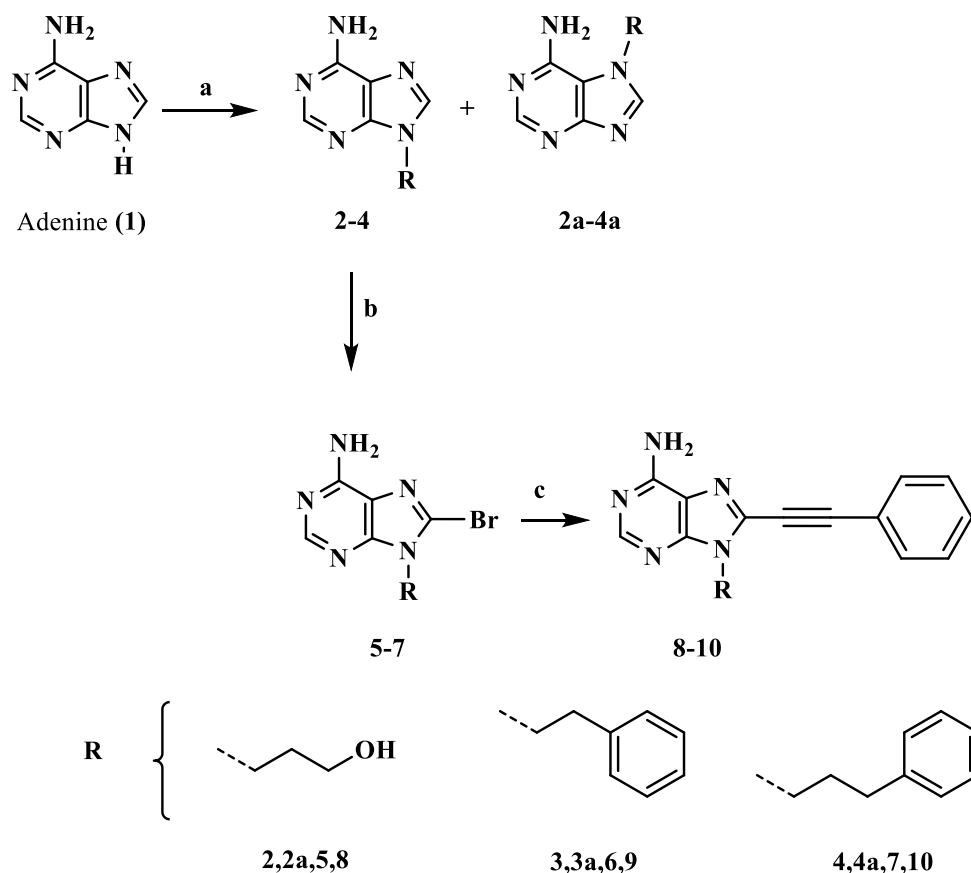
4.2 Chemistry

All the compounds were synthesized in three main steps starting with the introduction of the appropriate chain in 9-position of the commercial adenine or purine derivative, followed by bromination at C-8 position, and finally substitution of bromide with the suitable alkyne chain. In the case of compounds substituted at the N^6 position, the synthesis has been carried out first by introducing the 9-alkyl chain, then the substitution at the N^6 position, bromination at 8-position, and finally introduction of the 8-alkynyl chain.

4.2.1 First series of compounds

Compounds **2-10** were all synthesized from commercial adenine (**1**). Reaction of the suitable alkyl bromide with adenine (**1**) suspended in dry DMF and in presence dry K_2CO_3 furnished a mixture of N-9 and N-7 adenine derivatives isomers **2-4**, **2a-4a**, respectively. Mixture of the two isomers were separated through flash column chromatography to afford compounds **2-4** and **2a-4a** with yields ranging from 70-90% for the N-9 isomers, and 8-10% for the N-7 isomers. The N-9 and N-7 alkylation site was assigned on the base of different characteristics: N-9 isomers showed always an higher hydrophobic behavior and for this reason they always had an higher R_f on TLC run; furthermore the N-9 isomers were always obtained in much higher yields respect to the N-7 isomers, in addition 1H -NMR chemical shifts of the H-2, H-8, and NH_2 of the two isomers are different. In fact, in $DMSO-d_6$, pronounced downfield shifts were observed for the signals resulting from the H-8, 6-amino group, and the protons of the alkyl chain of all N-7 versus those of N-9 isomers (compare 1H -NMR shifts of compounds **2a-4a**, **22a**, **23a** with **2-4**, **22**, **23**, respectively). On the other hand, an opposite trend is highlighted in the case of H-2 signals for N-7 isomers, which were found to be shifted higher field relative to those of the corresponding N-9 isomers. All these data are in accordance with data obtained previously with similar compounds¹⁷¹. Bromination of the 9-alkyladenines **2-4** with N-bromosuccinimide (NBS) in DMF afforded the 8-bromoderivatives **5-7**. Following the Sonogashira cross-coupling reaction which used a palladium catalysis for the formation of the C-C bond of the terminal alkyne with the carbon bearing an halogen was used to introduce the alkynyl chain in 8-position. The reaction was conducted in a solution of **5-7** in dry DMF, triethylamine, and catalytic amount of Bis(triphenylphosphine)palladium(II) dichloride and copper iodide to afford **8-10** with yields ranging from 40-51% (Scheme 4.1).

Scheme 4.1



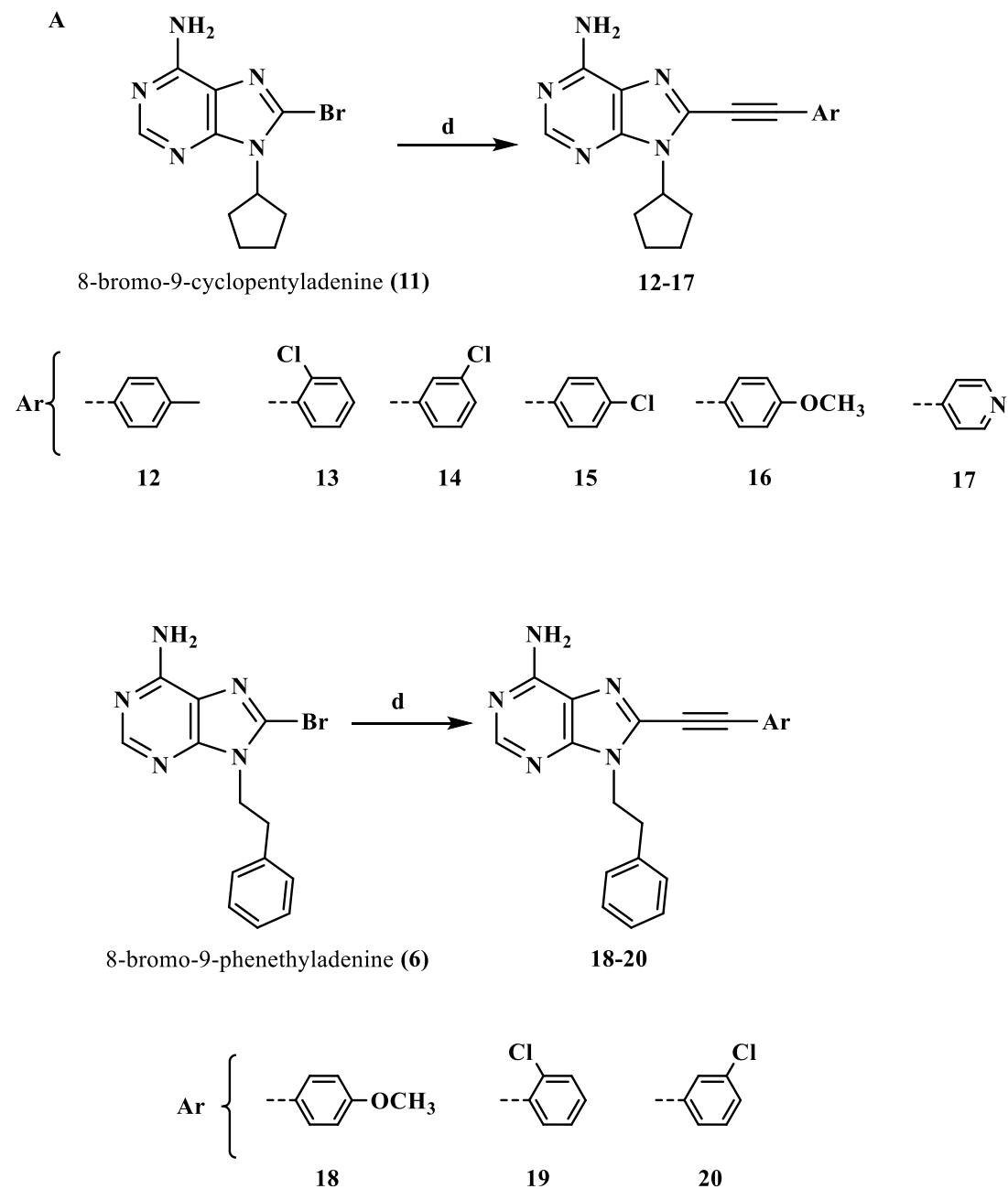
Reagents and conditions: (a) Alkylbromide, dry K_2CO_3 , DMF, r.t., 65 h, **2-4**: 70-90% yield, **2a-4a**: 8-10% yield; (b) NBS, DMF, 46 h, 39-43% yield; (d) phenylacetylene, Et_3N , $(PPh_3)_2PdCl_2$, CuI , DMF, 1 week, 36-51% yield.

4.2.2 Second series of compounds

The second series of compounds were characterized by a cyclopentyl and a phenethyl chain in 9-position. The desired **12-20** adenine derivatives were then synthesized from compounds **6** and **11**, previously reported¹⁷¹ by the Sonogashira cross-coupling reaction described previously (see first series of compounds) using the suitable terminal alkyne (Scheme 4.2). The cyclopentyl analogue, serie A (Scheme 4.2) were constituted by derivatives in which the phenyl group of the alkynyl chains in 8-position bears either a methyl or a methoxy in para position, or a chlorine atom in ortho, meta, and para position, a methoxy in para. The 4-ethynylpyridinyl chain in 8-position was also synthesized. For the second series bearing the phenethyl chain in 9-position (series B, Scheme 4.2), fewer derivatives were synthesized on the base of biological data

obtained with the cyclopentyl series. In fact, using the same procedure, only the ortho and meta-chloro derivative and para-methoxy derivative were synthesized.

Scheme 4.2



Reagents and conditions: (d): Arylalketylene, $(\text{PPh}_3)_2\text{PdCl}_2$, Et_3N , CuI , DMF , r.t, 1 week, 15-30%.

4.2.3 Third series of compounds

The third series of compounds include 9-cyclopentyladenine and 9-phenethyladenine derivatives bearing a chlorine atom in 2-position and, in the case of the second group of compounds, an alkyl chain in N^6 -position together with a para-methoxyphenylethynyl in 8-position.

Compounds **22-38** were all synthesized in four main steps by using 2,6-dichloropurine (**21**) commercially available, as starting material (Scheme 4.3).

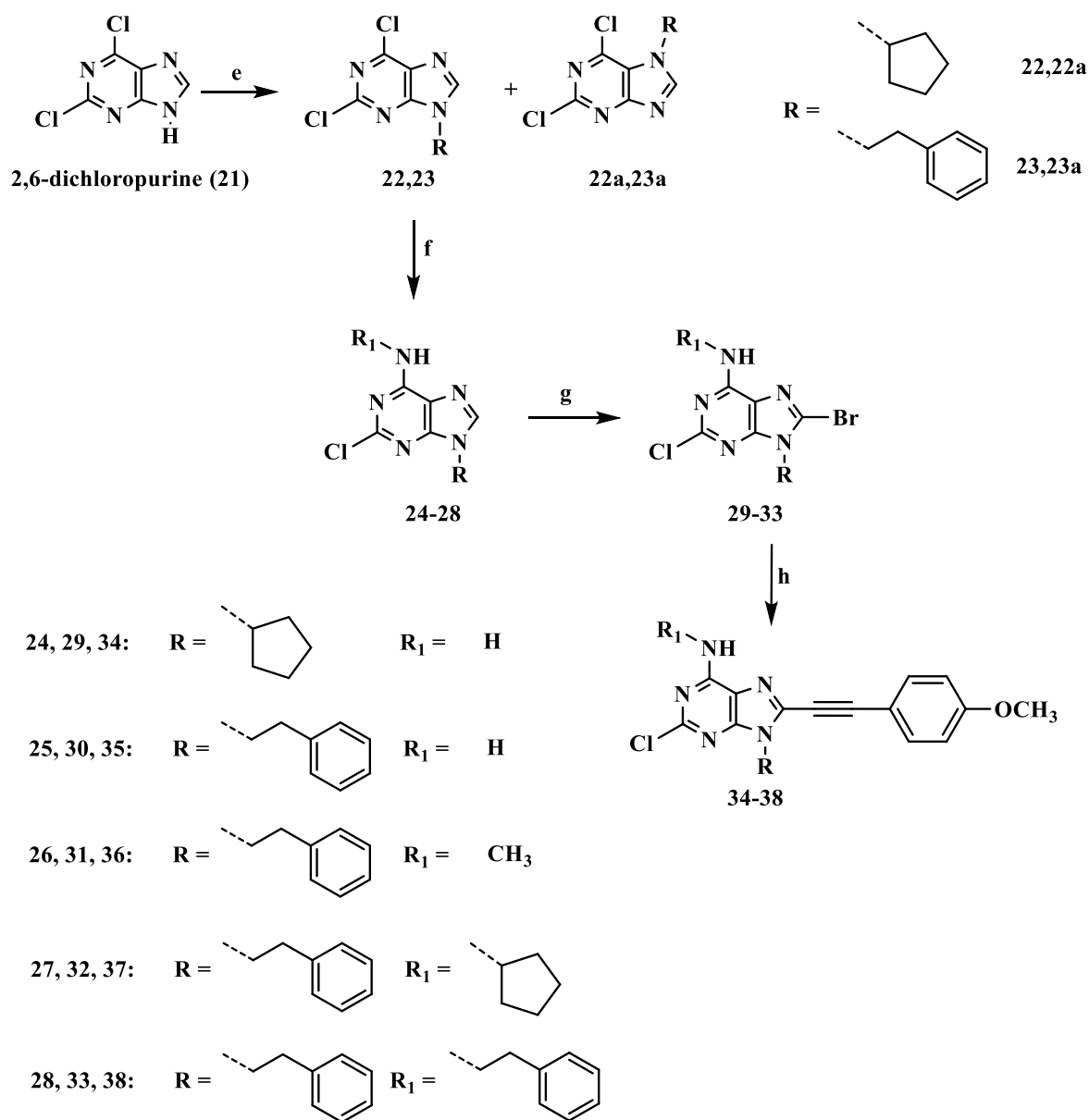
The alkylation of 2,6-dichloropurine (**1**) achieved in DMF in presence of dry K_2CO_3 and using the suitable alkyl bromide as alkylating agent led to mixtures of the N-9 and N-7 isomers **22-23** and **22a-23a**, respectively, which were separated through flash column chromatography. Also, in this case, the N-7 isomers were obtained with lower yield and they showed lower R_f during the development of TLC; furthermore, N-9 and N-7 isomers showed different chemical shifts for NH_2 and H-8, as it has been obtained for similar adenine derivatives discussed before. To confirm the alkylation position, the corresponding 6-amino derivatives of **22a** and **23a** (compounds **24** and **25**) have been hydrogenated in the presence of palladium and the reactions led to the respective 2-unsubstituted adenine yet described¹⁷². These data are the final proof that the alkylation have been obtained in 9-position.

The N-9 isomers **22** and **23** were in turn selectively aminated at 6-position. The reaction for the introduction of the amino group has been carried out by treatment with gaseous ammonia in tight closed steel vial at room temperature (r.t.). On the other hand, reaction with the other amines, methylamine, cyclopentylamine, phenethylamine has been carried out in DMF, using triethylamine as base catalyst, at r.t for 4-6 hrs. The 2-chloroadenine derivatives **24-28** have been obtained as pure compound after extraction with water and organic solvent followed by evaporation to dryness and crystallization with yield of about 90% (Scheme 4.3).

Compounds **24-28** were, then, treated with NBS in a mixture methanol-acetonitrile (1:1) to get the 2-chloro-8-bromo adenine derivatives **29-33** after reaction at r.t for 24 h. **29-33** were obtained as pure compounds after chromatography on a silica gel column with the yield 37-71%

The final desired derivatives were obtained through a Sonogashira cross-coupling in the same conditions described for the first and second series of derivatives reported here but heating the reactions at 100 °C for 4h-6 h to get the 8-*para*-methoxyphenylethyladenine derivatives **34-38**. The yield of the reactions are very low due to side products formed and also to the difficult purification of those compounds which required silica gel flash chromatography and then a second purification by reverse-phase silica chromatography. The compounds were obtained after crystallization with yields ranging from 15-40% (Scheme 4.3).

Scheme 4.3



Reagents and conditions: (e) Alkylbromide, dry K₂CO₃, DMF, r.t., 1 week, 39% (**22**); 70% (**23**); (f) gaseous NH₃ or R₁-NH₂, Et₃N, DMF, r.t., 4-6 h, 90%; (g) NBS, MeOH-CH₃CN (1:1), 24 h, 37-71%; (h) *para*-methoxyphenylacetylene, (PPh₃)₂PdCl₂, CuI, Et₃N, DMF, 100 °C, 6 h, 15-40%.

4.3 Results and discussion

All the newly synthesized adenine derivatives **8-10**, **12-20**, **24-38** were tested in binding or functional studies at human A₁, A_{2A}, A_{2B}, and A₃ ARs cloned and transfected in CHO cells by the research group of Prof. Klotz K.-N., at the University of Wuerzburg (Germany), and by the research group of Prof. Marucci G., at the University of Camerino. Binding studies were performed at the A₁, A_{2A}, and A₃ AR subtypes using the [³H]-N⁶-cyclopentyl-2-chloroAdo ([³H]-CCPA), the [³H]-NECA, and the [³H]-2-hexynyl-N⁶-methylAdo ([³H]-HEMADO) as radioligands, respectively. At A_{2B}R subtype a functional study was performed by the evaluation of adenylyl cyclase activity inhibition, through the measure of the cAMP levels^{173,174}.

The results of binding studies are summarized in Tables 4.1-4.3 where the 9-cyclopentyl-8-(phenylethynyl)adenine (ANR 235) has been reported as reference compound.

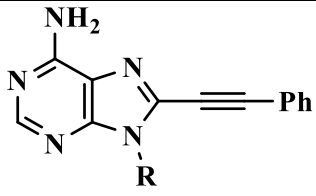
All the compounds showed IC₅₀ values at A_{2B}R higher than 30,000 nM, for this reason these data are not reported in the tables.

The reference compound ANR 235 is endowed with high affinity and good selectivity for the A₃R (K_i A₃R = 30 nM; selectivity A₁/A₃ = 110 and A_{2A}/A₃ = 44; Table 4.1). Replacement of the 9-cyclopentyl group with different substituents led to compounds **8-10** (first series), which maintained the preference for the A₃R subtype, although with a slight decrease of affinity. In particular, the introduction of a hydroxypropyl chain at the 9-position decreases both the affinity and the selectivity for the A₃R (**8**: K_i A₃R = 274 nM; selectivity A₁/A₃ = 5 and A_{2A}/A₃ = 4; Table 4.1). On the contrary, the introduction at the same position of a phenylethyl and a phenylpropyl chains improved the A₃R selectivity (**9**, K_i A₃R = 67 nM; selectivity A₁/A₃ and A_{2A}/A₃ > 1,492; **10**: K_i A₃R = 103 nM; selectivity A₁/A₃ > 291 and A_{2A}/A₃ > 970; Table 4.1).

Since compounds ANR 235 and **9**, bearing in 9-position a cyclopentyl and a phenylethyl chains, showed the best A₃R affinity and selectivity, respectively, these two substitutions have been chosen for the synthesis of the further compounds (series 2 and 3).

Hence, in the second series of compounds, which maintained in N-9 position either a cyclopentyl or a phenylethyl chain, different substituents at the ortho, meta, and para position of the 8-phenylalkyne were introduced. Furthermore in one case, the phenyl ring of the 8-phenylalkyne was replaced by a pyridine. The results reported in Table 4.2 showed that, also in this case, the resulted compounds **12-20** showed a preference for the A₃R, with two exceptions represented by **12** and **17**, which bear a cyclopentyl at 9-position and a para-methyphenylethynyl and a 4-ethynylpyridine in 8-position, respectively.

Table 4.1: Biological profile of 8-phenylethyladenine derivatives **8–10** (first series of compounds) at human A₁, A_{2A}, A₃ ARs stably transfected in CHO cells; values are expressed as K_i nM; 9-cyclopentyl-8-phenylethyladenine has been reported as reference compound.

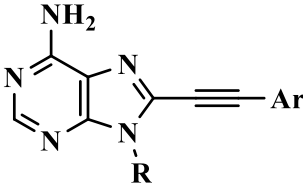
				
Cpds	R	hA ₁ ^a	hA _{2A} ^b	hA ₃ ^c
9-cyclopentyl-8-phenylethyladenine	cC ₅ H ₉	3,320 (3,082-3,580)	1,320 (871-1,990)	30 (18-50)
8	HO(CH ₂) ₃	1,500 (1,430-1,570)	1,080 (875-1,320)	274 (169-444)
9	Ph(CH ₂) ₂	>100,000	>100,000	67 (43-103)
10	Ph(CH ₂) ₃	>30,000	>100,000	103 (74.1-142)

^aDisplacement of specific [³H]CCPA binding at human A₁AR expressed in CHO cells (n = 3–6). ^bDisplacement of specific [³H]NECA binding at human A_{2A}AR expressed in CHO cells. ^cDisplacement of specific [³H]HEMADO binding at human A₃AR expressed in CHO cells. Data are expressed as geometric means, with 95% confidence limits.

In fact, **12** (K_i A₁R > 30,000 nM, K_i A_{2A}R = 660 nM, K_i A₃R = 1,010 nM) showed a slight preference for the A_{2A}R, while **17** (K_i A₁R = 851 nM, K_i A_{2A}R = 855 nM, K_i A₃R = 851 nM) resulted unselective. The introduction of an ortho-chloro substituent in the phenyl ring of ANR 235 led to a derivative which maintains affinity for the A₃AR (**13**: K_i A₃R = 27 nM *versus* ANR 235: K_i hA₃R = 30 nM) but decreased selectivity for the A_{2A}AR more than 6 fold respect to the reference compound (**13**: selectivity A_{2A}/A₃ = 7 *versus* ANR 235: selectivity A_{2A}/A₃ = 44 see Tables 4.1 and 4.2). The presence of meta-chloro decreased affinity for the A₃AR of only 2 fold but the noticeable effect was that selectivity for the A₁AR which decreased of 20 fold (**14**: selectivity A₁/A₃ = 5 ANR *versus* 235: selectivity A₁/A₃ = 110). The para-chloro substitution led to a significant reduction of both affinity and selectivity. Among the different substituents, the para-methoxy group seems to be the most favorable. In fact, **16** showed the best A₃ affinity (**16**: K_i A₃R = 5.5 nM) and increased selectivity for A₁R for more than 50 fold, although the selectivity *versus* the A_{2A}AR decreased (**7**: selectivity A₁/A₃ = 6000 and A₁/A_{2A} = 22 *versus* ANR 235: selectivity A₁/A₃ = 110 and A₁/A_{2A} = 44). These data suggest that the phenyl group para-position should be substituted with groups, like the methoxy able to accept a hydrogen bond from the receptor (e.g methyl or chlorine as found in **12** and **15**, respectively). Surely, this

hypothesis should be verified with the synthesis and evaluation of other derivatives bearing different hydrogen bond acceptors in the para-position of the phenyl ring.

Table 4.2: Biological profile of synthesized compounds **12–20** (second series of compounds) at human A₁, A_{2A}, A₃ ARs stably transfected in CHO cells; values are expressed as K_i nM.

					
Cpds	R	Ar	hA ₁ ^a	hA _{2A} ^b	hA ₃ ^c
12	cC ₅ H ₉	Ph-(<i>p</i> -CH ₃)	>30,000	660±64	1,010±17
13	cC ₅ H ₉	Ph-(<i>o</i> -Cl)	1,589±47	192±54	27±2
14	cC ₅ H ₉	Ph-(<i>m</i> -Cl)	334±75	1,442±138	61±15
15	cC ₅ H ₉	Ph-(<i>p</i> -Cl)	>30,000	>30,000	983±81
16	cC ₅ H ₉	Ph-(<i>p</i> -OCH ₃)	>30,000	124±23	5.5±1
17	cC ₅ H ₉	4-pyridine	851±104	855±10	851±104
18	Ph(CH ₂) ₂	Ph-(<i>p</i> -OCH ₃)	>30,000	>30,000	19±4
19	Ph(CH ₂) ₂	Ph-(<i>o</i> -Cl)	8,119±924	>30,000	40±9
20	Ph(CH ₂) ₂	Ph-(<i>m</i> -Cl)	>30,000	>30,000	284 ± 73

^aDisplacement of specific [³H]CCPA binding at human A₁AR expressed in CHO cells (n = 3–6). ^bDisplacement of specific [³H]NECA binding at human A_{2A}AR expressed in CHO cells. ^cDisplacement of specific [³H]HEMADO binding at human A₃AR expressed in CHO cells. Data are expressed as means ± SE.

As expected, replacement of the 9-cyclopentyl group in compounds **13**, **14**, and **16** with a phenylethyl chain, to obtain **18–20**, led to an increase of the A₃R selectivity in most cases, although with a slight decrease of the affinity for the same receptor subtype. The presence of the para-methoxyphenyl ring in the 8-position gave the compound endowed with the best A₃R affinity and, in this case, with a very good selectivity profile (**18**: K_i A₃R = 19 nM, selectivity A₁/A₃ and A₁/A_{2A} > 1,578).

The third series of compounds focused the interest on the contribution of C-2 chlorine combined with alkyl chain in N⁶-position, maintaining the 8-*p*-methoxyphenyl group and the 9-cyclopentyl or 9-phenylethyl chains. The goal of this third series was mainly to increase the selectivity ratio

A_{2A}/A_3 of cyclopentyl derivatives **16** or to increase the A_3R affinity of the phenylethyl derivative **18**, maintaining the same highest A_1/A_3 and A_{2A}/A_3 selectivity ratio.

Table 4.3: Biological profile of synthesized compounds **24–38** (third series of compounds) at human A_1 , A_{2A} , A_3 ARs stably transfected in CHO cells; values are expressed as K_i nM.

Cpd	R	R ₁	R ₂	hA ₁ ^a	hA _{2A} ^b	hA ₃ ^d
24	cC ₅ H ₉	H	H	1893±160	465±129	631±61
29	cC ₅ H ₉		Br	ND	ND	ND
34	cC ₅ H ₉	H	C≡C-(<i>p</i> -OCH ₃)Ph	>30,000	>30,000	376±94
25	Ph(CH ₂) ₂	H	H	9,147±1233	>30,000	57±12
30	Ph(CH ₂) ₂	H	Br	6,548±424	3,802±399	58±5
35	Ph(CH ₂) ₂	H	C≡C-(<i>p</i> -OCH ₃)Ph	>30,000	>30,000	26±3
26	Ph(CH ₂) ₂	CH ₃	H	>30,000	>30,000	50±9
31	Ph(CH ₂) ₂	CH ₃	Br	>30,000	>30,000	329±28
36	Ph(CH ₂) ₂	CH ₃	C≡C(<i>p</i> -OCH ₃)Ph	>30,000	>30,000	35±4
27	Ph(CH ₂) ₂	cC ₅ H ₉	H	ND	ND	ND
32	Ph(CH ₂) ₂	cC ₅ H ₉	Br	1,002±171	2,155±218	1,289±58
37	Ph(CH ₂) ₂	cC ₅ H ₉	C≡C(<i>p</i> -OCH ₃)Ph	>30,000	>30,000	61±12
28	Ph(CH ₂) ₂	Ph(CH ₂) ₂	H	2,279±403	>30,000	29±1.2
33	Ph(CH ₂) ₂	Ph(CH ₂) ₂	Br	2,435±3	>30,000	44±8
38	Ph(CH ₂) ₂	Ph(CH ₂) ₂	C≡C(<i>p</i> -OCH ₃)Ph	>30,000	>30,000	8.4±1.1

^aDisplacement of specific [³H]CCPA binding at human A_1 AR expressed in CHO cells (n = 3–6). ^bDisplacement of specific [³H]NECA binding at human A_{2A} AR expressed in CHO cells. ^cDisplacement of specific [³H]HEMADO binding at human A_3 AR expressed in CHO cells. Data are expressed as means ± SE.

In the case of this series also the 8-unsubstituted adenine derivatives and **24-26**, **28** and the 8-bromo derivatives **30-33** and were evaluated in binding assay. Compounds **27** and **29** were not available in sufficient amount for their evaluation. The results reported in Table 4.3.

The introduction of a C-2 chlorine atom at the 9-cyclopentyl derivative **16** was detrimental for the A₃AR affinity leading to **34** (K_i A₃R = 5.5 nM and 376 nM, respectively). On the contrary, the same substitution on the 9-phenylethyl derivative **18** led to a maintaining of the A₃ affinity and selectivity ((**18**: K_i A₃R = 19 nM, selectivity A₁/A₃ and A₁/A_{2A} > 1,578 *versus* **35**: K_i A₃R = 26 nM, selectivity A₁/A₃ and A₁/A_{2A} > 1,154). These findings suggested the further substitution only in the 9-phenylethyl derivative **35**.

The introduction of a methyl or a cyclopentyl group at the N⁶-position of **35** did not improve or slightly decreased the A₃R affinity (**36**: K_i A₃R = 35 nM and **37**: K_i A₃R = 61 nM), while the presence of a more hindered phenylethyl chain, in the same position, favored the interaction with the A₃R subtype leading to the most active and selective compound of the newly synthesized ligands (**38**: K_i A₃R = 8.4 nM, selectivity A₁/A₃ and A₁/A_{2A} > 3,571).

The intermediate derivatives bearing at C-8 position an hydrogen or a bromine atom displayed in general good affinity and different degree of selectivity, the 8-bromo substituted derivatives.

4.3.1 Functional studies at human A₃AR

In order to verify the antagonistic behaviour of new ligands, selected compounds **16**, **18**, and **38** were evaluated in functional assay at the human A₃ receptors. In this assay, the ability of the compounds to counteract the inhibition of adenylyl cyclase activity in CHO cells expressing such receptors was evaluated. In table 4.4, the IC₅₀ values of such compounds are reported in comparison with their binding affinity.

Table 4.4: Functional data, as IC₅₀ value (nM), at human A₃ARs in comparison with binding affinity data (K_i, nM) of compounds **16**, **18**, and **38**.

Compound	hA ₃ R ^a (K _i nM)	hA ₃ R ^b (IC ₅₀ nM)
16	5.5 ± 1	86 ± 11
18	18.5 ± 4	152 ± 22
38	8.4 ± 1.1	110 ± 18

^aDisplacement of specific [³H]-HEMADO binding at human A₃R expressed in CHO cells. ^bIC₅₀ values obtained counteracting NECA inhibition of adenylyl cyclase activity in CHO cells expressing hA₃R. Data are expressed as means ± SE.

The compounds confirmed antagonist behaviour as they were able to reverse the inhibition of the adenylyl cyclase activity induced by the full agonist NECA at the A₃ subtype. Furthermore, they showed IC₅₀ values in the high nanomolar range with compound **16** acting as the best antagonist with IC₅₀ equal to 86 nM.

In conclusion, three different series of di-, tri-, and tetra-substituted adenine derivatives have been designed and synthesized as A₃AR antagonists. Binding studies at human ARs demonstrated that most of the new compounds are endowed with high affinity and different degree of selectivity for the A₃AR subtype. In particular, the tetra-substituted adenine derivative **38** (K_i A₃R = 8.4 nM; K_i A₁R and K_i A_{2A}R >30,000 nM) resulting the most active and selective ligand.

The functional studies confirmed the antagonistic behavior of the selected newly synthesized adenine derivatives. Calculated IC₅₀ values were in good agreement with the binding data and confirmed the 2-chloro-*N*⁶,9-diphenylethyl-8-paramethoxyphenylethynyladenine (**38**) as the most potent and selective A₃R antagonist of the three series. This compound represents a very good ligand to study the A₃AR and its functions.

4.4: Experimental section

4.4.1: Materials and methods

The materials and methods have been described earlier in the experimental section of Chapter 3.

4.4.2: Chemistry

General procedure for the synthesis of 9-alkyladenines 2–4 and 7-alkyladenines 2a–4a, 9-alkyl-2,6-dichloro-9H-purine (22, 23) and 7-alkyl-2,6-dichloro-9H-purine (22a, 23a): To 1.0 mmol of adenine (**1**) or 2,6-dichloropurine (**21**), dissolved in 4 mL of dry DMF, dry K₂CO₃ (200 mg) and the suitable alkyl halide (1.2 mmol) were added. The mixture was stirred under a nitrogen atmosphere from 3-7 days. The solvent was evaporated and the residue was chromatographed on a silica gel column eluting with the suitable mixture of solvents (see the section below) to give compounds **2–4**, **2a-4a** and **22, 23, 22a, 23a**.

Compounds **2** and **2a** were obtained from **1** by reaction with 3-bromo-1-propanol as pure compounds after column chromatography eluting with CHCl₃–CH₃OH–NH₃/CH₃OH (94:4:2) with 28 and 27% yield, respectively.

9-(3-Hydroxypropyl)-9H-adenine (2): ¹H NMR (DMSO-*d*₆) δ: 1.91 (m, 2H, CH₂CH₂OH), 3.35 (m, 2H, CH₂OH), 4.17 (t, 2H, *J* = 7.0 Hz, CH₂N), 4.64 (t, 1H, *J* = 5.2 Hz, OH), 7.18 (br s, 2H, NH₂), 8.09 (s, 1H, H-8), 8.10 (s, 1H, H-2).

7-(3-Hydroxypropyl)-7H-adenine (2a): Compound **2a** was obtained after column chromatography eluting with CHCl₃–CH₃OH–NH₃/CH₃OH (94:4:2). ¹H NMR (DMSO-*d*₆) δ: 2.02 (m, 2H, CH₂CH₂OH), 3.39 (m, 2H, CH₂OH), 4.37 (t, 2H, *J* = 6.9 Hz, CH₂N), 4.85 (t, 1H, *J* = 5.2 Hz, OH), 7.76 (s, 1H, H-2), 7.87 (br s, 2H, NH₂), 8.31 (s, 1H, H-8).

Compounds **3** and **3a** were obtained from **1** by reaction with 1-bromo-2-phenylethane as pure compounds after column chromatography eluting with CHCl₃–CH₃OH (95:5) with 82 and 8% yield, respectively.

9-Phenylethyl-9H-adenine (3): ¹H NMR (DMSO-*d*₆) δ: 3.11 (t, 2H, *J* = 7.0 Hz, CH₂Ph), 4.36 (t, 2H, *J* = 7.2 Hz, CH₂N), 7.18 (m, 7H, H-Ph and NH₂), 7.90 (s, 1H, H-8), 8.12 (s, 1H, H-2).

7-Phenylethyl-9H-adenine (3a): ¹H NMR (DMSO-*d*₆) δ: 3.24 (t, 2H, *J* = 7.1 Hz, CH₂Ph), 4.54 (t, 2H, *J* = 7.2 Hz, CH₂N), 7.21 (m, 5H, H-Ph), 7.81 (s, 1H, H-2), 7.87 (br s, 2H, NH₂), 8.12 (s, 1H, H-8).

Compounds **4** and **4a** were obtained from **1** by reaction with 1-bromo-2-phenylpropane as pure compounds after column chromatography eluting with CHCl₃–NH₃/CH₃OH (99:2) with 82 and 11% yield, respectively.

9-Phenylpropyl-9H-adenine (4): ¹H-NMR (DMSO-*d*₆) δ: 2.13 (m, 2H, CH₂CH₂CH₂), 2.59 (m, 2H, CH₂Ph), 4.16 (t, *J* = 7.1 Hz, 2H, CH₂N), 7.24 (m, 7H, NH₂ and H-Ph), 8.13 (s, 1H, H-2), 8.15 (s, 1H, H-8).

7-Phenylpropyl-9H-adenine (4a): ¹H-NMR (DMSO-*d*₆) δ: 2.22 (m, 2H, CH₂CH₂CH₂); 2.62 (m, 2H, CH₂Ph); 4.33 (t, *J* = 7.0 Hz, 2H, CH₂N); 7.23 (m, 5H, H-Ph); 7.75 (s, 1H, H-2); 7.83 (br s, 2H, NH₂); 8.32 (s, 1H, H-8).

Compounds **22** and **22a** were obtained from **21** by reaction with bromocyclopentane as pure compounds after column chromatography eluting with cC₆H₁₂-EtOAc (90:10 to 70:30) with 37 and 7% yield, respectively.

9-Cyclopentyl-2,6-dichloro-9H-purine (22): ¹H-NMR (DMSO-*d*₆) δ: 1.69 (m, 2H, H-cyclopentyl), 1.86 (m, 2H, H-cyclopentyl), 2.00 (m, 2H, H-cyclopentyl), 2.18 (m, 2H, H-cyclopentyl), 4.92 (m, 1H, NCH), 8.82 (s, 1H, H-8).

7-Cyclopentyl-2,6-dichloro-9H-purine (22a): ¹H-NMR (DMSO-*d*₆) δ: 1.67 (m, 2H, H-cyclopentyl), 1.85 (m, 2H, H-cyclopentyl), 1.99 (m, 2H, H-cyclopentyl), 2.14 (m, 2H, H-cyclopentyl), 5.01 (m, 1H, NCH), 8.97 (s, 1H, H-8).

Compounds **23** and **23a** were obtained from **21** by reaction with 1-bromo-2-phenylethane as pure compounds after column chromatography eluting with cC₆H₁₂-EtOAc (90:10 to 70:30) with 64 and 16% yield, respectively.

2,6-Dichloro-9-phenylethyl-9H-purine (23): ¹H-NMR (DMSO-*d*₆) δ: 3.17 (t, *J* = 7.0 Hz, 2H, CH₂Ph), 4.52 (t, *J* = 7.5 Hz, 2H, CH₂N), 7.14-7.27 (m, 5H, H-Ph), 8.55 (s, 1H, H-8).

2,6-Dichloro-7-phenylethyl-9H-purine (23a): ¹H-NMR (DMSO-*d*₆) δ: 3.16 (t, *J* = 7.5 Hz, 2H, CH₂Ph), 4.70 (t, *J* = 7.5 Hz, 2H, CH₂N), 7.15-30 (m, 5H, H-Ph), 8.63 (s, 1H, H-8).

General procedure for the synthesis of 9-alkyl-8-bromoadenines 5–7 and 29-33: To 1.0 mmol of the appropriate 9-alkyladenines **2–4** dissolved in 4 mL of dry DMF, N-bromosuccinimide (NBS, 2.0 mmol) was added. The mixture was stirred under a nitrogen atmosphere at room temperature for the suitable time (see below).

For the synthesis of compounds **29-33**, to 1.0 mmol of the appropriated 9-alkyl-2-chloro-9H-adenine **24** or **25** or *N*⁶,9-dialkyl-2-chloro-9H-adenines **26-28** solubilized in a mixture of dry MeOH-dry CH₃CN (50:50) NBS (3.37 mmol) was added. The mixture was stirred under a nitrogen atmosphere at room temperature for 12 hours after which an equal amount of NBS was added (3.37mmol) and the mixture left under stirring at room temperature for others 12 hours. The solvent was removed in vacuo and the residue was chromatographed on a silica gel column

eluting with the suitable mixture of solvents for **5-7** (see below) and with C_6H_{12} -EtOAc (90:10 to 70:30) for **29-33**.

8-Bromo-9-(3-hydroxypropyl)-9H-adenine (5): Compound **5** was obtained from **2** as pure compound after chromatography eluting with CHCl_3 - CH_3OH (97:3) with 24% yield. $^1\text{H-NMR}$ ($\text{DMSO-}d_6$) δ : 1.89 (m, 2H, $\text{CH}_2\text{CH}_2\text{OH}$), 3.44 (m, 2H, CH_2OH), 4.19 (t, 2H, $J = 4.8$ Hz, CH_2 N), 4.66 (t, 1H, $J = 3.4$ Hz, OH), 7.39 (br s, 2H, NH_2), 8.13 (s, 1H, H-2).

8-Bromo-9-phenethyl-9H-adenine (6): Compound **6** was obtained from **3** as pure compound after chromatography eluting with CHCl_3 - CH_3OH (99:1) with 55% yield. $^1\text{H-NMR}$ ($\text{DMSO-}d_6$) δ : 3.10 (t, 2H, $J = 7.1$ Hz, CH_2Ph), 4.36 (t, 2H, $J = 7.1$ Hz, CH_2N), 7.11 (d, 2H, $J = 7.4$ Hz, H-Ph), 7.26 (m, 3H, H-Ph), 7.39 (br s, 2H, NH_2), 8.15 (s, 1H, H-2).

8-Bromo-9-phenylpropyl-9H-adenine (7): Compound **7** was obtained from **4** as pure compound after chromatography eluting with C_6H_{12} -EtOAc (75:25 to 60:40) with 43% yield. $^1\text{H-NMR}$ ($\text{DMSO-}d_6$) δ : 2.05 (m, 2H, $\text{CH}_2\text{CH}_2\text{Ph}$), 2.61 (m, 2H, CH_2 -Ph), 4.15 (t, $J = 7.0$ Hz, 2H, CH_2N), 7.22 (m, 5H, H-Ph), 7.38 (bs, 2H, NH_2), 8.13 (s, 1H, H-2).

8-Bromo-2-chloro-9-cyclopentyl-9H-adenine (29): Compound **29** was obtained from **24** with the yield of 51%. M. p.: 198-201 °C; $^1\text{H-NMR}$ ($\text{DMSO-}d_6$) δ : 1.68 (m, 2H, H-cyclopentyl), 2.00 (m, 2H, H-cyclopentyl), 2.01 (m, 2H, H-cyclopentyl), 2.20 (m, 2H, H-cyclopentyl), 4.86 (m, 1H, NCH), 7.88 (br s, 2H, NH_2).

8-Bromo-2-chloro-9-phenethyl-9H-adenine (30): Compound **30** was obtained from **25** with the yield of 60%. M. p.: 139-144 °C; $^1\text{H-NMR}$ ($\text{DMSO-}d_6$) δ : 3.07 (t, $J = 7.00$ Hz, 2H, CH_2Ph), 4.34 (t, $J = 7.00$ Hz, 2H, CH_2N), 7.08 (m, 2H, H-Ph), 7.24 (m, 3H, H-Ph), 7.87 (s, 2H, NH_2).

8-Bromo-2-chloro-9-phenethyl- N^6 -methyl-9H-adenine (31): Compound **31** was obtained from **26** with the yield of 37%. M. p.: 163-166 °C; $^1\text{H-NMR}$ ($\text{DMSO-}d_6$) δ : 2.91 (d, $J = 4.50$ Hz, 3H, CH_3N), 3.07 (t, $J = 7.00$ Hz, 2H, CH_2Ph), 4.32 (t, $J = 7.00$ Hz, 2H, CH_2N), 7.08 (m, 2H, H-Ph), 7.24 (m, 3H, H-Ph), 8.36 (br m, 1H, NH).

8-Bromo-2-chloro-9-phenethyl- N^6 -cyclopentylamino-9H-adenine (32): Compound **32** was obtained from **27** with the yield of 71%. M.p.: 115-120 °C; $^1\text{H-NMR}$ ($\text{DMSO-}d_6$) δ : 1.56 (m, 2H, H-cyclopentyl), 1.71 (m, 2H, H-cyclopentyl), 1.92 (m, 2H, H-cyclopentyl), 3.06 (t, $J = 7.00$ Hz, 2H, CH_2Ph), 4.33 (t, $J = 7.00$ Hz, 2H, CH_2N), 4.40 (m, 1H, NCH), 7.10 (m, 2H, H-Ph), 7.25 (m, 3H, H-Ph), 8.41 (m, 1H, NH).

8-Bromo-2-chloro- N^6 ,9-diphenylethyl-9H-adenine (33): Compound **33** was obtained from **28** with the yield of 37%. M.p.: 157-160 °C; $^1\text{H-NMR}$ ($\text{DMSO-}d_6$) δ : 2.91 (m, 2H, CH_2Ph), 3.06 (t,

$J = 7.00$ Hz, 2H, CH₂Ph), 3.64 (m, 2H, CH₂NH), 4.32 (t, $J = 7.00$ Hz, 2H, CH₂N), 7.08 (m, 2H, H-Ph), 7.25 (m, 8H, H-Ph), 8.49 (br m, 1H, NH).

General procedure for the synthesis of 6-aminopurine derivatives 24 and 25: Gaseous NH₃ was condensed into a steel vessel at -78 °C and **22** or **23** (0.85 mmol) was added. The steel vessel was tightly closed and left to react at r.t. for 6 hs. The content was then transferred into a flask by solvent and co-evaporated with MeOH (5 x 10 mL). The residue was extracted with water (H₂O) and EtOAc (15 ml x 3 times). The organic phase was collected washed with brine and dried over anhydrous sodium sulphate (Na₂SO₄). The organic phase was filtered and evaporated under vacuum to dryness to afford a yellowish solid. The yellowish solid was crystallized from in CH₂Cl₂/n-hexane to afford **24** and **25** as white solids.

2-Chloro-9-cyclopentyl-9H-adenine (24): Compound **24** was obtained from **22** with the yield of 70%. M. p.: 225-229 °C; ¹H-NMR (DMSO-*d*₆) δ: 1.69 (m, 2H, H-cyclopentyl), 1.86 (m, 2H, H-cyclopentyl), 1.94 (m, 2H, H-cyclopentyl), 2.14 (m, 2H, H-cyclopentyl), 4.77 (m, 1H, NCH), 7.72 (s, 2H, NH₂), 8.23 (s, 1H, H-8). ESI-MS: positive mode m/z 238.0 [M+H]⁺, 260.0 [M+Na]⁺.

2-Chloro-9-phenylethyl-9H-adenine (25): Compound **25** was obtained from **23** with the yield of 91%. M. P.: 217-221 °C; ¹H-NMR (DMSO-*d*₆) δ 3.12 (t, $J = 7.00$ Hz, 2H, CH₂Ph), 3.36 (t, $J = 7.00$ Hz, 2H, CH₂N), 7.15 (m, 2H, H-Ph), 7.21 (m, 1H, H-Ph), 7.27 (m, 2H, H-Ph), 7.12 (s, 2H, NH₂), 7.94 (s, 1H, H-8). ESI-MS: positive mode m/z 274.1 [M+H]⁺, 295.9 [M+Na]⁺.

General procedure for the synthesis of 6-alkyladenine derivatives 26-28: Intermediate **23** (1.36 mmol) was solubilized in dry DMF (10 mL) under N₂ atmosphere. Et₃N (1.2 mL, 0.009 mmol) and the suitable amine (5.3 mmol) were added and the mixture was left under stirring at r.t for 4 hs. The reaction mixture was stopped: volatiles were removed under vacuum and the residue was extracted with water (H₂O) and EtOAc (15 mL x 3 times). The organic phase was collected, washed with brine and dried over anhydrous Na₂SO₄. The dry organic phase was filtered and evaporated under vacuum to dryness to afford a yellowish solid. The yellowish solid was crystallized CHCl₃/n-hexane afford **26-28** as white solids.

2-Chloro-*N*⁶-methyl-9-phenethyl-9H-adenine (26): Yield: 92%. M.P.: 126-131°C; ¹H-NMR (DMSO-*d*₆) δ: 2.91 (d, $J = 4.50$ Hz, 3H, CH₃-NH), 3.12 (t, $J = 7.00$ Hz, 2H, CH₂Ph), 4.36 (t, $J = 7.00$ Hz, 2H, CH₂N), 7.16 (m, 2H, H-Ph), 7.21 (m, 1H, H-Ph), 7.26 (m, 2H, H-Ph), 7.91 (br s, 1H, HNCH₃), 8.13 (br s, 1H, H-8). ESI-MS: positive mode m/z 288.0 [M+H]⁺, 310.0 [M+Na]⁺.

2-Chloro-*N*⁶-cyclopentyl-9-phenethyl-9H-adenine (27): Yield: 81%. Vitreous solid; ¹H-NMR (DMSO-*d*₆) δ: 1.56 (m, 4H, H-cyclopentyl), 1.71 (m, 2H, H-cyclopentyl), 1.92 (m, 2H, H-cyclopentyl), 3.12 (t, $J = 7.00$ Hz, 2H, CH₂Ph), 4.37 (t, $J = 7.00$ Hz, 2H, CH₂N), 4.42 (m, 1H,

NCH), 7.18 (m, 2H, Ph), 7.22 (m, 1H, Ph), 7.26 (m, 2H, 7.91 (br s, 1H, H-8), 8.17 (br s, 1H, NH). ESI-MS: positive mode m/z 342.1 $[M+H]^+$, 364.0 $[M+Na]^+$.

2-Chloro-*N*⁶,9-diphenylethyl-9*H*-adenine (28): Yield: 70%. M.p.: 157-160 °C; ¹H-NMR (DMSO-*d*₆) δ: 2.92 (t, $J = 7.00$ Hz, 2H, CH₂Ph), 3.12 (t, $J = 7.00$ Hz, 2H, CH₂Ph), 3.65 (t, $J = 7.00$ Hz, 2H, CH₂NH), 4.36 (t, $J = 7.00$ Hz, 2H, CH₂N), 7.23 (m, 10H, H-Ph), 7.93 (s, 1H, H-8), 8.26 (br s, 1H, NH). ESI-MS: positive mode m/z 378.0 $[M+H]^+$, 399.9 $[M+Na]^+$.

General procedure for the synthesis of 8-alkynyl-9-alkyladenines 8-10, 12-20, and 34-38.

The title compounds were synthesized following similar methodologies previously reported^{175, 176}. To a solution of **5-7**, **11**, **29-33** (0.84 mmol) in dry DMF, bis(triphenylphosphine)palladium dichloride (12 mg, 0.017 mmol), CuI (0.84 mg, 0.004 mmol), Et₃N (3.4 mL), and the appropriate terminal alkyne (4.2 mmol) were added. The reaction mixture was stirred under N₂ atmosphere, at room temperature, for 5-7 days. For the synthesis of compounds **34-38**, the reaction mixtures were heated at 100°C under stirring and under N₂ atmosphere for 4-6 hs. The solvent was removed in vacuo and the residue was chromatographed on a silica gel column eluting with CHCl₃-cC₆H₁₂-CH₃OH (85:10:5) (compounds **8-10**), CH₂Cl₂-MeOH (100:00 to 95:5) (compounds **12-20**), or cC₆H₁₂-EtOAc (90:10 to 70:30) (compounds **34-38**). Compounds **12-20** and **34-38** were further purified by reverse-phase chromatography eluting with H₂O:CH₃CN (80:20 to 50:50).

9-(3-Hydroxypropyl)-8-phenylethynyl-9*H*-adenine (8): Yield: 42%. M.P.: 204-208 °C; ¹H-NMR (DMSO-*d*₆) δ: 2.00 (m, 2H, CH₂CH₂CH₂), 3.49 (m, 2H, CH₂OH), 4.36 (t, $J = 7.2$ Hz, 2H, CH₂-N), 4.68 (t, $J = 5.1$ Hz, 1H, CH₂OH), 7.48 (bs, 2H, NH₂), 7.55 (m, 3H, H-Ph), 7.72 (m, 2H, H-Ph), 8.20 (s, 1H, H-2). ESI-MS: positive mode m/z 294.0 $[M+H]^+$, 316.0 $[M+Na]^+$.

9-Phenylethyl-8-phenylethynyl-9*H*-adenine (9): Yield: 40%. M. p.: 167-171°C; ¹H-NMR (DMSO-*d*₆) δ: 3.17 (t, $J = 6.8$ Hz 2H, CH₂-Ph), 4.51 (t, $J = 7.0$ Hz, 2H, CH₂-N), 7.05-7.65 (m, 12H, H-Ph and NH₂), 8.21 (s, 1H, H-2). ESI-MS: positive mode m/z 340.0 $[M+H]^+$, 361.9 $[M+Na]^+$.

8-Phenylethynyl-9-phenylpropyl-9*H*-adenine (10): Yield: 51%. M. p.: 197-199 °C; ¹H-NMR (DMSO-*d*₆) δ: 2.18 (m, 2H, CH₂CH₂CH₂), 2.68 (t, $J = 7.5$ Hz, 2H, CH₂-Ph), 4.30 (t, $J = 7.2$ Hz, 2H, CH₂-N), 7.24 (m, 5H, H-Ph), 7.48 (bs, 2H, NH₂), 7.55 (m, 5H, H-Ph), 8.21 (s, 1H, H-2). ESI-MS: positive mode m/z 354.0 $[M+H]^+$, 375.9 $[M+Na]^+$.

9-Cyclopentyl-8-(para-methylphenylethynyl)-9*H*-adenine (12): Yield: 15%. M.p.: 212-216 °C; ¹H-NMR (DMSO-*d*₆) δ: 1.73 (m, 2H, H-cyclopentyl), 2.06 (m, 2H, H-cyclopentyl); 2.12 (m, 2H, H-cyclopentyl); 2.21 (m, 2H, H-cyclopentyl); 5.12 (m, 1H, NCH); 7.33 (m, 2H, H-Ph);

7.45 (s, 2H, NH₂); 7.58 (m, 2H, H-Ph); 8.17 (s, 1H, H-2). ESI-MS: positive mode m/z 318.0 [M+H]⁺, 340.0 [M+Na]⁺, 657.1 [2M+Na]⁺.

9-Cyclopentyl-8-(ortho-chlorophenylethynyl)-9H-adenine (13): Yield: 12%. M. p.: 208-210 °C; ¹H-NMR (DMSO-*d*₆) δ: 1.71 (m, 2H, H-cyclopentyl), 1.99 (m, 2H, H-cyclopentyl), 2.12 (m, 2H, H-cyclopentyl), 2.37 (m, 2H, H-cyclopentyl), 5.18 (m, 1H, NCH), 7.50 (m, 4H, H-Ph and NH₂), 7.68 (m, 1H, H-Ph), 7.82 (m, 1H, H-Ph), 8.19 (s, 1H, H-2). ESI-MS: positive mode m/z 338.1 [M+H]⁺, 360.1 [M+Na]⁺, 697.2 [2M+Na]⁺.

9-Cyclopentyl-8-(meta-chlorophenylethynyl)-9H-adenine (14): Yield: 7%. M. p.: 197-203 °C; ¹H-NMR (DMSO-*d*₆) δ: 1.74 (m, 2H, H-cyclopentyl), 2.00 (m, 2H, H-cyclopentyl), 2.13 (m, 2H, H-cyclopentyl), 2.33 (m, 2H, H-cyclopentyl), 5.15 (m, 1H, NCH), 7.49 (br s, 2H, NH₂), 7.54 (m, 1H, H-Ph), 7.62 (m, 1H, H-Ph), 7.67 (m, 1H, H-Ph), 7.82 (s, 1H, H-Ph), 8.19 (s, 1H, H-2). ESI-MS: positive mode m/z 338.3 [M+H]⁺, 360.3 [M+Na]⁺, 697.3 [2M+Na]⁺.

9-Cyclopentyl-8-(para-chlorophenylethynyl)-9H-adenine (15): Yield: 20%. M. p.: 230-235 °C; ¹H-NMR (DMSO-*d*₆) δ: 1.73 (m, 2H, H-cyclopentyl), 1.99 (m, 2H, H-cyclopentyl), 2.14 (m, 2H, H-cyclopentyl), 2.31 (m, 2H, H-cyclopentyl), 5.13 (m, 1H, NCH), 7.49 (br s, 2H, NH₂); 7.60 (m, 2H, H-Ph), 7.72 (m, 2H, H-Ph), 8.18 (s, 1H, H-2). ESI-MS: positive mode m/z 338.0 [M+H]⁺.

9-Cyclopentyl-8-(para-methoxyphenylethynyl)-9H-adenine (16): Yield: 35%. M. p.: 188-194 °C; ¹H-NMR (DMSO-*d*₆) δ: 1.73 (m, 2H, H-cyclopentyl), 2.00 (m, 2H, H-cyclopentyl), 2.13 (m, 2H, H-cyclopentyl), 2.31 (m, 2H, H-cyclopentyl), 3.83 (s, 3H, OCH₃), 5.12 (m, 1H, NCH), 7.06 (m, 2H, H-Ph), 7.42 (br s, 2H, NH₂), 7.63 (m, 2H, H-Ph), 8.18 (s, 1H, H-2). ESI-MS: positive mode m/z 334.0 [M+H]⁺, 356.0 [M+Na]⁺, 689.1 [2M+Na]⁺.

9-Cyclopentyl-8-(pyridin-4-ylethynyl)-9H-adenine (17): Yield: 10%. M. p.: 231-234 °C; ¹H-NMR (DMSO-*d*₆) δ: 1.74 (m, 2H, H-cyclopentyl), 2.01 (m, 2H, H-cyclopentyl), 2.15 (m, 2H, H-cyclopentyl), 2.32 (m, 2H, H-cyclopentyl), 5.15 (m, 1H, NCH), 7.55 (br s, 2H, NH₂), 7.67 (d, $J = 5.8$ Hz, 2H, H-Ph), 8.20 (s, 1H, H-2), 8.73 (d, $J = 4.8$ Hz, 2H, H-Ph). ESI-MS: positive mode m/z 304.9 [M+H]⁺.

9-Phenylethyl-8-(para-methoxyphenylethynyl)-9H-adenine (18): Yield: 8%. M. p.: 188-193 °C; ¹H-NMR (DMSO-*d*₆) δ: 3.17 (t, $J = 7.0$ Hz, 2H, CH₂Ph), 3.84 (s, 3H, OCH₃), 4.50 (t, $J = 7.0$ Hz, 2H, CH₂N), 7.08 (m, 4H, H-Ph), 7.11 (m, 3H, H-Ph), 7.47 (br s, 2H, NH₂), 7.58 (m, 2H, H-Ph), 8.20 (s, 1H, H-2). ESI-MS: positive mode m/z 370.0 [M+H]⁺, 392.0 [M+Na]⁺.

9-Phenylethyl-8-(ortho-chlorophenylethynyl)-9H-adenine (19): Yield: 28%. M. p.: 190-194 °C; ¹H-NMR (DMSO-*d*₆) δ: 3.19 (t, $J = 7.0$ Hz, 2H, CH₂Ph), 4.55 (t, $J = 7.0$ Hz, 2H, CH₂N),

7.15 (m, 2H, H-Ph), 7.18 (m, 3H, H-Ph), 7.50 -7.77 (m, 6H, H-Ph and NH₂), 8.23 (s, 1H, H-2). ESI-MS: positive mode m/z 373.9 [M+H]⁺, 395.8 [M+Na]⁺.

9-Phenethyl-8-(meta-chlorophenylethynyl)-9H-adenine (20): Yield: 9%. M. p.: 222-225 °C; ¹H-NMR (DMSO-*d*₆) δ: 3.17 (t, $J = 7.0$ Hz, 2H, CH₂Ph), 4.54 (t, $J = 7.0$ Hz, 2H, CH₂N), 7.07-7.18 (s, 5H, H-Ph), 7.49 (br s, 2H, NH₂), 7.63 (m, 3H, H-Ph), 7.72 (s, 1H, H-Ph), 8.23 (s, 1H, H-2). ESI-MS: positive mode m/z 373.9 [M+H]⁺, 395.8 [M+Na]⁺, 768.9 [2M+Na]⁺.

2-Chloro-9-cyclopentyl-8-(para-methoxyphenylethynyl)-9H-adenine (34): Yield: 15%. M. p.: 232-234 °C; ¹H-NMR (DMSO-*d*₆) δ: 1.73 (m, 2H, H-cyclopentyl), 1.99 (m, 2H, H-cyclopentyl), 2.14 (m, 2H, H-cyclopentyl), 2.25 (m, 2H, H-cyclopentyl), 3.84 (s, 3H, OCH₃), 5.01 (1H, NCH), 7.07 (m, 2H, H-Ph); 7.63 (m, 2H, H-Ph), 7.98 (s, 2H, NH₂). ESI-MS: positive mode m/z 368.1 [M+H]⁺, 390.1 [M+Na]⁺, 757.2 [2M+Na]⁺.

2-Chloro-9-phenylethyl-8-(para-methoxyphenylethynyl)-9H-adenine (35): Yield: 16%. M. p.: 232-236 °C; ¹H-NMR (DMSO-*d*₆) δ: 3.14 (t, $J = 7.0$ Hz, 2H, CH₂Ph), 3.84 (s, 3H, OCH₃), 4.46 (t, $J = 7.0$ Hz, 2H, CH₂N), 7.08 (m, 4H, H-Ph), 7.36 (m, 3H, H-Ph), 7.58 (d, $J = 2.0$ Hz, 2H, H-Ph), 7.93 (br s, 2H, NH₂). ESI-MS: positive mode m/z 404.0 [M+H]⁺, 425.9 [M+Na]⁺.

2-Chloro-*N*⁶-methyl-9-phenylethyl-8-(para-methoxyphenylethynyl)-9H-adenine (36): Yield: 17%. M. p.: 137-144 °C; ¹H-NMR (DMSO-*d*₆) δ: 2.94 (d, $J = 4.5$ Hz, 3H, CH₃NH), 3.14 (t, $J = 7.0$ Hz, 2H, CH₂Ph), 3.84 (s, 3H, OCH₃); 4.47 (t, $J = 7.0$ Hz, 2H, CH₂N), 7.07 (m, 4H, H-Ph), 7.18 (m, 3H, H-Ph), 7.56 (d, $J = 8.5$ Hz, 2H, H-Ph); 8.40 (s, 1H, CH₃NH). ESI-MS: positive mode m/z 338.1 [M+H]⁺, 360.1 [M+Na]⁺, 697.2 [2M+Na]⁺.

2-Chloro-*N*⁶-cyclopentyl-9-phenylethyl-8-(para-methoxyphenylethynyl)-9H-adenine (37): Yield: 23%. M. p.: 151-154 °C; ¹H-NMR (DMSO-*d*₆) δ: 1.57 (m, 4H, H-cyclopentyl), 1.72 (m, 2H, H-cyclopentyl), 1.93 (m, 2H, H-cyclopentyl), 3.14 (t, $J = 7.0$ Hz, 2H, CH₂Ph), 3.84 (s, 3H, OCH₃), 4.46 (t, $J = 7.0$ Hz, 2H, CH₂N), 7.10 (m, 4H, H-Ph), 7.19 (m, 3H, H-Ph), 7.55 (m, 2H, H-Ph), 8.48 (br m, 1H, NH). ESI-MS: positive mode m/z 472.0 [M+H]⁺, 494.0 [M+Na]⁺, 965.3 [2M+Na]⁺.

2-Chloro-*N*⁶,9-diphenylethyl-8-(para-methoxyphenylethynyl)-9H-adenine (38): Yield: 40%. M. p.: 204-206 °C; ¹H-NMR (DMSO-*d*₆) δ: 3.00 (m, 4H, 2 x CH₂Ph), 3.65 (m, 2H, CH₂NH); 3.87 (s, 3H, OCH₃), 4.50 (m, 2H, CH₂N), 7.20 (m, 4H, H-Ph), 7.30 (m, 4H, H-Ph), 7.45 (m, 4H, H-Ph), 7.55 (m, 2H, H-Ph), 8.51 (s, 1H, NH). ESI-MS: positive mode m/z 507.9 [M+H]⁺, 529.9 [M+Na]⁺.

4.5: Biological assay

The cell culture, preparation of membranes and binding Assay were done as described before in chapter 3 in experimental section. In addition the non-specific binding was determined in the presence of 1 mM theophylline for the A₁ receptor, or 100 μM R-PIA (*N*⁶-(1-methyl-2-phenylethyl)Ado) for the A_{2A} and A₃ receptors.

REFERENCES

1. Bruce, A.; Alexander, J.; Julian, L.; Martin, R.; Keith, R.; Peter, W., How Cells Obtain Energy from Food NCBI 2002, Molecular Biology of the Cell. 4th edition.
2. Bonora, M.; Patergnani, S.; Rimessi, A.; De Marchi, E.; Suski, J. M.; Bononi, A.; Giorgi, C.; Marchi, S.; Missiroli, S.; Poletti, F.; Wieckowski, M. R.; Pinton, P., ATP synthesis and storage. Purinergic signalling 2012, 8 (3), 343-57.
3. Whittaker, V. P.; Dowdall, M. J.; Dowe, G. H.; Facino, R. M.; Scotto, J., Proteins of cholinergic synaptic vesicles from the electric organ of Torpedo: characterization of a low molecular weight acidic protein. Brain research 1974, 75 (1), 115-31.
4. Chan, C. M.; Unwin, R. J.; Burnstock, G., Potential functional roles of extracellular ATP in kidney and urinary tract. Experimental nephrology 1998, 6 (3), 200-7.
5. Burnstock, G., Do some nerve cells release more than one transmitter? Neuroscience 1976, 1 (4), 239-48.
6. Burnstock, G., Purine and pyrimidine receptors. Cellular and Molecular Life Sciences 2007, 64 (12), 1471-83.
7. Burnstock, G.; Kennedy, C., Is there a basis for distinguishing two types of P2-purinoceptor? General pharmacology 1985, 16 (5), 433-40.
8. Burnstock, G., Introduction: P2 receptors. Current topics in medicinal chemistry 2004, 4 (8), 793-803.
9. Burnstock, G., Purinergic signalling. British journal of pharmacology 2006, 147 Suppl 1, S172-81.
10. Burnstock, G., Discovery of purinergic signalling, the initial resistance and current explosion of interest. British journal of pharmacology 2012, 167 (2), 238-55.
11. Burnstock, G., Purinergic signalling and disorders of the central nervous system. Nature Reviews Drug Discovery 2008, 7 (7), 575-90.
12. Jerry, B., ATP: The Perfect Energy Currency for the Cell Creation Research Society Quarterly 1999, 36 (1).
13. Kunji, E. R. S.; Aleksandrova, A.; King, M. S.; Majd, H.; Ashton, V. L.; Cerson, E.; Springett, R.; Kibalchenko, M.; Tavoulari, S.; Crichton, P. G.; Ruprecht, J. J., The transport mechanism of the mitochondrial ADP/ATP carrier Bba-Mol Cell Res 2016, 1863 (12), 3169-3169.
14. Ralevic, V.; Burnstock, G., Receptors for purines and pyrimidines. Pharmacological reviews 1998, 50 (3), 413-92.
15. Burnstock, G.; Knight, G. E., Cellular distribution and functions of P2 receptor subtypes in different systems. International review of cytology 2004, 240, 31-304.
16. Metzger, M. W.; Walser, S. M.; Aprile-Garcia, F.; Dedic, N.; Chen, A.; Holsboer, F.; Arzt, E.; Wurst, W.; Deussing, J. M., Genetically dissecting P2RX7 expression within the central nervous system using conditional humanized mice. Purinergic signalling 2017, 13 (2), 153-170.
17. Miras-Portugal, M. T.; Diaz-Hernandez, J. I.; Gomez-Villafuertes, R.; Diaz-Hernandez, M.; Artalejo, A. R.; Gualix, J., Role of P2X7 and P2Y2 receptors on alpha-secretase-dependent APP processing: Control of amyloid plaques formation "in vivo" by P2X7 receptor. Computational and structural biotechnology journal 2015, 13, 176-81.
18. Woods, L. T.; Ajit, D.; Camden, J. M.; Erb, L.; Weisman, G. A., Purinergic receptors as potential therapeutic targets in Alzheimer's disease. Neuropharmacology 2016, 104, 169-79.

19. Wang, X. H.; Xie, X.; Luo, X. G.; Shang, H.; He, Z. Y., Inhibiting purinergic P2X7 receptors with the antagonist brilliant blue G is neuroprotective in an intranigral lipopolysaccharide animal model of Parkinson's disease. *Molecular medicine reports* 2017, 15 (2), 768-776.
20. Kimbler, D. E.; Shields, J.; Yanasak, N.; Vender, J. R.; Dhandapani, K. M., Activation of P2X7 promotes cerebral edema and neurological injury after traumatic brain injury in mice. *PloS one* 2012, 7 (7), e41229.
21. Masuch, A.; Shieh, C. H.; van Rooijen, N.; van Calker, D.; Biber, K., Mechanism of microglia neuroprotection: Involvement of P2X7, TNFalpha, and valproic acid. *Glia* 2016, 64 (1), 76-89.
22. Ren, M.; Liu, Y.; Zhao, H.; Dong, S.; Jiang, Z.; Li, K.; Tian, J., Adenosine triphosphate postconditioning is associated with better preserved global and regional cardiac function during myocardial ischemia and reperfusion: a speckle tracking imaging-based echocardiologic study. *Cardiovascular therapeutics* 2016, 34 (5), 343-51.
23. Burnstock, G., Purinergic Signalling: Therapeutic Developments. *Frontiers in pharmacology* 2017, 8, 661.
24. Sarafoff, N.; Byrne, R. A.; Sibbing, D., Clinical use of clopidogrel. *Current pharmaceutical design* 2012, 18 (33), 5224-39.
25. Christopher, A. B.; Yishai, M. E.; Andres, P.; and Bolton, M. M., Cellular resolution circuit mapping with temporal-focused excitation of soma-targeted channelrhodopsin. *Elife* 2016, 5.
26. Basoglu, O. K.; Barnes, P. J.; Kharitonov, S. A.; Pelleg, A., Effects of Aerosolized Adenosine 5'-Triphosphate in Smokers and Patients With COPD. *Chest* 2015, 148 (2), 430-435.
27. Tsuda, M.; Inoue, K., Neuron-microglia interaction by purinergic signaling in neuropathic pain following neurodegeneration. *Neuropharmacology* 2016, 104, 76-81.
28. Tsuda, M., P2 receptors, microglial cytokines and chemokines, and neuropathic pain. *Journal of neuroscience research* 2017, 95 (6), 1319-1329.
29. Amoroso, F.; Capece, M.; Rotondo, A.; Cangelosi, D.; Ferracin, M.; Franceschini, A.; Raffaghello, L.; Pistoia, V.; Varesio, L.; Adinolfi, E., The P2X7 receptor is a key modulator of the PI3K/GSK3beta/VEGF signaling network: evidence in experimental neuroblastoma. *Oncogene* 2015, 34 (41), 5240-51.
30. Gomez-Villafuertes, R.; Garcia-Huerta, P.; Diaz-Hernandez, J. I.; Miras-Portugal, M. T., PI3K/Akt signaling pathway triggers P2X7 receptor expression as a pro-survival factor of neuroblastoma cells under limiting growth conditions. *Scientific reports* 2015, 5, 18417.
31. Mishra, A.; Guo, Y.; Zhang, L.; More, S.; Weng, T.; Chintagari, N. R.; Huang, C.; Liang, Y.; Pushparaj, S.; Gou, D.; Breshears, M.; Liu, L., A Critical Role for P2X7 Receptor-Induced VCAM-1 Shedding and Neutrophil Infiltration during Acute Lung Injury. *J Immunol* 2016, 197 (7), 2828-37.
32. Zimmermann, H., Extracellular metabolism of ATP and other nucleotides. *Naunyn-Schmiedeberg's archives of pharmacology* 2000, 362 (4-5), 299-309.
33. Drury, A. N.; Szent-Gyorgyi, A., The physiological activity of adenine compounds with especial reference to their action upon the mammalian heart. *The Journal of physiology* 1929, 68 (3), 213-37.
34. Sattin, A.; Rall, T. W., The effect of adenosine and adenine nucleotides on the cyclic adenosine 3', 5'-phosphate content of guinea pig cerebral cortex slices. *Molecular Pharmacology* 1970, 6 (1), 13-23.
35. Phillis, J. W.; Edstrom, J. P.; Kostopoulos, G. K.; Kirkpatrick, J. R., Effects of adenosine and adenine nucleotides on synaptic transmission in the cerebral cortex. *Canadian journal of physiology and pharmacology* 1979, 57 (11), 1289-312.

36. Kostopoulos, G. K.; Limacher, J. J.; Phillis, J. W., Action of various adenine derivatives on cerebellar Purkinje cells. *Brain research* 1975, 88 (1), 162-5.
37. Kuroda, Y.; Saito, M.; Kobayashi, K., Concomitant changes in cyclic AMP level and postsynaptic potentials of olfactory cortex slices induced by adenosine derivatives. *Brain research* 1976, 109 (1), 196-201.
38. Michaelis, M. L.; Michaelis, E. K.; Myers, S. L., Adenosine modulation of synaptosomal dopamine release. *Life sciences* 1979, 24 (22), 2083-92.
39. Harms, H. H.; Wardeh, G.; Mulder, A. H., Adenosine modulates depolarization-induced release of 3H-noradrenaline from slices of rat brain neocortex. *European journal of pharmacology* 1978, 49 (3), 305-8.
40. Corradetti, R.; Lo Conte, G.; Moroni, F.; Passani, M. B.; Pepeu, G., Adenosine decreases aspartate and glutamate release from rat hippocampal slices. *European journal of pharmacology* 1984, 104 (1-2), 19-26.
41. Harms, H. H.; Wardeh, G.; Mulder, A. H., Effect of adenosine on depolarization-induced release of various radiolabelled neurotransmitters from slices of rat corpus striatum. *Neuropharmacology* 1979, 18 (7), 577-80.
42. Fredholm, B. B.; IJzerman, A. P.; Jacobson, K. A.; Klotz, K.-N.; Linden, J., International Union of Pharmacology. XXV. Nomenclature and classification of adenosine receptors. *Pharmacological reviews* 2001, 53 (4), 527-52.
43. Linden, J., Adenosine in tissue protection and tissue regeneration. *Mol Pharmacol* 2005, 67 (5), 1385-7.
44. Snyder, S. H., Adenosine as a Neuromodulator. *Annu Rev Neurosci* 1985, 8, 103-124.
45. Corti, F.; Cellai, L.; Melani, A.; Donati, C.; Bruni, P.; Pedata, F., Adenosine is present in rat brain synaptic vesicles. *Neuroreport* 2013, 24 (17), 982-7.
46. Polosa, R.; Holgate, S. T., Adenosine receptors as promising therapeutic targets for drug development in chronic airway inflammation. *Current Drug Targets* 2006, 7 (6), 699-706.
47. Snyder, S. H., Adenosine as a neuromodulator. *Annual review of neuroscience* 1985, 8, 103-24.
48. Jarvis, S. M.; Young, J. D., Nucleoside transport in rat erythrocytes: two components with differences in sensitivity to inhibition by nitrobenzylthioinosine and p-chloromercuriphenyl sulfonate. *The Journal of membrane biology* 1986, 93 (1), 1-10.
49. Anderson, C. M.; Xiong, W.; Geiger, J. D.; Young, J. D.; Cass, C. E.; Baldwin, S. A.; Parkinson, F. E., Distribution of equilibrative, nitrobenzylthioinosine-sensitive nucleoside transporters (ENT1) in brain. *Journal of neurochemistry* 1999, 73 (2), 867-73.
50. Ritzel, M. W.; Yao, S. Y.; Huang, M. Y.; Elliott, J. F.; Cass, C. E.; Young, J. D., Molecular cloning and functional expression of cDNAs encoding a human Na⁺-nucleoside cotransporter (hCNT1). *American Journal of Physiology* 1997, 272 (2 Pt 1), C707-14.
51. Griffith, D. A.; Jarvis, S. M., Nucleoside and nucleobase transport systems of mammalian cells. *Biochimica et biophysica acta* 1996, 1286 (3), 153-81.
52. Dunwiddie, T. V.; Diao, L., Regulation of extracellular adenosine in rat hippocampal slices is temperature dependent: role of adenosine transporters. *Neuroscience* 2000, 95 (1), 81-8.
53. Jacobson, K. A.; Gao, Z. G., Adenosine receptors as therapeutic targets. *Nature Reviews Drug Discovery* 2006, 5 (3), 247-64.
54. Franco, R.; Canela, E. I.; Bozal, J., Heterogeneous localization of some purine enzymes in subcellular fractions of rat brain and cerebellum. *Neurochem Research* 1986, 11 (3), 423-35.

55. Latini, S.; Pedata, F., Adenosine in the central nervous system: release mechanisms and extracellular concentrations. *Journal of neurochemistry* 2001, 79 (3), 463-84.
56. Van Calker, D.; Muller, M.; Hamprecht, B., Adenosine regulates via two different types of receptors, the accumulation of cyclic AMP in cultured brain cells. *Journal of neurochemistry* 1979, 33 (5), 999-1005.
57. Daly, J. W.; Butts-Lamb, P.; Padgett, W., Subclasses of adenosine receptors in the central nervous system: interaction with caffeine and related methylxanthines. *Cellular and Molecular Neurobiology* 1983, 3 (1), 69-80.
58. Legerski, R.; Zhou, X.; Dresback, J.; Eberspaecher, H.; McKinney, S.; Segarini, P.; de Crombrughe, B., Molecular cloning and characterization of a novel rat activin receptor. *Biochem Biophys Res Commun* 1992, 183 (2), 672-9.
59. Sajjadi, F. G.; Firestein, G. S., Cdna Cloning and Sequence-Analysis of the Human A3-Adenosine Receptor. *Biochimica et biophysica acta* 1993, 1179 (1), 105-107.
60. Salvatore, C. A.; Jacobson, M. A.; Taylor, H. E.; Linden, J.; Johnson, R. G., Molecular cloning and characterization of the human A3 adenosine receptor. *Proceedings of the National Academy of Sciences of the United States of America* 1993, 90 (21), 10365-9.
61. Stone, T. W., Receptors for adenosine and adenine nucleotides. *General pharmacology* 1991, 22 (1), 25-31.
62. Varani, K.; Gessi, S.; Dalpiaz, A.; Borea, P. A., Pharmacological and biochemical characterization of purified A2a adenosine receptors in human platelet membranes by [3H]-CGS 21680 binding. *British journal of pharmacology* 1996, 117 (8), 1693-1701.
63. Olah, M. E.; Stiles, G. L., Adenosine receptor subtypes: characterization and therapeutic regulation. *Annual Review of Pharmacology and Toxicology* 1995, 35, 581-606.
64. Baldwin, J. M., Structure and function of receptors coupled to G proteins. *Current opinion in cell biology* 1994, 6 (2), 180-90.
65. Fredholm, B. B.; IJzerman, A. P.; Jacobson, K. A.; Klotz, K.-N.; Linden, J., International Union of Pharmacology. XXV. Nomenclature and classification of adenosine receptors. *Pharmacological reviews* 2001, 53 (4), 527-552.
66. Jaakola, V. P.; Griffith, M. T.; Hanson, M. A.; Cherezov, V.; Chien, E. Y.; Lane, J. R.; IJzerman, A. P.; Stevens, R. C., The 2.6 angstrom crystal structure of a human A2A adenosine receptor bound to an antagonist. *Science* 2008, 322 (5905), 1211-7.
67. Xu, F.; Wu, H.; Katritch, V.; Han, G. W.; Jacobson, K. A.; Gao, Z. G.; Cherezov, V.; Stevens, R. C., Structure of an agonist-bound human A2A adenosine receptor. *Science* 2011, 332 (6027), 322-7.
68. Lebon, G.; Edwards, P. C.; Leslie, A. G. W.; Tate, C. G., Molecular Determinants of CGS21680 Binding to the Human Adenosine A2A Receptor. *Mol Pharmacol* 2015.
69. Lebon, G.; Warne, T.; Edwards, P. C.; Bennett, K.; Langmead, C. J.; Leslie, A. G.; Tate, C. G., Agonist-bound adenosine A2A receptor structures reveal common features of GPCR activation. *Nature* 2011, 474 (7352), 521-5.
70. Reppert, S. M.; Weaver, D. R.; Stehle, J. H.; Rivkees, S. A., Molecular cloning and characterization of a rat A1-adenosine receptor that is widely expressed in brain and spinal cord. *Molecular endocrinology* 1991, 5 (8), 1037-48.
71. Sajjadi, F. G.; Firestein, G. S., cDNA cloning and sequence analysis of the human A3 adenosine receptor. *Biochimica et Biophysica Acta (BBA)-Molecular Cell Research* 1993, 1179 (1), 105-107.

72. Cooper, D. M.; Londos, C.; Rodbell, M., Adenosine receptor-mediated inhibition of rat cerebral cortical adenylate cyclase by a GTP-dependent process. *Molecular Pharmacology* 1980, 18 (3), 598-601.
73. Megson, A. C.; Dickenson, J. M.; Townsend-Nicholson, A.; Hill, S. J., Synergy between the inositol phosphate responses to transfected human adenosine A1-receptors and constitutive P2-purinoceptors in CHO-K1 cells. *British journal of pharmacology* 1995, 115 (8), 1415-1424.
74. Nisha, J.; Nicola, K.; Olasumbo, A.; Patricia, B.; & revor, W. S., Anxiolytic activity of adenosine receptor activation in mice. *British journal of pharmacology* 1995, 116 (3), 2127-2133.
75. Trost, T.; Schwabe, U., Adenosine Receptors in Fat Cells Identification by (-)-N6-[3H] Phenylisopropyladenosine Binding. *Molecular Pharmacology* 1981, 19 (2), 228-235.
76. Ollson, R. A.; pearson, J. D.; Straub, R. W., Cardiovascular purinoceptor. 1990; p 70, 761-845.
77. Ferré, S.; Fuxe, K.; Fredholm, B. B.; Morelli, M.; Popoli, P., Adenosine–dopamine receptor–receptor interactions as an integrative mechanism in the basal ganglia. *Trends in neurosciences* 1997, 20 (10), 482-487.
78. Le, F.; Townsend-Nicholson, A.; Baker, E.; Sutherland, G. R.; Schofield, P. R., Characterization and chromosomal localization of the human A2A adenosine receptor gene: ADORA2A. *Biochemical and Biophysical Research Communications* 1996, 223 (2), 461-467.
79. Svenningsson, P.; Le Moine, C.; Kull, B.; Sunahara, R.; Bloch, B.; Fredholm, B. B., Cellular expression of adenosine A 2A receptor messenger RNA in the rat central nervous system with special reference to dopamine innervated areas. *Neuroscience* 1997, 80 (4), 1171-1185.
80. Varani, K.; Gessi, S.; Dalpiaz, A.; Ongini, E.; Borea, P. A., Characterization of A2A adenosine receptors in human lymphocyte membranes by [3H]-SCH 58261 binding. *British journal of pharmacology* 1997, 122 (2), 386-392.
81. Moreau, J.-L.; Huber, G., Central adenosine A2A receptors: an overview. *Brain research reviews* 1999, 31 (1), 65-82.
82. Fuxe, K.; Ferre, S.; Canals, M.; Torvinen, M.; Terasmaa, A.; Marcellino, D.; Goldberg, S. R.; Staines, W.; Jacobsen, K. X.; Lluís, C.; Woods, A. S.; Agnati, L. F.; Franco, R., Adenosine A2A and dopamine D2 heteromeric receptor complexes and their function. *Journal of Molecular Neuroscience* 2005, 26 (2-3), 209-20.
83. Ferre, S.; Goldberg, S. R.; Lluís, C.; Franco, R., Looking for the role of cannabinoid receptor heteromers in striatal function. *Neuropharmacology* 2009, 56 Suppl 1, 226-34.
84. Ferre, S.; Karcz-Kubicha, M.; Hope, B. T.; Popoli, P.; Burgueno, J.; Gutierrez, M. A.; Casado, V.; Fuxe, K.; Goldberg, S. R.; Lluís, C.; Franco, R.; Ciruela, F., Synergistic interaction between adenosine A2A and glutamate mGlu5 receptors: implications for striatal neuronal function. *Proceedings of the National Academy of Sciences of the United States of America* 2002, 99 (18), 11940-5.
85. Navarro, G.; Carriba, P.; Gandia, J.; Ciruela, F.; Casado, V.; Cortes, A.; Mallol, J.; Canela, E. I.; Lluís, C.; Franco, R., Detection of heteromers formed by cannabinoid CB1, dopamine D2, and adenosine A2A G-protein-coupled receptors by combining bimolecular fluorescence complementation and bioluminescence energy transfer. *ScientificWorldJournal* 2008, 8, 1088-97.
86. Bouma, M. G.; van den Wildenberg, F. A.; Buurman, W. A., Adenosine inhibits cytokine release and expression of adhesion molecules by activated human endothelial cells. *American Journal of Physiology* 1996, 270 (2 Pt 1), C522-9.

87. Hettinger, B. D.; Lee, A.; Linden, J.; Rosin, D. L., Ultrastructural localization of adenosine A2A receptors suggests multiple cellular sites for modulation of GABAergic neurons in rat striatum. *Journal of Comparative Neurology* 2001, 431 (3), 331-46.
88. Sebastiao, A. M.; Ribeiro, J. A., Adenosine A2 receptor-mediated excitatory actions on the nervous system. *Progress in neurobiology* 1996, 48 (3), 167-89.
89. Kull, B.; Ferre, S.; Arslan, G.; Svenningsson, P.; Fuxe, K.; Owman, C.; Fredholm, B. B., Reciprocal interactions between adenosine A2A and dopamine D2 receptors in Chinese hamster ovary cells co-transfected with the two receptors. *Biochemical pharmacology* 1999, 58 (6), 1035-45.
90. Ferre, S.; Ciruela, F.; Woods, A. S.; Lluís, C.; Franco, R., Functional relevance of neurotransmitter receptor heteromers in the central nervous system. *Trends in neurosciences* 2007, 30 (9), 440-6.
91. Pinna, A.; di Chiara, G.; Wardas, J.; Morelli, M., Blockade of A2a adenosine receptors positively modulates turning behaviour and c-Fos expression induced by D1 agonists in dopamine-denervated rats. *European Journal of Neuroscience* 1996, 8 (6), 1176-81.
92. Schiffmann, S. N.; Vanderhaeghen, J.-J., Adenosine A2 receptors regulate the gene expression of striatopallidal and striatonigral neurons. *The Journal of neuroscience* 1993, 13 (3), 1080-1087.
93. Aoyama, S.; Kase, H.; Borrelli, E., Rescue of locomotor impairment in dopamine D2 receptor-deficient mice by an adenosine A2A receptor antagonist. *Neuroscience - Journal* 2000, 20 (15), 5848-52.
94. Dubey, R. K.; Gillespie, D. G.; Osaka, K.; Suzuki, F.; Jackson, E. K., Adenosine Inhibits Growth of Rat Aortic Smooth Muscle Cells Possible Role of A2b Receptor. *Hypertension* 1996, 27 (3), 786-793.
95. Feoktistov, I.; Biaggioni, I., Characterization of adenosine receptors in human erythroleukemia cells and platelets: further evidence for heterogeneity of adenosine A2 receptor subtypes. *Molecular Pharmacology* 1993, 43 (6), 909-914.
96. Feoktistov, I.; Biaggioni, I., Adenosine A2B receptors evoke interleukin-8 secretion in human mast cells. An enprofylline-sensitive mechanism with implications for asthma. *Journal of Clinical Investigation* 1995, 96 (4), 1979.
97. Yakel, J. L.; Warren, R. A.; Reppert, S. M.; North, R. A., Functional expression of adenosine A2b receptor in *Xenopus* oocytes. *Molecular Pharmacology* 1993, 43 (2), 277-280.
98. Nicholls, J.; Brownhill, V. R.; Hourani, S. M. O., Characterization of P1-purinoceptors on rat isolated duodenum longitudinal muscle and muscularis mucosae. *British journal of pharmacology* 1996, 117 (1), 170-174.
99. Iwamoto, T.; Umemura, S.; Toya, Y.; Uchibori, T.; Kogi, K.; Takagi, N.; Ishii, M., Identification of adenosine A2 receptor-cAMP system in human aortic endothelial cells. *Current pharmaceutical design* 1994, 199 (2), 905-910.
100. Vallejo, A. I.; Arin, R. M.; Schijvarger, S. A.; Varela, A., Role of A2B receptors in the gastric mucosal cells. *Drug Development Research* 2000, 50, 87.
101. Forsythe, P.; Ennis, M., Adenosine, mast cells and asthma. *Inflammation Research* 1999, 48 (6), 301-7.
102. Dubey, R. K.; Gillespie, D. G.; Mi, Z.; Jackson, E. K., Exogenous and endogenous adenosine inhibits fetal calf serum-induced growth of rat cardiac fibroblasts: role of A2B receptors. *Circulation* 1997, 96 (8), 2656-66.

103. Morrison, R. R.; Talukder, M. A.; Ledent, C.; Mustafa, S. J., Cardiac effects of adenosine in A(2A) receptor knockout hearts: uncovering A(2B) receptors. *American Journal of Physiology-Heart and Circulatory Physiology* 2002, 282 (2), H437-44.
104. Linden, J., Cloned adenosine A3 receptors: pharmacological properties, species differences and receptor functions. *Trends in pharmacological sciences* 1994, 15 (8), 298-306.
105. Abbracchio, M. P.; Brambilla, R.; Ceruti, S.; Kim, H. O.; von Lubitz, D.; Jacobson, K. A.; Cattabeni, F., G protein-dependent activation of phospholipase C by adenosine A3 receptors in rat brain. *Molecular Pharmacology* 1995, 48 (6), 1038-1045.
106. Van Schaick, E. A.; Jacobson, K. A.; Kim, H. O.; IJzerman, A. P.; Danhof, M., Hemodynamic effects and histamine release elicited by the selective adenosine A3 receptor agonist 2-Cl-IB-MECA in conscious rats. *European journal of pharmacology* 1996, 308 (3), 311-4.
107. Ezeamuzie, C. I.; Elizabeth, P. E., Adenosine A3 receptors on human eosinophils mediate inhibition of degranulation and superoxide release. *British journal of pharmacology* 1999, 127, 188-194.
108. Fishman, P.; Bar-Yehuda, S.; Ohana, G.; Barer, F.; Ochaion, A.; Erlanger, A.; Madi, L., An agonist to the A3 adenosine receptor inhibits colon carcinoma growth in mice via modulation of GSK-3 beta and NF-kappa B. *Oncogene* 2004, 23 (14), 2465-71.
109. Marcel, Y. A.; Richard, A. S.; Mortimer, M. C., Knockout of A3 adenosine receptors reduces mouse intraocular pressure. *Investigative Ophthalmology & Visual Science* 2002, 43 (9), 3021-6.
110. Bodin, P.; Burnstock, G., Purinergic signalling: ATP release. *Neurochem Research* 2001, 26 (8-9), 959-69.
111. Burnstock, G., Noradrenaline and ATP as cotransmitters in sympathetic nerves. *Neurochemistry international* 1990, 17 (2), 357-68.
112. Gessi, S.; Merighi, S.; Varani, K.; Borea, P. A., Adenosine receptors in health and disease. *Naunyn-Schmiedeberg's archives of pharmacology* 2011, 61, 41-75.
113. Sheth, S.; Brito, R.; Mukherjea, D.; Rybak, L. P.; Ramkumar, V., Adenosine receptors: expression, function and regulation. *International journal of molecular sciences* 2014, 15 (2), 2024-52.
114. Layland, J.; Carrick, D.; Lee, M.; Oldroyd, K.; Berry, C., Adenosine: physiology, pharmacology, and clinical applications. *JACC: Cardiovascular Interventions* 2014, 7 (6), 581-91.
115. Eckle, T.; Krahn, T.; Grenz, A.; Kohler, D.; Mittelbronn, M.; Ledent, C.; Jacobson, M. A.; Osswald, H.; Thompson, L. F.; Unertl, K.; Eltzschig, H. K., Cardioprotection by ecto-5'-nucleotidase (CD73) and A2B adenosine receptors. *Circulation* 2007, 115 (12), 1581-90.
116. Meghji, P.; Newby, A. C., Sites of adenosine formation, action and inactivation in the brain. *Neurochemistry international* 1990, 16 (3), 227-32.
117. Dunwiddie, T. V.; Masino, S. A., The role and regulation of adenosine in the central nervous system. *Annual review of neuroscience* 2001, 24, 31-55.
118. Ryzhov, S.; Novitskiy, S. V.; Zaynagetdinov, R.; Goldstein, A. E.; Carbone, D. P.; Biaggioni, I.; Dikov, M. M.; Feoktistov, I., Host A(2B) adenosine receptors promote carcinoma growth. *Neoplasia* 2008, 10 (9), 987-95.
119. Chen, G. J.; Harvey, B. K.; Shen, H.; Chou, J.; Victor, A.; Wang, Y., Activation of adenosine A3 receptors reduces ischemic brain injury in rodents. *Journal of neuroscience research* 2006, 84 (8), 1848-55.
120. Martin, T. J.; Eisenach, J. C.; Mislser, J.; Childers, S. R., Chronic activation of spinal adenosine A1 receptors results in hypersensitivity. *Neuroreport* 2006, 17 (15), 1619-22.

121. Ohta, A.; Sitkovsky, M., Role of G-protein-coupled adenosine receptors in downregulation of inflammation and protection from tissue damage. *Nature* 2001, 414 (6866), 916-20.
122. Yaar, R.; Jones, M. R.; Chen, J. F.; Ravid, K., Animal models for the study of adenosine receptor function. *Journal of cellular physiology* 2005, 202 (1), 9-20.
123. Sachdeva, S.; Gupta, M., Adenosine and its receptors as therapeutic targets: An overview. *Saudi Pharmaceutical Journal* 2013, 21 (3), 245-53.
124. Yuzlenko, O.; Kiec-Kononowicz, K., Potent adenosine A1 and A2A receptors antagonists: recent developments. *Current medicinal chemistry* 2006, 13 (30), 3609-25.
125. Gronning, L. M.; Dahle, M. K.; Tasken, K. A.; Enerback, S.; Hedin, L.; Tasken, K.; Knutsen, H. K., Isoform-specific regulation of the CCAAT/enhancer-binding protein family of transcription factors by 3',5'-cyclic adenosine monophosphate in Sertoli cells. *Endocrinology* 1999, 140 (2), 835-43.
126. Fredholm, B. B.; Jacobson, K. A., Adenosine Receptors: The Contributions by John W. Daly. *Heterocycles* 2009, 79 (1), 73-83.
127. Livingston, M.; Heaney, L. G.; Ennis, M., Adenosine, inflammation and asthma--a review. *Inflamm Res* 2004, 53 (5), 171-8.
128. Jacobson, K. A., Adenosine A3 receptors: novel ligands and paradoxical effects. *Trends in pharmacological sciences* 1998, 19 (5), 184-91.
129. Yan, L.; Burbiel, J. C.; Maass, A.; Muller, C. E., Adenosine receptor agonists: from basic medicinal chemistry to clinical development. *Expert opinion on emerging drugs* 2003, 8 (2), 537-76.
130. Beukers, M. W.; Chang, L. C.; von Frijtag Drabbe Kunzel, J. K.; Mulder-Krieger, T.; Spanjersberg, R. F.; Brussee J.; IJzerman, A. P., New, non-adenosine, high-potency agonists for the human adenosine A_{2B} receptor with an improved selectivity profile compared to the reference agonist N-ethylcarboxamidoadenosine. *Journal of medicinal chemistry* 2004, 47 (15), 3707-9.
131. Schirok, H.; Kast, R.; Figueroa-Perez, S.; Bennabi, S.; Gnoth, M. J.; Feurer, A.; Heckroth, H.; Thutewohl, M.; Paulsen, H.; Knorr, A.; Hutter, J.; Lobell, M.; Munter, K.; Geiss, V.; Ehmke, H.; Lang, D.; Radtke, M.; Mittendorf, J.; Stasch, J. P., Design and synthesis of potent and selective azaindole-based Rho kinase (ROCK) inhibitors. *ChemMedChem* 2008, 3 (12), 1893-904.
132. Muller, C. E.; Jacobson, K. A., Recent developments in adenosine receptor ligands and their potential as novel drugs. *Biochimica et biophysica acta* 2011, 1808 (5), 1290-308.
133. Baraldi, P. G.; Tabrizi, M. A.; Gessi, S.; Borea, P. A., Adenosine receptor antagonists: translating medicinal chemistry and pharmacology into clinical utility. *Chemical reviews* 2008, 108 (1), 238-63.
134. Moro, S.; Deflorian, F.; Bacilieri, M.; Spalluto, G., Novel strategies for the design of new potent and selective human A3 receptor antagonists: an update. *Current medicinal chemistry* 2006, 13 (6), 639-45.
135. Schwartz, T. W.; Holst, B., Allosteric enhancers, allosteric agonists and ago-allosteric modulators: where do they bind and how do they act? *Trends in pharmacological sciences* 2007, 28 (8), 366-73.
136. Goblyos, A.; Ijzerman, A. P., Allosteric modulation of adenosine receptors. *Purinergic signalling* 2009, 5 (1), 51-61.
137. Goblyos, A.; Ijzerman, A. P., Allosteric modulation of adenosine receptors. *Biochimica et biophysica acta* 2011, 1808 (5), 1309-18.
138. Bruns, R. F.; Fergus, J. H.; Coughenour, L. L.; Courtland, G. G.; Pugsley, T. A.; Dodd, J. H.; Tinney, F. J., Structure-activity relationships for enhancement of adenosine A1 receptor binding by 2-amino-3-benzoylthiophenes. *Mol Pharmacol* 1990, 38 (6), 950-8.

139. Baraldi, P. G.; Zaid, A. N.; Lampronti, I.; Fruttarolo, F.; Pavani, M. G.; Tabrizi, M. A.; Shryock, J. C.; Leung, E.; Romagnoli, R., Synthesis and biological effects of a new series of 2-amino-3-benzoylthiophenes as allosteric enhancers of A1-adenosine receptor. *Bioorganic & medicinal chemistry letters* 2000, 10 (17), 1953-7.
140. Giorgi, I.; Biagi, G.; Bianucci, A. M.; Borghini, A.; Livi, O.; Leonardi, M.; Pietra, D.; Calderone, V.; Martelli, A., N6-1,3-diphenylurea derivatives of 2-phenyl-9-benzyladenines and 8-azaadenines: synthesis and biological evaluation as allosteric modulators of A2A adenosine receptors. *European journal of medicinal chemistry* 2008, 43 (8), 1639-47.
141. Borrmann, T.; Hinz, S.; Bertarell, D. C.; Li, W.; Florin, N. C.; Scheiff, A. B.; Muller, C. E., 1-alkyl-8-(piperazine-1-sulfonyl)phenylxanthines: development and characterization of adenosine A2B receptor antagonists and a new radioligand with subnanomolar affinity and subtype specificity. *Journal of medicinal chemistry* 2009, 52 (13), 3994-4006.
142. Gao, Z. G.; Van Muijlwijk-Koezen, J. E.; Chen, A.; Muller, C. E.; Ijzerman, A. P.; Jacobson, K. A., Allosteric modulation of A(3) adenosine receptors by a series of 3-(2-pyridinyl)isoquinoline derivatives. *Molecular Pharmacology* 2001, 60 (5), 1057-63.
143. van Muijlwijk-Koezen, J. E.; Timmerman, H.; Link, R.; van der Goot, H.; IJzerman, A. P., A novel class of adenosine A3 receptor ligands. 1. 3-(2-Pyridinyl)isoquinoline derivatives. *Journal of medicinal chemistry* 1998, 41 (21), 3987-93.
144. van Galen, P. J.; Nissen, P.; van Wijngaarden, I.; IJzerman, A. P.; Soudijn, W., 1H-imidazo[4,5-c]quinolin-4-amines: novel non-xanthine adenosine antagonists. *Journal of medicinal chemistry* 1991, 34 (3), 1202-6.
145. Lane, J. R.; Beukers, M. W.; Mulder-Krieger, T.; Ijzerman, A. P., The endocannabinoid 2-arachidonylglycerol is a negative allosteric modulator of the human A3 adenosine receptor. *Biochemical pharmacology* 2010, 79 (1), 48-56.
146. Carriba, P.; Navarro, G.; Ciruela, F.; Ferre, S.; Casado, V.; Agnati, L.; Cortes, A.; Mallol, J.; Fuxe, K.; Canela, E. I.; Lluís, C.; Franco, R., Detection of heteromerization of more than two proteins by sequential BRET-FRET. *Nature methods* 2008, 5 (8), 727-33.
147. Franco, R.; Casado, V.; Cortes, A.; Perez-Capote, K.; Mallol, J.; Canela, E.; Ferre, S.; Lluís, C., Novel pharmacological targets based on receptor heteromers. *Brain Research Reviews* 2008, 58 (2), 475-82.
148. Gao, Z. G.; Blaustein, J. B.; Gross, A. S.; Melman, N.; Jacobson, K. A., N6-Substituted adenosine derivatives: selectivity, efficacy, and species differences at A3 adenosine receptors. *Biochemical pharmacology* 2003, 65 (10), 1675-84.
149. Muller, C. E., Medicinal chemistry of adenosine A3 receptor ligands. *Current topics in medicinal chemistry* 2003, 3 (4), 445-62.
150. Holschbach, M. H.; Olsson, R. A., Applications of adenosine receptor ligands in medical imaging by positron emission tomography. *Current pharmaceutical design* 2002, 8 (26), 2345-52.
151. Holschbach, M. H.; Olsson, R. A., Applications of adenosine receptor ligands in medical imaging by positron emission tomography. *Current pharmaceutical design* 2002, 8 (26), 2345-52.
152. Avni, I.; Garzozzi, H. J.; Barequet, I. S.; Segev, F.; Varssano, D.; Sartani, G.; Chetrit, N.; Bakshi, E.; Zadok, D.; Tomkins, O.; Litvin, G.; Jacobson, K. A.; Fishman, S.; Harpaz, Z.; Farbstein, M.; Yehuda, S. B.; Silverman, M. H.; Kerns, W. D.; Bristol, D. R.; Cohn, I.; Fishman, P., Treatment of dry eye syndrome with orally administered CF101: data from a phase 2 clinical trial. *Ophthalmology* 2010, 117 (7), 1287-93.

153. Russo, C.; Arcidiacono, G.; Polosa, R., Adenosine receptors: promising targets for the development of novel therapeutics and diagnostics for asthma. *Fundamental & clinical pharmacology* 2006, 20 (1), 9-19.
154. Che, J.; Chan, E. S.; Cronstein, B. N., Adenosine A2A receptor occupancy stimulates collagen expression by hepatic stellate cells via pathways involving protein kinase A, Src, and extracellular signal-regulated kinases 1/2 signaling cascade or p38 mitogen-activated protein kinase signaling pathway. *Molecular Pharmacology* 2007, 72 (6), 1626-36.
155. Wilson, C. N., Adenosine receptors and asthma in humans. *British journal of pharmacology* 2008, 155 (4), 475-86.
156. Gisele, Z.-S.; Susumu, Z. S.; Allan, K. N.; Alencar and Roberto, T. S., Targeting of the Adenosine Receptors as A Novel Strategy for the Treatment of Arterial Hypertension. *Journal of Neurology & Neurophysiology* 2014.
157. Dungo, R.; Deeks, E. D., Istradefylline: first global approval. *Drugs* 2013, 73 (8), 875-82.
158. Bosch, M. P.; Campos, F.; Niubo, I.; Rosell, G.; Diaz, J. L.; Brea, J.; Loza, M. I.; Guerrero, A., Synthesis and biological activity of new potential agonists for the human adenosine A2A receptor. *Journal of medicinal chemistry* 2004, 47 (16), 4041-53.
159. Manuel de, L. R.; Yeon-Hee, L.; and Junying, Z., Adenosine A2A Receptor as a Drug Discovery Target. 2014, 57 (9), 3623-3650.
160. pubchem.ncbi.nlm.nih.gov/compound/3086599.
161. <https://www.drugbank.ca/drugs/DB05009>.
162. Genovese, T.; Melani, A.; Esposito, E.; Mazzon, E.; Di Paola, R.; Bramanti, P.; Pedata, F.; Cuzzocrea, S., The selective adenosine A2A receptor agonist CGS 21680 reduces JNK MAPK activation in oligodendrocytes in injured spinal cord. *Shock* 2009, 32 (6), 578-85.
163. Christopher, P. A.; Yann, D.; David, A. E.; Lynsey, C.; Hesmondhalgh.; Adrian, L.; and Julian, D. S., Route Selection and Process Development of a Multikilogram Route to the Inhaled A2A Agonist UK-432,097. *Organic Process Research & Development* 2012, 16 (3), 470-483.
164. Volpini, R.; Costanzi, S.; Lambertucci, C.; Portino, F. R.; Taffi, S.; Vittori, S.; Klotz, K.-N.; Cristalli, G., Adenosine receptor agonists: synthesis and binding affinity of 2-(aryl)alkylthioadenosine derivatives *ARKIVOC* 2004, 301-311.
165. Rodríguez, A.; Guerrero, A.; Gutierrez-de-Terán, H.; Rodríguez, D.; Brea, J. Loza, M. I. Roselle, G.; Bosch M. P., New selective A2A agonists and A3 antagonists for human adenosine receptors: synthesis, biological activity and molecular docking studies. *Medchemcomm* 2015, 6.
166. Petrelli, R.; Scortichini, M.; Kachler, S.; Boccella, S.; Carmen, C.; Torquati, I.; Del Bello, F.; Salvemini, D.; Novellino, E.; Livio Luongo, L.; Maione, S.; Kenneth, A. J.; Lavecchia, A.; Klotz, K.-N., and Cappellacci, L., Exploring the Role of N6-Substituents in Potent Dual Acting 5'-C-Ethyltetrazolyladenosine Derivatives: Synthesis, Binding, Functional Assays, and Antinociceptive Effects in Mice. *Journal of medicinal chemistry* 2017, 60 (10), 4327-4341.
167. Ajiroghene, T.; Buccioni, M.; Dal Ben, D.; Lambertucci, C.; Marucci, G.; Santinelli, C.; Spinaci, A.; Kachler, S.; Klotz, K.-N.; Volpini, R., The length and flexibility of the 2-substituent of 9-ethyladenine derivatives modulate affinity and selectivity for the human A2A adenosine receptor. *ChemMedChem* 2016, 11, 1829-1839.
168. Buccioni, M.; Santinelli, C.; Angeli, P.; Dal Ben, D.; Lambertucci, C.; Thomas, A.; Volpini, R.; Marucci, G., Overview on radiolabel-free in vitro assays for GPCRs. *Mini-Rev. Med. Chem.* 2017, 17, 3-14.

169. Caprioli, G.; Iannarelli, R.; Innocenti, M.; Bellumori, M.; Fiorini, D.; Sagratini, G.; Vittori, S.; Buccioni, M.; Santinelli, C.; Bramucci, M.; Quassinti, L.; Lupidi, G.; Vitali, L. A.; Petrelli, D.; Beghelli, D.; Cavallucci, C.; Bistoni, O.; Trivisonno, A.; Maggi, F., Blue honeysuckle fruit (*Lonicera caerulea* L.) from eastern Russia: phenolic composition, nutritional value and biological activities of its polar extracts. *Food & Function* 2016, 7, 1892–1903.
170. Volpini, R.; Dal Ben, D.; Lambertucci, C.; Marucci, G.; Mishra, R. C.; Ramadori, A. T.; Klotz, K.-N.; Trincavelli, M. L.; Martini, C.; Cristalli, G., Adenosine A2A receptor antagonists: new 8-substituted 9-ethyladenines as tools for in vivo rat models of Parkinson's disease. *ChemMedChem*. 2009, 4 (6), :1010-9.
171. Lambertucci, C.; Antonini, I.; Buccioni, M.; Dal Ben, D.; Kachare, D. D.; Volpini, R.; Klotz, K.-N.; Cristalli, G., 8-Bromo-9-alkyl adenine derivatives as tools for developing new adenosine A2A and A2B receptors ligands. *Bioorganic & Medicinal Chemistry* 2009, 17, 2812–2822.
172. Lambertucci, C.; Antonini, I.; Buccioni, M.; Dal Ben, D.; Kachare, D. D.; Volpini, R.; Klotz, K.-N.; Cristalli, G., 8-Bromo-9-alkyl adenine derivatives as tools for developing new adenosine A2A and A2B receptors ligands. *Bioorganic & Medicinal Chemistry* 2009, 17, 2812–2822.
173. Klotz, K.-N.; Hessling, J.; Hegler, J.; Owman, C.; Kull, B.; Fredholm, B. B.; Lohse, M. J., Comparative pharmacology of human adenosine receptor subtypes - characterization of stably transfected receptors in CHO cells. *Naunyn-Schmiedeberg's archives of pharmacology* 1998, 357 (1), 1-9.
174. Klotz, K.-N.; Falgner, N.; Kachler, S.; Lambertucci, C.; Vittori, S.; Volpini, R.; Cristalli, G., [3H]HEMADO--a novel tritiated agonist selective for the human adenosine A3 receptor. *European Journal of Pharmacology* 2007, 556 (1-3), 14-18.
175. Volpini, R.; Costanzi, S.; Lambertucci, C.; Vittori, S.; Martini, C.; Trincavelli, M. L.; Klotz, K.-N.; Cristalli, G., 2- And 8-alkynyl-9-ethyladenines: synthesis and biological activity at human and rat adenosine receptors. *Purinergic signalling* 2005, 173-181.
176. Camaioni E, Costanzi S, Vittori S, Volpini R, Klotz K.-N., Cristalli G., New substituted 9-alkylpurines as adenosine receptor ligands. *Bioorganic & Medicinal Chemistry* 1998, 6 (5), 523-533.